



**UNIVERSITY OFTM
KWAZULU-NATAL**

**INYUVESI
YAKWAZULU-NATALI**

Synthesis and immobilization of triazolium based ionic liquids
as recyclable organocatalysts for the transfer hydrogenation of
ketones

By

George Dhimba

Dissertation submitted in fulfilment of the academic requirements for the
degree of Masters of Science, School of Chemistry and Physics,
University of KwaZulu-Natal, Durban

As the candidate's supervisor I have approved this dissertation for
submission.

Supervisor:

Signature: Name: Muhammad D. BALA

Date:.....

ABSTRACT

The aim of the study was to bridge the gap between homogeneous and heterogeneous catalysis by combining the advantages offered by single phase homogeneous catalysts with the ease of separation of heterogeneous catalysts while minimizing the disadvantages of both systems. A common method used is catalyst immobilization on solid supports. Hence, triazoles and corresponding salts have been synthesized by adopting the versatile, green and regioselective Cu(I) catalyzed cycloaddition reaction of organic azides and terminal alkynes. The triazolium salts were characterized by various spectroscopic techniques and then tested for activity in the transfer hydrogenation of ketones. Selected triazoles were then immobilized onto straight chain polyethylene glycols (PEGs) of various chain lengths. The immobilization was achieved by the tosylation of PEGs to yield PEG ditosylates followed by *N*-alkylation which created binding O-N covalent bonds. Characterization by NMR and mass spectrometry confirmed successful immobilization. Salt metathesis was done using sodium iodide in dichloromethane that yielded brick red colored ionic liquids. The formed ionic liquids were then tested for activity in the transfer hydrogenation of acetophenone with isopropanol as a hydrogen donor and solvent. The effects of polymer chain length, electronic effect of the triazolium moiety, reaction temperature and time on the catalysis were investigated. Results indicate that the immobilized triazoles bearing tosylate counter ions were inactive as catalysts. However, the results indicate that for optimum reactivity, PEG₆₀₀ was the ideal chain length for the immobilized systems. The ionic liquids were then tested for transfer hydrogenation of different substituted ketones. The catalyst system was easily recovered by the addition of diethyl ether after the reaction followed by simple decantation. The immobilized catalysts were recycled three times with a percentage conversion of 82% being observed in the third cycle.

DECLARATION: PLAGIARISM

I, George Dhimba, declare that the experimental work described in this dissertation was carried out at the School of Chemistry and Physics, University of KwaZulu-Natal, Westville Campus, between August 2013 and June 2015, under the supervision of Prof. Muhammad D. Bala, and that:

1. The research reported in this dissertation, except where otherwise indicated is my original research.
2. This dissertation has not been submitted for any degree or examination at any other university.
3. This dissertation does not contain other persons' data, pictures, graphs or other information, unless specifically acknowledged as being sourced from other persons.
4. This dissertation does not contain other persons' writing, unless specifically acknowledged as being sourced from other researchers. Where other written sources have been quoted, then:
 - a. Their words have been re-written but the general information attributed to them has been referenced.
 - b. Where their exact words have been used, then their writing has been placed in italics and inside quotation marks, and referenced.
5. This dissertation does not contain texts, graphics or tables copied and pasted from the Internet, unless specifically acknowledged, and the source being detailed in the dissertation and in the references sections.

Signed

George Dhimba

Table of Contents

Contents	page
ABSTRACT	i
DECLARATION: PLAGIARISM	ii
Table of contents	iii
List of Schemes	viii
List of tables.....	ix
List of Abbreviations	x
List of Symbols	xii
Dedication	xiii
Acknowledgements	xiv
Chapter one	1
1.1 Introduction	1
1.1.1 Genesis of click chemistry.....	1
1.1.2 The 1, 3-dipolar cycloaddition of azides and alkynes	1
1.1.3 Mechanism of the CuAAC	2
1.1.4 The Cu(I) catalysts and pre-catalysts.....	3
1.1.5 Solvents	4
1.1.6 <i>N</i> -alkylation of triazolium compounds	4
1.2 Application of 1,2,3-triazolium ionic salts	5
1.3 Catalysis.....	6
1.3.1 Organocatalysis	7
1.4 Immobilization of organocatalysts on supports	7
1.4.1 Immobilization strategies	9
1.4.2 Adsorption	9

Contents	Page
1.4.3 Encapsulation.....	10
1.4.4 Covalent tethering.....	11
1.4.5 Covalent immobilization on inorganic supports.....	11
1.4.6 Covalent immobilization on polymers	11
1.4.7 Liquid-liquid biphasic immobilization	13
1.5 Metal free transfer hydrogenation	14
1.6 Aims.....	15
1.7 Objectives	15
1.8 References	16
Chapter two	20
Preparation of 1,3,4-trisubstituted-1,2,3-triazolium salts	20
2.1 Introduction	20
2.1.1 Materials	20
2.1.2 Instrumentation	20
2.2 Experimental protocols.....	21
2.2.1 General procedure for the synthesis of compounds 2.1-2.6	21
2.2.2 General procedure for the synthesis of 1,4-disubstituted-1,2,3-triazoles 2.7-2.12	24
2.2.3 N-alkylation of the 1,4-disubstituted-1,2,3-triazoles.....	26
2.2.4 Typical procedure for salt metathesis of triazolium salts	30
2.5 Attempted immobilization of triazoles on silanes	31
2.6 General procedure for synthesis of PEG ditosylates	32
2.7 General procedure for the immobilization of 1-butyl-4-phenyl-1H-1,2,3-triazole onto PEGs	34
2.8 Typical Procedure for covalent immobilization of 1-benzyl-4-phenyl-1H-1,2,3-triazole onto PEG.....	38

Contents	Page
2.9 Results and discussion.....	41
2.9.1 NMR	41
2.9.2 Tosylation of PEG diols	46
2.9.3 Covalent immobilization of triazoles onto PEGs	47
2.10 Melting point	48
2.11 IR spectra.....	50
2.12 Mass spectrometry	51
2.13 Elemental analysis (EA)	54
2.14 Single crystal XRD studies.....	55
2.15 References	62
Chapter three	64
Covalent immobilization of triazoles onto PEGs and their application as catalysts for the transfer hydrogenation of ketones	64
3.1 Introduction	64
3.2 Organocatalytic transfer hydrogenation of ketones.....	64
3.3 Experimental.....	64
3.4 Typical protocol for transfer hydrogenation of ketones	65
3.5 Transfer hydrogenation of acetophenone by triazolium ionic salts.....	65
3.6 Catalyst recycle.....	73
3.7 References	75
Chapter four	76
Conclusion and recommendations.....	76
4.1 Synthesis and N-alkylation of triazoles	76
4.2 Immobilization and catalysis	79
4.3 Future outlook.....	79

List of Figures

Contents	Page
Figure 1.1: Immobilization of Rh ⁺ [R–R–BDPBzPSO ₃]- complex by adsorption. ⁶²	9
Figure 1.2: Silane modified L- proline precursor P₁ and P₂ .	11
Figure 1.3: Thermoregulated behaviour of PEG ₁₀₀₀ -DAIL/ toluene system. ⁸³	14
Figure 2.1: Typical triazole numbering.....	41
Figure 2.2: ¹ H NMR spectrum of 2.7	42
Figure 2.3: ¹³ C NMR spectrum of 2.7	43
Figure 2.4: ¹ H NMR spectrum of 2.7a	44
Figure 2.5: ¹³ C NMR spectrum of 2.7a	45
Figure 2.6: NOESY NMR spectrum of 2.11a	46
Figure 2.7: ¹ H NMR spectrum of PEG ₃₀₀ ditosylate 2.17	47
Figure 2.8: ¹ H NMR spectrum of PEG ₃₀₀ ditriazole 3a	48
Figure 2.9: IR spectrum of 2.7	51
Figure 2.10: Mass spectrum of 2.10	53
Figure 2.11: Mass spectrum of 2.29	53
Figure 2.12: Mass spectrum of 2.29	54
Figure 2.13: ORTEP representation of the structure of 2.7 with the displacement ellipsoids drawn at the 50% probability level.	56
Figure 2.14: Crystal packing of 2.7	57
Figure 2.15: ORTEP representation of the structure of 2.11 with the displacement ellipsoids drawn at the 50% probability level.	57
Figure 2.16: Crystal Packing of 2.11	57
Figure 2.17: ORTEP representations of the structure of 2.8a with the displacement ellipsoids drawn at the 50% probability level.	58
Figure 2.18: Crystal packing of 2.8a	58

Figure 2.19: ORTEP representations of the structure of 2.12a with the displacement ellipsoids drawn at the 50% probability level.	58
Figure 2.20: crystal packing of 2.12a	59
Figure 2. 21: Solid state structure of 2.8a (top) and 2.12a (bottom) showing halogen bonding; (brown = bromide purple = iodide).....	59
Figure 3.1: Triazolium salts 2.1a-2.12a	65
Figure 3.2: Time dependance of the transfer hydrogenation of cyclohexanone catalysed by 2.5a	68
Figure 3.3: Behaviour of PEG ₆₀₀ IL in ether.	73
Figure 3.4: Recycling studies for the PEG immobilized catalyst 3.19	74
Figure 4.1: Summary of the synthesized triazoles.....	77
Figure 4.2: Summary of the synthesized triazolium salts.	78

List of Schemes

Contents

Page

Scheme 1.1: The Huisgen 1, 3-dipolar cycloaddition of alkynes and azides. ^{11,14}	2
Scheme 1.2: Schematic representation of CuAAC click chemistry reaction. ¹⁶	2
Scheme 1.3: Adopted mechanism for the CuAAC. ^{2, 3, 12}	3
Scheme 1.4: Synthesis of 1,3,4-trialkylated-1,2,3-triazolium salts. ²⁸	5
Scheme 1.5: Synthesis of (S)-proline derived 1,2,3-triazolium ionic liquid tagged organocatalyst. ²⁵	6
Scheme 1.6: Immobilization of [Mn(saldPh)Cl] within Al-WYO by encapsulation.....	10
Scheme 1. 7: Synthetic route of PEG-DIAL. ^{66a}	12
Scheme 1.8: Synthesis of immobilized pyridine organocatalysts. ⁷⁵	12
Scheme 2.1: Synthesis of 1,4-disubstituted-1,2,3-triazoles.	22
Scheme 2.2: Synthesis of 1,4-disubstituted-1,2,3-triazoles 2.7-2.12	24
Scheme 2.3: N-alkylation of triazolium salts.	27
Scheme 2.4: salt metathesis of 2.6a	31
Scheme 2.5: Synthesis of PEG ditosylate.	32
Scheme 2.6: Covalent immobilization of 1-butyl-4-phenyl-1H-1,2,3-triazole onto PEG.	34
Scheme 2.7: Covalent Immobilization of 1-benzyl-4-phenyl-1H-1,2,3-triazole onto PEG.....	38

List of Tables

Contents	Page
Table 2.1: Variations in mp and the triazole chemical shift of the compounds.....	49
Table 2.2: The m/z ratios obtained for triazoles.	51
Table 2.3: The m/z ratios obtained for triazolium salts.	52
Table 2.4: CHN EA results for triazoles and triazolium salts.....	55
Table 2.5: Summary of crystallographic data for 2.7 , 2.11 , 2.8a , and 2.12a	60
Table 2.6: Selected bond lengths (Å) and angles (°) for 2.7 , 2.11 , 2.8a and 2.12a	61
Table 3.1: Transfer hydrogenation of acetophenone catalyzed by triazolium salts 2.1a-2.12a	66
Table 3.2: Transfer hydrogenation of different sources of ketones.	69
Table 3.3: Effect of polymer chain length on catalysis.	71
Table 3.4: Effect of toluene blending on catalysis.....	72

List of Abbreviations

ATR	-	Attenuated total reflectance
Cald	-	Calculated
CIF	-	Crystallographic information file
cm ⁻¹	-	wavenumber
d	-	Doublet
DEPT	-	Distortionless enhancement by polarization transfer
EA	-	Elemental Analysis
EDTA	-	Ethylenediaminetetraacetic acid,
ESI	-	Electron spray ionization
GC	-	Gas chromatography
HRMS	-	High resolution mass spectrometry
IR	-	Infrared
M	-	Molecular ion
m	-	Multiplet
mg	-	Milligrams
MHz	-	Mega Hertz
mmol	-	Millimoles
m/z	-	Mass to charge ratio
mp	-	Melting point
N/A	-	Not applicable
NMR	-	Nuclear magnetic resonance

ORTEP	-	-	Oakridge thermal ellipsoid plot
PEG	-		Polyethylene glycol
PEG Mn ₃₀₀	-		Polyethylene glycol average molecular mass 300 g
RBF	-		Round bottom flask
s	-		Singlet
t	-		Triplet
TOF	-		Time of flight
TLC	-		Thin layer chromatograph
TON	-		Turnover number
q	-		Quartet

List of Symbols

δ	-	Chemical shift
%	-	Percentage
\AA	-	Angstrom unit, 10^{-10} m
α	-	Alpha
β	-	Beta
γ	-	Gamma
$^{\circ}\text{C}$	-	Degrees Celsius
$(^{\circ})$	-	Degrees

Dedication

To my late Father

Acknowledgements

I would like to give all the glory to God the Almighty and most high, in the name of our Lord and Savior Jesus Christ, through Him we earn eternity.

I would like to thank my mother for the love, and support.

I would like to thank my supervisor, Prof. MD Bala for initiating this project, support, guidance and constructive criticisms during my time as a Masters student.

I would like to thank the University of KwaZulu-Natal and the School of Chemistry and Physics for accepting me as a Masters student in their campus and the National Research Foundation (NRF) for their financial support.

I would like to thank all my colleagues in the laboratory.

Chapter one

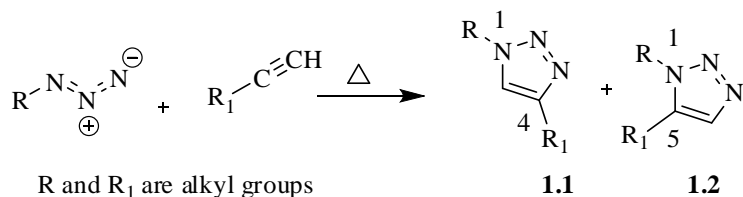
1.1 Introduction

1.1.1 Genesis of click chemistry

The versatile “green” concept of “click” reaction was first coined and defined by Kolb, Finn and Sharpless in 2001. The objective was to bind two molecular building blocks together in a simple, selective, high yield reaction under mild aqueous conditions with little or negligible byproducts.¹ The term “click” refers to energetically favored, specific, and versatile chemical transformations, which lead to a single reaction product.² Reactions classified as “click” require only mild conditions and facile workup and purification procedures.³ In addition, the reaction must be modular, wide in scope and provide high yields generating only innocuous byproducts.⁴ The Cu(I)-catalyzed cycloaddition reaction of organic azides and terminal alkynes to give 1,4-substituted-1,2,3-triazoles fulfils all the click requirements, exhibits remarkable broad scope and exquisite selectivity.^{4,5} The cycloaddition of alkynes and azides to give triazoles is arguably the best click reaction to date,⁶ it has evolved as a powerful strategy with myriad applications in synthetic and medicinal chemistry,⁷ bio conjugations,⁸ materials science,⁹ and polymer chemistry.¹⁰ The click reaction is one type of Huisgen cycloaddition reaction,¹¹ in which dipolarophiles react with 1,3-dipoles to form five-membered heterocycles including triazoles. Thermal Huisgen 1,3-dipolar cycloaddition reactions normally give 1:1 mixtures of 1,4 and 1,5-disubstituted regioisomers, whereas the Cu-catalyzed reactions are highly regioselective and only give 1,4-disubstituted triazoles.¹²

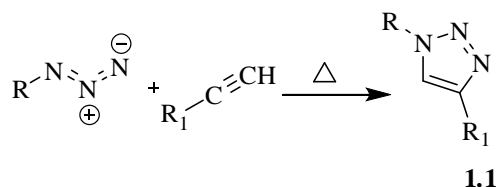
1.1.2 The 1, 3-dipolar cycloaddition of azides and alkynes

A “1,3-dipole” is a species which contains one or more heteroatoms and can be described as having at least one mesomeric structure which undergoes 1,3-cycloaddition to a multiple bond system, the “dipolarophile”.¹³ The formation of 1,2,3-triazoles by 1,3-dipolar cycloaddition of azides and alkynes has been extensively studied in the 1960s by Rolf Huisgen.¹¹ Illustrated in Scheme 1.1 is the thermal unselective Huisgen 1,3-cycloaddition reaction. The reaction does not satisfy the requirements for click chemistry as it is not regioselective and usually gives equimolar mixtures of the 1,4-disubstituted-1,2,3-triazole **1.1** and its 1,5- regioisomer **1.2**. In addition, the reaction only proceeds by refluxing at higher temperatures and requires long reaction time.¹¹



Scheme 1.1: The Huisgen 1, 3-dipolar cycloaddition of alkynes and azides.^{11,14}

In 2002, the groups of Sharpless⁶ and Meldal¹⁵ described the use of Cu(I) salts as catalysts for the 1,3-dipolar cycloaddition reaction, which gives the 1,4-triazolic isomer **1.1** as the exclusive product at room temperature. The reaction (Scheme 1.2) has been labelled as the Cu(I) catalyzed azide/alkyne cycloaddition (CuAAC) and as earlier mentioned, it has been categorized as the best click reaction to date.⁵



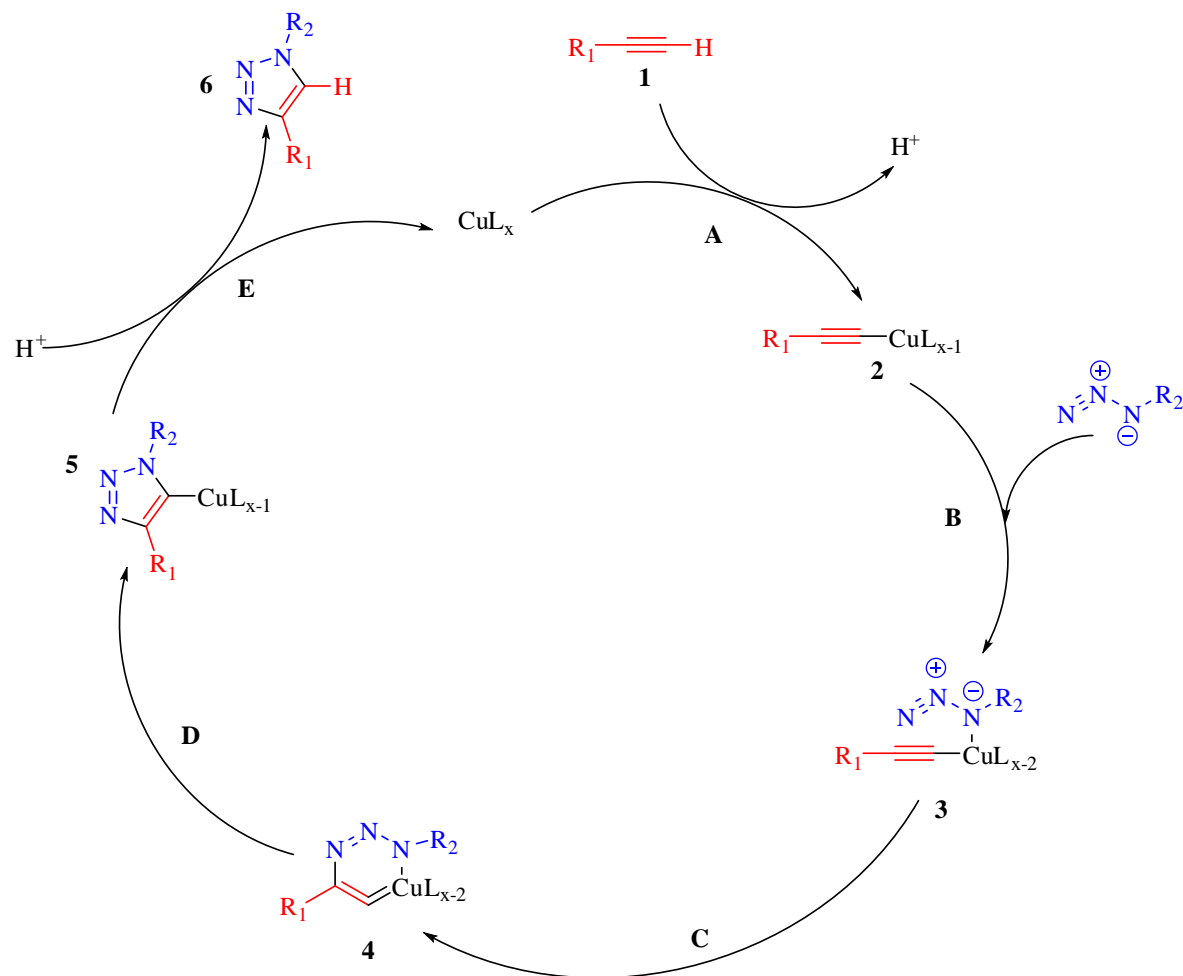
Scheme 1.2: Schematic representation of CuAAC click chemistry reaction.¹⁶

Sharpless *et al.*,⁴ highlighted that the CuAAC couplings of terminal alkynes and azides is characterized by a high thermodynamic force (>20 kcal/mol),¹⁷ which gives rise to highly modular and stereospecific reactions. The mechanism of the Cu(I) catalyzed cycloaddition reaction of azides and terminal alkynes has been studied comprehensively.¹⁸

1.1.3 Mechanism of the CuAAC

The mechanism of CuAAC appears to be relatively complex. Although it has been extensively studied,^{5,18} it is still not yet fully understood in terms of the exact nature of the Cu-containing species involved in the catalytic cycle.¹⁹ The proposed mechanistic sequence (Scheme 1.3) initiates with the coordination of the alkyne to the Cu(I) species, displacing one of the ligands **L**.^{2,6} This initial step has been well documented in which Cu(I) readily inserts into terminal alkynes in the presence of a base, for example the case of Sonogashira coupling.²⁰ It has been calculated to be slightly endothermic, however when water is used as a solvent or co-solvent the process becomes exothermic.

The conversion of alkyne **1** to acetylide **2** is well known to be involved in many C-C bond forming reactions in which the Cu acetylide species is the only exclusive intermediate. The second step is the reaction of Cu(I) acetylides with organic azides to give Cu(I) azide **3**, presumably via a six-membered metallacycle **4**. Next is the formation of triazolide species **5** via a ring contraction reaction, which finally undergoes proton transfer to form **6**. The final step is the proteolysis of **5** to give a 1,4-substituted-1,2,3-triazole and recovery of the Cu(I) catalyst.¹⁹



Scheme 1.3: Adopted mechanism for the CuAAC.^{2, 3, 12}

1.1.4 The Cu(I) catalysts and pre-catalysts

Different sources of copper catalysts have been used for the CuAAC provided that the active Cu(I) species are generated *in situ*.^{18b} Liang and Astruc¹ emphasized that the Cu(I) concentration need to be maintained at its maximum in order to facilitate this reaction. The pioneers of the CuAAC, Meldal

and coworkers initially described the use of Cu(I) salts on a solid phase,⁶ while Sharpless reported solution phase *in situ* reduction of Cu(II) salts or comproportionation of Cu(0) and Cu(II).^{3,20a} A variety of different Cu(I) sources can be employed in the CuAAC reaction, as recently demonstrated in necessarily partial fashion by Meldal and Tornøe.²¹ Cu(I) salts (iodide, bromide, chloride, acetate) and coordination complexes such as [Cu(CH₃CN)₄]PF₆ and [Cu(CH₃CN)₄]OTf have been commonly employed.²² Various diacetylenes, bis-triazoles, and 5-hydroxytriazoles are usually the byproducts obtained when the reaction is done in the absence of a base.²³ It is noteworthy that the use of Cu(I) iodide should be avoided as the iodide readily coordinate as a bridging ligand for the metal, resulting in the formation of polynuclear acetylide complexes.^{22b}

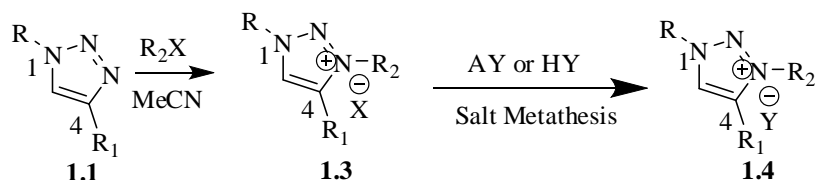
1.1.5 Solvents

The most important feature of the CuAAC is that it can tolerate a wide variety of solvents,²⁴ and functional groups,²⁵ hence target functionalities can be incorporated as substituents of the resulting triazoles ring. A variety of solvents and solvent conditions have been used,⁶ non-coordinating solvents such as dichloromethane, toluene and chloroform, weakly coordinating solvents such as dioxane, pyridine and tetrahydrofuran, polar solvents such as acetone, acetonitrile and dimethylformamide (DMF) and aqueous organic biphasic mixtures of two or even three solvent systems have been reported to produce moderate to high yields.¹ The main function of the solvent or solvent mixtures is to dissolve the Cu(I) catalyst and ensure a spontaneous reaction. However, as coordinating solvents could inhibit the crucial metal-substrate coordination, solvents like (DMF) are ideal for the Cu(Br) catalyst without supplementary ligands.¹

1.1.6 *N*-alkylation of triazolium compounds

The second step in the synthesis of 1,2,3-triazolium salts is *N*-Alkylation. This step can either produce a 2-alkylated²⁶ or 3-alkylated²⁷ 1,4-disubstituted triazolium salts which present a problem of regioselectivity. However, if soft alkylating reagents (tosylates, allyl halides, benzyl, sulfates and sulfonates) are used, only 1,3,4-trisubstituted 1,2,3-triazolium salts are obtained.²⁸ Hence, the major steps in the synthesis of 1,2,3-triazolium salts can be achieved in a highly regioselective manner.²⁵ To obtain pure *N*-alkylated products it is essential to start with pure 1,2,3-triazoles and conduct the reaction neat but with excess of the alkylating reagents. The target 1,2,3-triazolium salts are obtained in pure form by removing excess alkylating reagent and washing with non-polar solvents. It is

important to demonstrate at this point that if the leaving group is considered as an unsuitable counter ion, it can be exchanged with another counter ion via salt metathesis⁵ as illustrated in Scheme 1.4.



where AY and HY are salts or acids

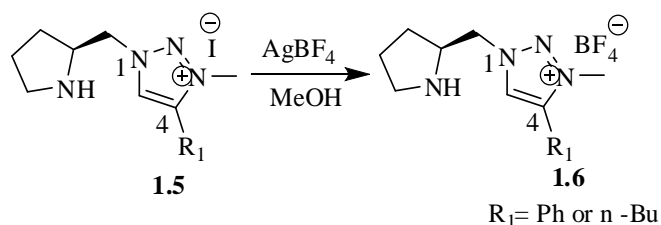
$X = Cl^-, Br^-, \text{ and } I^-$

$Y^- = BF_4^-, PF_6^-, NO_3^- \text{ etc}$

Scheme 1.4: Synthesis of 1,3,4-trialkylated-1,2,3-triazolium salts.²⁸

1.2 Applications of 1,2,3-triazolium ionic salts

The application of 1,2,3-triazolium based ionic salts as reaction solvents is rare probably due to the fact that they are expensive and not commercially available. However, 1,3-dialkyl-1,2,3-triazolium ionic liquids have been developed as chemically inert and recyclable catalysts for the Baylis-Hillman reaction²⁹. At present, the major use of 1,2,3-triazolium salts is in ionic liquid tagging of organocatalysts.³⁰ In this procedure 1,2,3-triazolium ionic salts are covalently bonded to organocatalytic structures yielding ionic liquid tagged organocatalysts. Tagging affords better catalytic activity, solubility, and most importantly easier recyclability of catalysts.³¹ Ionic liquids tagged organocatalysts can be dissolved in various polar solvents and hence act as homogeneous catalysts which is an advantage when compared to catalysts fixed on solid supports that are often insoluble in the reaction media.³² Catalyst recovery and reuse is achieved by extracting the products from the reaction mixture using non polar organic solvents leaving behind the ionic liquid tagged organocatalyst which can be used for the next cycle. (S)-proline derived 1,2,3-triazolium ionic liquid tagged organocatalysts **1.5** and **1.6** (Scheme 1.5) were found to be effective as enantioselective catalysts for the Michael addition of different unmodified aldehydes and ketones.²⁵ Another important application of 1,2,3-triazolium salts is in *N*-heterocyclic carbene (NHC) based metal complexes where 1,2,3-triazolium salts are used as precursors towards the synthesis of NHC ligands.³³ In addition to catalysis, triazolium salts have been used in fuel industry. The 1-amino-1,2,3-triazolium ionic salt have been used as energy rich ligand in explosives and fuels in which the high heat of formation is directly attributable to the large number of energetic N-N and C-N bonds present.³⁴



Scheme 1.5: Synthesis of (S)-proline derived 1,2,3-triazolium ionic liquid tagged organocatalyst.²⁵

1.3 Catalysis

The term catalysis was first coined by Berzelius³⁵ to identify a new entity capable of promoting the occurrence of a chemical reaction by contact. According to his definition a catalyst is viewed as something that is added to a reaction to speed up the rate of the reaction (catalytic force) without being consumed in the process.³⁶ The concept can also be explained by adopting a Sharpless statement, “*catalysis is the engine that drives the development of chemistry*”.³⁷ Theoretically, a catalyst should approach 100% selectivity while reaching high levels of productivity; however this is not always the case in practice. Historically, catalysts were categorized as homogeneous or heterogeneous catalysts but recently, heterogenized catalysts were also introduced.³⁸ Homogeneous catalysts have the advantage of producing high selectivity at relatively mild operating conditions.³⁹ This is attributed to their molecular nature and being in the same phase as the reactants. Conversely, heterogeneous catalysts like metals and their oxides, have several advantages which include high thermal and mechanical stability, high activity for a wide range of catalytic reactions, ease of separation and catalyst recovery.⁴⁰ The major disadvantages of heterogeneous catalysts include design and improvement limits due to frequently ill-defined active sites, limited accessibility of the organic substrates to the active sites and the use of severe reaction conditions such as high temperatures and pressures. In homogeneous systems, each catalytic molecule is available for the reaction. This results in efficient, reproducible and highly active catalytic system. However, their only major drawback is the problem of separating the catalyst from products for reactivation and re-use. It is worthwhile to combine the advantages offered by homogeneous catalysts, specifically high activity and selectivity, with the ease separation of heterogeneous catalysts. A common methodology is to anchor homogeneous catalysts to inert supports (immobilization) such that the catalyst sphere remains unaltered. The long term objective of immobilizing catalysts onto solid supports is that they

would result in the superior hybrid catalysts retaining advantageous features of homogeneous and heterogeneous catalysts while eliminating the disadvantages of both systems.

1.3.1 Organocatalysis

In 2000, MacMillan coined and defined the term organocatalysis as the use of organic molecules with low molecular weight as catalysts in organic reactions.⁴¹ The definition corresponds to low molecular weight organic molecules which in sub-stoichiometric amounts catalyzes chemical reactions.⁴² Catalysis with small organic molecules, where an inorganic element is not part of the active species has become a highly dynamic area in chemical research.⁴³ This new field of catalysis has emerged as a powerful and promising synthetic field that is complementary to enzyme-catalysis and metal-catalyzed transformations and has accelerated the development of new methodologies for synthesizing diverse chiral molecules.⁴⁴ Interest in this kind of catalysis is increased by other attractive benefits such as ready availability and stability of the catalysts, their simple handling, operational simplicity and storage, and the possibility of performing reactions in wet solvents and in air.⁴⁵ Organocatalysts may be Lewis or Brønsted acids or bases. The action of most organocatalysts reported so far are explained by two main organocatalytic mechanisms: the covalent and non-covalent mechanism. The former strategy utilizes formation of a covalent bond between the catalyst and substrate molecule which maintains the asymmetric center very close to the reactive moiety. Conversely, non-covalent organocatalysts is based on small organic molecules designed as catalysts capable of forming hydrogen bonding interactions with oxygen or nitrogen lone electron pairs in the substrate. A common drawback associated with the use of organocatalysts is that most of them are required in stoichiometric amounts,⁴⁶ this is probably the reason why they have seldom been applied in industry,⁴⁷ a fact that can also be attributed to their insufficient efficiency. In addition, the workup procedure for separation of organocatalysts from the product is often tedious and laborious hence the need for immobilization.

1.4 Immobilization of organocatalysts on supports

Immobilization or heterogenization of catalysts onto solid supports for catalytic reactions represents an attractive approach towards increased sustainability in organic synthesis. In comparison to metal mediated reactions, organocatalysis results in agglomeration and aggregation of the active sites which often leads to a higher required mole % of catalyst.⁴⁶ Isolation of these catalysts from the reaction is

often cumbersome, hence interest in the design of recoverable catalysts has recently increased profoundly in catalysis research.⁴⁸ In fact, catalyst deactivation mainly due to leaching of the active species and its decomposition have to be taken into account. Heterogenization of active organic entities promises to be a viable method to alleviate these shortcomings.⁴⁹ Although this invariably increases the stages of the synthetic pathway, the design of an effective heterogenized organocatalyst will improve activity, selectivity and recoverability;⁵⁰ the benefits of which will by far offset the additional synthetic challenges. Despite the above merits, there are very few reports of heterogenized organocatalysts that are able to replicate the levels of activity and selectivity observed in homogeneous systems.⁵¹ As a result, there is an urgent need for the development of a design rationale that could serve as a basis for anchoring homogeneous organocatalysts in a robust fashion.⁴⁹ The two support systems that have widely been used to immobilize organocatalysts are organic polymers like PEGs⁵² and inorganic oxides like silica.⁵³ When compared to inorganic supports, polymers offer several advantages. They can easily be functionalized and most of the hydrocarbon polymers are chemically inert hence the supports will not interfere with the catalyst.⁵⁴ Since polymers can be prepared with a wide range of physical properties, their porosity, surface area and solution characteristics can be altered to suit the catalyst conditions. In addition, immobilization of homogeneous catalysts can sometimes improve catalyst activity and selectivity by preventing the formation of inactive dimers, agglomerates and aggregates.⁵⁵ This condition is usually referred to as site-isolation that is immobilizing a catalyst on a support in such a way that the catalytic sites cannot interact with each other. However, the catalytic activity of some cross linked polymeric catalysts is generally decreased when compared to the corresponding low molecular weight catalysts in solution. In addition, polymers often show poor heat transfer ability and in many cases they show poor mechanical properties which prevents them from being used in stirred reactors.⁵⁶ Due to their high viscosity, polymeric catalysts often result in reduced diffusion properties which subsequently leads to a decrease in catalytic activity. Polymer supported catalysts usually resulted in deactivation through intermolecular aggregation or condensation.⁵⁷ On the other hand, inorganic supported catalysts show better mechanical and thermal stabilities coupled with reasonable heat transfer properties.⁵⁸

1.4.1 Immobilization strategies

There are four broad types of procedures that have been developed for the heterogenization of homogeneous catalysts. The following section consists of examples of given methodologies and a comparison of the homogeneous equivalent wherever possible.

1.4.2 Adsorption

Physical adsorption is probably the simplest and most common method of catalyst immobilization. It is based on physical binding or ionic bonding or both of the catalyst to the surface of the support.⁵⁹ In most cases, weak interaction between the catalyst and support are established, namely (van der Waals and hydrophobic interactions) which have little effect on catalytic activity.⁶⁰ In a typical adsorption procedure a solution of catalyst, usually aqueous is brought into contact with a support material, if the catalyst support interactions are strong enough adsorption will occur.⁶¹ Since catalyst-support interactions are usually weak, the catalyst will easily leach into solution as it reaches equilibrium between the surface absorbed species and solution species. Supported catalysts can be stabilized by improving the surfaces of the catalyst and its support such that hydrogen bonding is facilitated. An example of this type of catalyst system is a rhodium phosphine catalyst (Figure 1.1) which has been immobilized onto silica, the sulfonic groups incorporated onto the phosphine ligand formed hydrogen bonds with the silanol groups of silica.⁶²

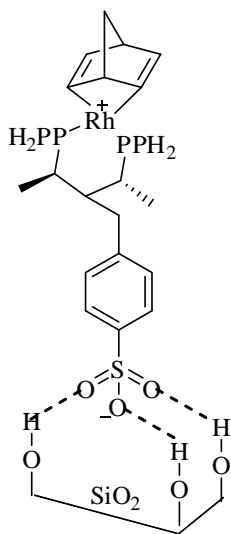
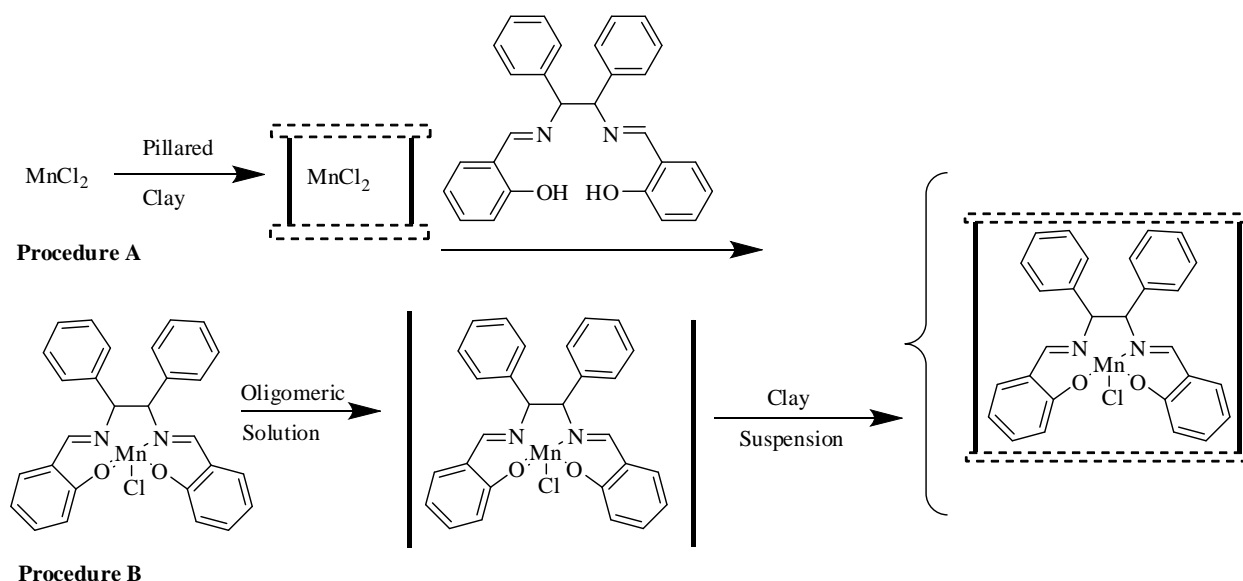


Figure 1.1: Immobilization of Rh^+ [R–R–BDPBzPSO₃]⁻ complex by adsorption.⁶²

1.4.3 Encapsulation

Encapsulation is the only catalyst immobilization procedure that sometimes resemble homogeneous catalyzed reactions, this is because it does not involve interaction between the catalyst and support, other methods by necessity results in the catalyst being altered.⁶¹ For encapsulation to take place, the catalyst must be larger than the pores of the support otherwise the catalyst will leach into solution during the catalytic reaction. The encapsulated catalyst can either be prepared by synthesizing it inside the pores of the support⁶³ or assembling the support around it.⁶⁴ The encapsulation procedure to be chosen depends on the chemistry of both the catalyst and its support. For example, if the catalyst is to be prepared inside the support then the support need to be stable under the reaction conditions used. Conversely, if the support is to be made around the catalyst then the catalyst have to be stable to the synthesis conditions of that support.⁶¹ Therefore, if a catalyst can be easily made in a few simple steps then synthesis inside the pores is favored. On the other hand, if catalyst synthesis involve complicated steps then formation of support around the catalyst is preferred. Illustrated in Scheme 1.6 is the immobilization procedure of a Mn^{3+} complex ($\text{Mn}(\text{saldPh})\text{Cl}$) by encapsulation.⁶⁵ In Procedure A, the catalyst is prepared inside the support (ship in a bottle) material while in procedure B the support is assembled around the catalyst.



Scheme 1.6: Immobilization of $[\text{Mn}(\text{saldPh})\text{Cl}]$ within Al-WYO by encapsulation.

1.4.4 Covalent tethering

Tethering of organocatalysts through the formation of covalent bonding enhances long term stability of anchored molecules. It is currently the most popular technique for designing stable immobilized asymmetric catalysts. Various strategies have been developed depending upon the reaction being catalyzed.⁶⁵ Common supports for immobilization include functionalized polymers,⁶⁶ inorganic oxides⁶⁷ and nanoparticles.⁹

1.4.5 Covalent immobilization on inorganic supports

Inorganic supports like silica, alumina, zeolites, zirconia, zinc oxide, clays and other mesoporous materials have high surface areas and readily accessible pores.⁶⁸ Additionally, they exhibit high thermal and mechanical stabilities⁶⁹ under catalytic conditions as compared to polymer and organic supports.⁷⁰ Organocatalysts are grafted onto the surface of the supports (usually silica) either via direct linkage, making use of existing functional groups, or by modification of the ligand to include an (SiOR)₃ functionality which can be grafted on the support via condensation.⁷¹ Silica is the most popular matrix for inorganic solid catalytic support because of its lower cost, availability, mechanical robustness and ease of synthesis.⁷² Zamboulis and co-workers have immobilized L-proline onto the surface of mesoporous silica and successfully applied it for asymmetric aldol reaction.⁶⁷ The two modified L-proline precursor P₁ and P₂ (Figure 1.2) were easily grafted onto the surface of mesoporous silica by a simple condensation reaction.

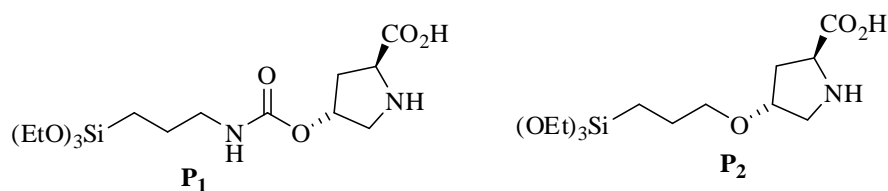
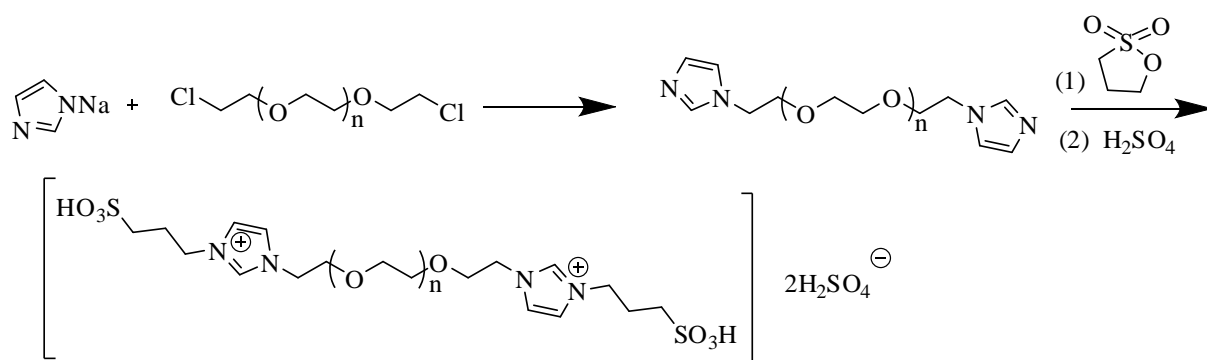


Figure 1.2: Silane modified L- proline precursor P₁ and P₂.

1.4.6 Covalent immobilization on polymers

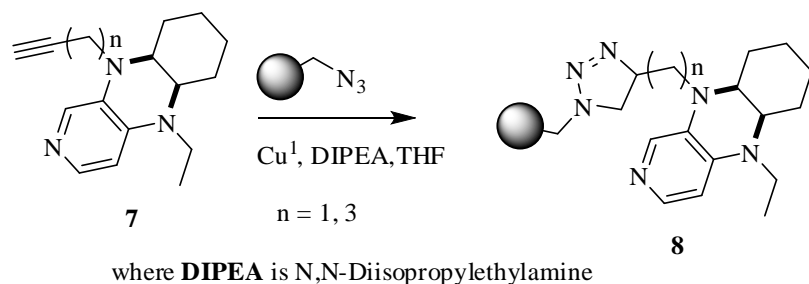
Covalent tethering can also be applied to attach organocatalysts onto polymers via the formation of covalent bonds between the catalyst and polymer. This procedure is the most popular and versatile one. It can be achieved either by grafting the catalyst onto a polymeric support that was synthesized in advance (Scheme 1.7) or by copolymerization of a modified catalyst with a suitable monomer (Scheme 1.8) The major disadvantage of covalent grafting is that the catalyst has to be modified to

insert attachable units. This modification usually increase catalyst cost by the addition of several synthetic steps. This might have detrimental effect on the catalyst performance due to new conformational preference of the modified catalyst.⁷³ Although this problem can be reduced by anchoring the catalytically active center as far away as possible from the point of attachment which invariably disturbs chiral induction. Parameters like type of the polymeric backbone of the support, spacer type and length, flexibility, and degree of catalyst loading need to be seriously considered if catalytic performance comparable to non-supported analogues are to be obtained.⁷⁴ The incredible advantage of covalent tethering is that catalyst leaching is relatively low due to the stable covalent bond formed; in addition, leached organocatalysts are not toxic pollutants. For example Luo and his research group were the first to develop a PEG₁₀₀₀-DIAL catalyst (Scheme 1.7).



Scheme 1.7: Synthetic route of PEG-DIAL.^{66a}

This catalyst exhibited a temperature-dependent phase-separation behavior in toluene and was successfully applied for a one-pot three component condensation reaction to prepare benzopyrans in excellent yields.^{66a} Valerio and co-workers have attached catalytically active pyridine units onto polystyrene support by using the copper-catalyzed Huisgen cycloaddition reaction between azides and alkynes (Scheme 1.8).



Scheme 1.8: Synthesis of immobilized pyridine organocatalysts.⁷⁵

1.4.7 Liquid-liquid biphasic immobilization

The recent development in green chemistry has been concentrated in replacing volatile organic solvents with environmentally innocuous solvents such as ionic liquids and PEGs.⁷⁶ Owing to their polar nature these solvents are widely explored in the biphasic immobilization of organocatalysts. However, catalyst leaching and contamination of product in ionic liquids coupled with their high costs are issues to be further addressed.⁴⁷ More recently intense research has been focused towards the development of temperature-dependent solvent systems that afford ease of recycling; an approach that combines features of the liquid/liquid two-phase technique with the principles of the thermoregulated phase-transfer catalysis.⁷⁷ The use of temperature-dependent solvent systems afford a greatly improved catalysis by maintaining both a high reaction rate and a good separation of catalyst and product phases.⁷⁸ Normally, a temperature-dependent solvent system consists of three liquid components; a polar, a non-polar, and a semi-polar solvents. The semi polar solvent introduced suppresses the miscibility gap of the polar and non-polar solvents such that the solvent mixture forms into one phase at high temperatures but separates into two phases at lower temperatures.⁷⁹ Chandrasekhar and co-workers successfully utilized low molecular weight polyethylene glycol (PEG Mn₄₀₀) as immobilization phase for proline catalyzed aldol reactions.⁸⁰ This system allowed the catalyst and solvent to be recycled 10 times without loss of activity. Luo and his research group recently reported a new PEG₁₀₀₀-based dicationic ionic liquid demonstrating temperature-dependent phase behavior with toluene as illustrated in (Figure 1.3) and had effectively applied it in one pot synthesis of benzopyrans.^{66a} Loh *et al.*, described an organic biphasic system containing PEG₃₃₅₀, heptane and either CH₂Cl₂ or CH₃OH. This system has been tested in the hydrogenation of 1-hexene.⁸¹

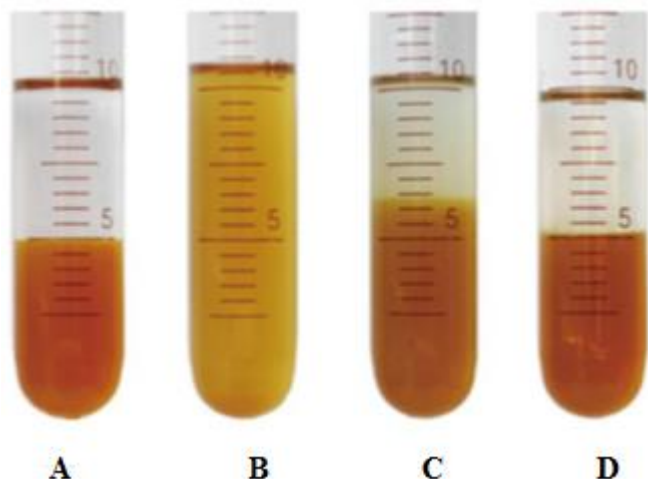


Figure 1.3: Thermoregulated behaviour of PEG₁₀₀₀-DAIL/ toluene system.⁸³

(A) Two phases at room temperature; (B) homogeneous phase at 80 °C; (C) phase separation along with cooling; (D) complete phase separation after cooling to room temperature.

1.5 Metal free transfer hydrogenation

Since the discovery of Rh and Ru catalyzed homogeneous hydrogenation of unsaturated substrates by Wilkinson and co-workers in the 1960s, a variety of other promising systems have been developed.⁸² Despite promising levels of activity and selectivity derived from the use of these metal systems, alternative hydrogenation strategies using non-transition-metal catalysts are being explored, probably due to the requirements of green chemistry or the fact that these exotic systems are very expensive and prone to poisoning.⁸³ In their quest to develop a transitional metal free catalytic system, Berkessel and co-workers described the reduction of benzophenone using KO^tBu and H₂ under stringent conditions⁸⁴ that employed high temperature (200 °C) and pressure (135 bar) hence the term forcing conditions. Stephan and coworkers introduced the concept of frustrated Lewis pair (FLP) which is a fundamental strategy of developing catalysts based on main-group elements for small-molecule activation.⁸² Nevertheless, all the efforts at achieving metal free hydrogenation utilize high temperatures and pressures and require specialized apparatus to operate hence the shift towards transfer hydrogenation. Transfer hydrogenation is a reaction process where organic molecules other than conventional molecular hydrogen are used as hydrogen donors.⁸⁵ Recent interest in this type of catalysis is driven by the fact that molecular hydrogen, a gas of low molecular weight and consequently high diffusibility, easily ignites and is substantially hazardous to handle

especially at a large scale. The use of hydrogen donors obviates these difficulties such that no gas control is necessary, no expensive pressure vessels are required, and simple solution stirring is all that is required.⁸⁶ Varma and co-workers serendipitously discovered an efficient, high yielding base catalyzed ligand free, transfer hydrogenation of carbonyl compounds, however the system required high base loading of 25%.⁸⁷ Recently Bala and co-workers reported a viable, mild and high yielding metal free imidazolium salt catalytic system for transfer hydrogenation of ketones.⁸⁸

1.6 Aims

The aim of this research is to immobilize triazolium ionic salts onto PEGs and to test their activity as recyclable organocatalysts in transfer hydrogenation of ketones.

1.7 Objectives

- To synthesize triazolium based ionic salts using the Cu(I) catalyzed cycloaddition reaction of azides and terminal alkynes.
- To determine the most active catalyst by screening the synthesized salts for catalytic activity in transfer hydrogenation of acetophenone with isopropanol as the proton source.
- To anchor the selected catalyst onto PEGs of various chain lengths and deduce the optimum chain length.
- To perform catalyst recycling studies using the immobilized catalyst under optimum conditions.

1.8 References

- (1) Liang, L.; Astruc, D. *Coord. Chem. Rev.* **2011**, 255, 2933.
- (2) Díez-González, S.; Correa, A.; Cavallo, L.; Nolan, S. P. *Eur. J. Chem.* **2006**, 12, 7558.
- (3) Bock, V. D.; Hiemstra, H.; Van Maarseveen, J. H. *Eur. J. Chem.* **2006**, 2006, 51.
- (4) Kolb, H. C.; Finn, M.; Sharpless, K. B. *Angew. Chem., Int. Ed.* **2001**, 40, 2004.
- (5) Himo, F.; Lovell, T.; Hilgraf, R.; Rostovtsev, V. V.; Noodleman, L.; Sharpless, K. B.; Fokin, V. V. *J. Am. Chem. Soc.* **2005**, 127, 210.
- (6) Rostovtsev, V. V.; Green, L. G.; Fokin, V. V.; Sharpless, K. B. *Angew. Chem., Int. Ed.* **2002**, 41, 2596.
- (7) Kolb, H. C.; Sharpless, K. B. *Drug Discovery Today* **2003**, 8, 1128.
- (8) Lutz, J.-F.; Zarafshani, Z. *Adv. Drug. Deliv. Rev.* **2008**, 60, 958.
- (9) Zhang, Q.; Su, H.; Luo, J.; Wei, Y. *Catal. Sci. Technol.* **2013**, 3, 235.
- (10) Helms, B.; Mynar, J. L.; Hawker, C. J.; Fréchet, J. M. J. *J. Am. Chem. Soc.* **2004**, 126, 15020.
- (11) Huisgen, R. *Angew. Chem. Int. Ed.* **1963**, 2, 565.
- (12) Buckley, B. R.; Dann, S. E.; Heaney, H. *Chem. Eur. J.* **2010**, 16, 6278.
- (13) Padwa, A. *Angew. Chem. Int. Ed.* **1976**, 15, 123.
- (14) Lutz, J. F. *Angew. Chem. Int. Ed.* **2008**, 47, 2182.
- (15) Tornøe, C.; Christensen, C.; Meldal, M. *Angew. Chem. Int. Ed* **2002**, 41, 2596.
- (16) Shao, C.; Wang, X.; Xu, J.; Zhao, J.; Zhang, Q.; Hu, Y. *J. Org. Chem.* **2010**, 75, 7002.
- (17) Aragão-Leoneti, V.; Campo, V. L.; Gomes, A. S.; Field, R. A.; Carvalho, I. *Tetrahedron* **2010**, 66, 9475.
- (18) (a) Liang, L.; Astruc, D. *Coord. Chem. Rev.* **2011**, 255, 2933 (b) Rostovtsev, V. V.; Green, L. G.; Fokin, V. V.; Sharpless, K. B. *Angew. Chem.* **2002**, 114, 2708.
- (19) Geng, J.; Lindqvist, J.; Mantovani, G.; Haddleton, D. M. *Angew. Chemie Int. Ed.* **2008**, 47, 4180.
- (20) (a) Tornøe, C. W.; Christensen, C.; Meldal, M. *J. Org. Chem.* **2002**, 67, 3057 (b) Sonogashira, K.; Tohda, Y.; Hagihara, N. *Tetrahedron Lett.* **1975**, 16, 4467 (c) Li, J.-H.; Li, J.-L.; Wang, D.-P.; Pi, S.-F.; Xie, Y.-X.; Zhang, M.-B.; Hu, X.-C. *J. Org. Chem.* **2007**, 72, 2053.

- (21) Meldal, M.; Tornøe, C. W. *Chem. Rev.* **2008**, *108*, 2952.
- (22) (a) Hein, J. E.; Fokin, V. V. *Chem. Soc. Rev.* **2010**, *39*, 1302 (b) Hein, J. E.; Fokin, V. V. *Chem. Soc. Rev.* **2010**, *39*, 1302.
- (23) Schindler, S. *Eur. J. Inorg. Chem.* **2000**, *2000*, 2311.
- (24) Wang, Q.; Chan, T. R.; Hilgraf, R.; Fokin, V. V.; Sharpless, K. B.; Finn, M. J. *Am. Chem. Soc.* **2003**, *125*, 3192.
- (25) Yacob, Z.; Liebscher, J. *Ionic liquids classes and properties, InTech* **2011**.
- (26) Wang, X.-j.; Sidhu, K.; Zhang, L.; Campbell, S.; Haddad, N.; Reeves, D. C.; Krishnamurthy, D.; Senanayake, C. H. *Org. Lett.* **2009**, *11*, 5490.
- (27) Tseng, M.-C.; Cheng, H.-T.; Shen, M.-J.; Chu, Y.-H. *Org. Lett.* **2011**, *13*, 4434.
- (28) Khan, S. S.; Hanelt, S.; Liebscher, J. *Arkivoc* **2009**, *12*, 1939.
- (29) Jeong, Y.; Ryu, J.-S. *J. Org. Chem.* **2010**, *75*, 4183.
- (30) Shah, J.; Khan, S. S.; Blumenthal, H.; Liebscher, J. *Synthesis* **2009**, *2009*, 3975.
- (31) Chauvin, Y.; Musmann, L.; Olivier, H. *Angew. Chem. Int Ed* **1996**, *34*, 2698.
- (32) Gu, Y.; Li, G. *Adv. Synth. Catal.* **2009**, *351*, 817.
- (33) Mathew, P.; Neels, A.; Albrecht, M. *J. Am. Chem. Soc.* **2008**, *130*, 13534.
- (34) Singh, R. P.; Verma, R. D.; Meshri, D. T.; Shreeve, J. n. M. *Angew. Chem. Int. Ed.* **2006**, *45*, 3584.
- (35) Roberts, M. *Catal. Lett.* **2000**, *67*, 1.
- (36) Averill, B.; Moulijn, J.; van Santen, R.; van Leeuwen, P. *Catal. Int. Appro* **1999**, *123* 195
- (37) Sharpless, K. B. *Adv. Synth. Catal.* **2007**, *349*, 2533.
- (38) Bailar, J. C. *Catal. Rev.* **1974**, *10*, 17.
- (39) Cole-Hamilton, D. J. *Science* **2003**, *299*, 1702.
- (40) Sheldon, R.; Downing, R. *Appl. Catal. A* **1999**, *189*, 163.
- (41) MacMillan, D. W. *Nature* **2008**, *455*, 304.
- (42) Shaikh, I. R. *J Catal.*, **2014**, *2014*.
- (43) List, B. *Chem. Rev.* **2007**, *107*, 5413.
- (44) He, R.; Shirakawa, S.; Maruoka, K. *J. Am. Chem. Soc.* **2009**, *131*, 16620.
- (45) Hong, L.; Wang, R. *Adv. Synth. Catal.* **2013**, *355*, 1023.
- (46) Itsuno, S.; Hassan, M. M. *RSC Advances* **2014**, *4*, 52023.

- (47) Zhang, L.; Luo, S.; Cheng, J.-P. *Catal. Sci. Technol.* **2011**, *1*, 507.
- (48) Leadbeater, N. E.; Marco, M. *Chem. Rev.* **2002**, *102*, 3217.
- (49) Newland, S. H.; Xuereb, D. J.; Gianotti, E.; Marchese, L.; Rios, R.; Raja, R. *Catal. Sci. Technol.* **2015**.
- (50) Krishnan, G. R.; Sreekumar, K. *Eur. J. Org. Chem.* **2008**, 2008, 4763.
- (51) (a) Font, D.; Jimeno, C.; Pericas, M. A. *Org. Lett.* **2006**, *8*, 4653 (b) Takahashi, T.; Watahiki, T.; Kitazume, S.; Yasuda, H.; Sakakura, T. *Chem. Commun.* **2006**, 1664(c) Wight, A.; Davis, M. *Chem. Rev.* **2002**, *102*, 3589.
- (52) Benaglia, M.; Cinquini, M.; Cozzi, F.; Puglisi, A.; Celentano, G. *Adv. Synth. Catal.* **2002**, *344*, 533.
- (53) Zhao, Y.-B.; Zhang, L.-W.; Wu, L.-Y.; Zhong, X.; Li, R.; Ma, J.-T. *Tetrahedron: Asymmetry* **2008**, *19*, 1352.
- (54) Zalipsky, S. *Bioconjugate Chem.* **1993**, *4*, 296.
- (55) Drago, R. S.; Pribich, D. C. *Inorg. Chem.* **1985**, *24*, 1983.
- (56) Floyd, S.; Choi, K. Y.; Taylor, T. W.; Ray, W. H. *J. Appl. Polym. Sci.* **1986**, *32*, 2935.
- (57) Kunitake, T.; Shinkai, S. *J. Am. Chem. Soc.* **1971**, *93*, 4247.
- (58) Hartley, F. R. *Supported Metal Complexes* **1985**. vol 6, 14
- (59) Knežević, Z. D.; Šiler-Marinković, S. S.; Mojović, L. V. *Acta Tech.* **2004**, 151.
- (60) Wahlgren, M.; Arnebrant, T. *Trends Biotechnol.* **1991**, *9*, 201.
- (61) McMorn, P.; Hutchings, G. J. *Chem. Soc. Rev.* **2004**, *33*, 108.
- (62) Bianchini, C.; Barbaro, P.; Dal Santo, V.; Gobetto, R.; Meli, A.; Oberhauser, W.; Psaro, R.; Vizza, F. *Adv. Synth. Catal.* **2001**, *343*, 41.
- (63) Cardoso, B.; Pires, J.; Carvalho, A. P.; Kuźniarska-Biernacka, I.; Silva, A. R.; de Castro, B.; Freire, C. *Micropor. Mesopor. Mat.* **2005**, *86*, 295.
- (64) Slagt, V. F.; Kamer, P. C. J.; van Leeuwen, P. W. N. M.; Reek, J. N. H. *J. Am. Chem. Soc.* **2004**, *126*, 1526.
- (65) J. Sabater, M.; Corma, A.; Domenech, A.; Fornes, V.; Garcia, H. *Chem Commun* **1997**, 1285.
- (66) (a) Zhi, H.; Lü, C.; Zhang, Q.; Luo, J. *Chem. Commun.* **2009**, 2878 (b) Lu, J.; Toy, P. H. *Chem. Rev.* **2009**, *109*, 815.

- (67) Zamboulis, A.; Rahier, N. J.; Gehringer, M.; Cattoën, X.; Niel, G.; Bied, C.; Moreau, J. J. E.; Man, M. W. C. *Tetrahedron: Asymmetr.* **2009**, *20*, 2880.
- (68) Yang, P.; Zhao, D.; Margolese, D. I.; Chmelka, B. F.; Stucky, G. D. *Nature* **1998**, *396*, 152.
- (69) Inagaki, S.; Guan, S.; Fukushima, Y.; Ohsuna, T.; Terasaki, O. *J. Am. Chem. Soc.* **1999**, *121*, 9611.
- (70) Beyler, C. L.; Hirschler, M. M. *SFPE handbook of fire protection engineering* **2002**, *2*.
- (71) Brunel, D.; Cauvel, A.; Fajula, F.; DiRenzo, F. *Stud. Surf. Sci. Catal.* **1995**, *97*, 173.
- (72) Song, C. E.; Lee, S.-g. *Chem. Rev.* **2002**, *102*, 3495.
- (73) Fraile, J. M.; García, J. I.; Mayoral, J. A. *Chem. Rev.* **2008**, *109*, 360.
- (74) Hodge, P. *Chem. Soc. Rev.* **1997**, *26*, 417.
- (75) D'Elia, V.; Liu, Y.; Zipse, H. *Eur. J. Org. Chem.* **2011**, *2011*, 1527.
- (76) Eastoe, J.; Gold, S.; Rogers, S. E.; Paul, A.; Welton, T.; Heenan, R. K.; Grillo, I. *J. Am. Chem. Soc.* **2005**, *127*, 7302.
- (77) Jin, Z.; Zheng, X.; Fell, B. *J. Mol. Catal. A: Chem.* **1997**, *116*, 55.
- (78) Behr, A.; Obst, D.; Turkowski, B. *J. Mol. Catal. A: Chem.* **2005**, *226*, 215.
- (79) Behr, A.; Miao, Q. *J. Mol. Catal. A: Chem.* **2004**, *222*, 127.
- (80) Chandrasekhar, S.; Narsihmulu, C.; Reddy, N. R.; Sultana, S. S. *Tetrahedron Lett.* **2004**, *45*, 4581.
- (81) da Rosa, R. G.; Martinelli, L.; da Silva, L. H.; Loh, W. *Chem. Commun.* **2000**, 33.
- (82) Mahdi, T.; del Castillo, J. N.; Stephan, D. W. *Organometallics* **2013**, *32*, 1971.
- (83) Junge, K.; Schröder, K.; Beller, M. *Chem Commun* **2011**, *47*, 4849.
- (84) Berkessel, A.; Schubert, T. J. S.; Müller, T. N. *J. Am. Chem. Soc.* **2002**, *124*, 8693.
- (85) Zheng, C.; You, S.-L. *Chem. Soc. Rev.* **2012**, *41*, 2498.
- (86) Johnstone, R. A. W.; Wilby, A. H.; Entwistle, I. D. *Chem. Rev.* **1985**, *85*, 129.
- (87) Polshettiwar, V.; Varma, R. S. *Green. Chem.* **2009**, *11*, 1313.
- (88) Ikhile, M. I.; Nyamori, V. O.; Bala, M. D. *Tetrahedron Lett.* **2012**, *53*, 4925.

Chapter two

Preparation of 1,3,4-trisubstituted-1,2,3-triazolium salts

2.1 Introduction

This chapter gives an account of the synthetic routes followed in the preparation of 1,4-disubstituted-1,2,3-triazoles. The triazolium salts were synthesized by adapting the versatile, green and regioselective Cu(I) catalysed cycloaddition reaction of organic azides and terminal alkynes. This was followed by *N*-alkylation to afford the corresponding 1,3,4-trisubstituted-1,2,3-triazolium salts. The immobilization of selected triazoles onto PEGs to yield ionic liquids is also presented. The results obtained and detailed characterization techniques employed to elucidate the structures of the compounds is also presented.

2.1.1 Materials

All chemicals and solvents were analytical grade purchased from commercial suppliers and were used without further purification. Sodium azide 95.5%, sodium ascorbate 98%, PEGs, CuBr 99.99%, phenylacetylene 98%, benzyl bromide 98%, were purchased from Sigma- Aldrich. Diethyl ether 98% and DMF 98% were purchased from Merck. Distilled water was utilized whenever the use of water was necessary. All reactions were performed under atmospheric conditions. Crystals which were used for single crystal X-ray crystallographic studies were obtained by slow evaporation of the solvent.

2.1.2 Instrumentation

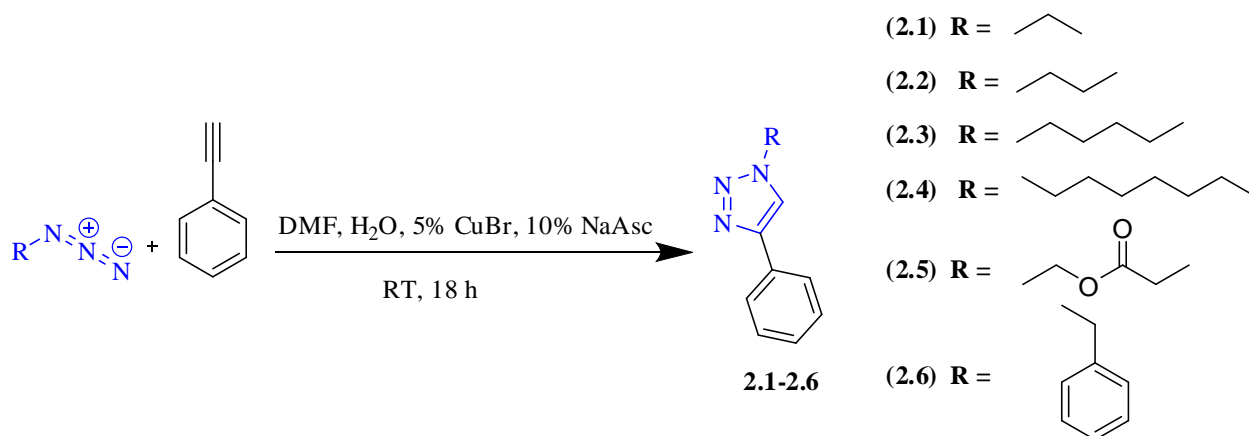
Structural elucidation of the compounds was achieved by the use of NMR spectroscopy. All NMR spectra were recorded in deuterated solvents using a Bruker Ultra-Shield™ spectrometer AVANCE^{III} operating at a frequency of 400 MHz and ambient temperature. Chemical shifts were recorded as δ values in reference to SiMe₃ at 0.00 parts per million (ppm) at 25 °C. ¹H NMR were reported as: chemical shift (δ , ppm) and referenced to the solvent peak CDCl₃ (7.26 ppm); multiplicity and number of protons are presented in parentheses. The ¹³CPD was conducted to obtain the carbon skeleton of the triazoles and was presented as: chemical shift (δ , ppm) and referenced to the solvent peak CDCl₃ (77.16 ppm) with the specific carbon indicated in the parentheses. Infrared (IR) spectroscopy was

conducted to examine the vibrational modes of the functional groups present in the triazolium salts, this further elucidated the structures of the compounds. The IR spectra were recorded on a Perkin Elmer Attenuated Total Reflectance (ATR) spectrophotometer with only the significant bands reported in cm^{-1} . A CHN Thermo Scientific Flash 2000 Elemental Analyzer was used to determine the elemental composition and the purity of the triazolium salts. Melting point was performed using a Stuart Scientific melting point apparatus, this further provided information about the purity of the salts. The mass-to-charge ratio (m/z) of the compounds was determined using a high resolution mass spectrometry to confirm the molecular masses of the salts. The mass spectrometric data were collected using a Bruker Micro TOF-Q11 with electron spray ionisation (ESI) and a sample concentration of approximately 1 ppm.

2.2 Experimental protocols

2.2.1 General procedure for the synthesis of compounds 2.1-2.6

The 1,2,3-triazoles were synthesized following a literature procedure.¹ We prepared six compounds **2.1-2.6** (scheme 2.1) that have been reported before. To a stirred solution of 1-bromoalkane (4.68 g, 28 mmol) in DMF (20 ml) was added NaN_3 (1.84 g, 1 equiv.) the mixture was stirred under reflux at 80 °C. The reaction progress was monitored by TLC for the disappearance of alkyl halide, when the reaction was complete, CuBr (0.05 equiv.), sodium ascorbate (0.1 equiv.), phenylacetylene (2.89 g, 1.0 equiv.) and 5 ml of water were added. The reaction mixture was stirred at ambient temperature for 24 hours. The resulting suspension was partitioned between aqueous $\text{NH}_4\text{OH}/\text{EDTA}$ (100 ml) and CH_2Cl_2 (100 ml) and the organic layer separated. The organic layer was washed with H_2O (100 ml) and dried over MgSO_4 and the solvent was removed under reduced pressure using rotary evaporation to give an off-white crystalline product.



Scheme 2.1: Synthesis of 1,4-disubstituted-1,2,3-triazoles.

4-phenyl-1-propyl-1H-1,2,3-triazole **2.1**²

The starting materials used were bromo propane (4.065 g, 33.0 mmol), NaN₃ (2.578 g, 39.6 mmol), and phenylacetylene (3.376 g, 33.0 mmol). White solid, 4.022 g, 65% yield, mp 42-43 °C. ¹H NMR (400 MHz, CDCl₃, ppm): δ 7.84-7.82 (t, 2H, Ar) 7.75 (s, 1H, triazole, C=CH) 7.43-7.39 (q, 2H, Ar) 7.34-7.30 (q, 1H, Ar) 4.36-4.33 (t, 2H, CH₂), 1.99-1.94 (m, 2H, CH₂) 0.99-0.96 (m, 3H, CH₃); ¹³C NMR (400 MHz, CDCl₃, ppm): δ 147.6, 130.7, 128.8, 128.0, 125.6, 119.5, 51.9, 23.7, 11.0; IR (ATR, cm⁻¹) 3134, 3045, 2965, 2874, 2732, 1669, 1608, 1579, 1482, 1461, 1436, 1355, 1218, 1181, 1075, 1050, 761, 695.

1-butyl-4-phenyl-1H-1,2,3-triazole **2.2**³

Starting materials were bromo butane (3.810 g, 27.8 mmol), NaN₃ (2.169 g, 33.4 mmol) and phenyl acetylene (2.809 g, 27.8 mmol). White solid 4.646 g, 83% yield, mp 46-47 °C. ¹H NMR (400 MHz, CDCl₃, ppm): δ 7.84-7.82 (t, 2H, Ar) 7.74 (s, 1H, triazole, C=CH) 7.44-7.40 (t, 2H, Ar) 7.34-7.30 (m, 1H, Ar) 4.41-4.38 (t, 2H, CH₂) 1.97-1.91 (m, 2H, CH₂) 1.44-1.34 (m, 2H, CH₂) 0.99-0.95 (t, 3H, CH₃); ¹³C NMR (400 MHz, CDCl₃, ppm): δ 147.7, 130.7, 128.8, 128.0, 125.6, 119.4, 50.1, 32.3, 19.7, 13.4; IR (ATR, cm⁻¹): 3118, 3090, 2955, 2871, 2451, 1950, 1809, 1675, 1608, 1579, 1484, 1464, 1438, 1216, 1078, 1050, 976, 913, 839, 761, 693, 523.

1-hexyl-4-phenyl-1H-1,2,3-triazole 2.3⁴

Starting materials were bromo hexane (2.352 g, 14.2 mmol), NaN₃ (1.111 g, 17.0 mmol) and phenyl acetylene (1.455 g, 14.2 mmol). White solid 2.549 g, 78% yield, mp 64-65 °C. ¹H NMR (400 MHz, CDCl₃, ppm): δ 7.84-7.82 (m, 2H, Ar) 7.74 (s, 1H, triazole, C=CH) 7.44-7.40 (t, 2H, Ar) 7.34-7.31 (t, 1H, Ar) 4.40-4.37 (t, 2H, CH₂) 1.98-1.90 (m, 2H, CH₂) 1.36-1.30 (m, 6H, 3x CH₂) 0.91-0.87 (m, 3H, CH₃); ¹³C NMR (400 MHz, CDCl₃, ppm): δ 147.7, 132.1, 130.7, 128.8, 128.0, 125.6, 119.4, 50.4, 31.1, 30.2, 26.1, 22.4, 13.9; IR (ATR, cm⁻¹) 3395, 2954, 1615, 1586, 1498, 1454, 1409, 1301, 1201, 1151, 1038, 760, 729, 703.

1-octyl-4-phenyl-1H-1,2,3-triazole 2.4⁵

Starting materials were bromo octane (2.224 g, 11.5 mmol), NaN₃ (0.898 g, 13.8 mmol) and phenyl acetylene (1.455 g, 14.2 mmol). White solid 2.697 g, 91% yield, mp 75-76 °C. ¹H NMR (400 MHz, CDCl₃, ppm): δ 7.84-7.82 (d, 2H, Ar) 7.75 (s, 1H, triazole, C=CH) 7.44-7.42 (t, 2H, Ar) 7.35-7.31 (t, 1H, Ar) 4.41-4.38 (t, 2H, CH₂) 1.99-1.91 (t, 2H, CH₂) 1.35-1.27 (m, 10H, 5 x CH₂) 0.89-0.86 (m, 3H, CH₃); ¹³C NMR (400 MHz, CDCl₃, ppm): δ 147.7, 130.7, 128.8, 125.6, 119.3, 50.4, 31.6, 31.4, 30.3, 29.0, 28.9, 26.5, 22.5, 14.0; IR (ATR, cm⁻¹) 3120, 3093, 3065, 2954, 2917, 2848, 2871, 1671, 1609, 1484, 1463, 1439, 1356, 1215, 1190, 1078, 1052, 976, 839, 760, 694.

ethyl 2-(4-phenyl-1H-1,2,3-triazol-1-yl)acetate 2.5⁶

Starting materials were ethyl bromo acetate (3.020 g, 18 mmol), NaN₃ (1.404 g, 21.6 mmol) and phenylacetylene (1.838 g, 18 mmol). White solid 3.471 g, 83% yield, mp 90-91 °C. ¹H NMR (400 MHz, CDCl₃, ppm): δ 7.91 (s, 1H, triazole, C=CH) 7.86-7.84 (q, 2H, Ar) 7.45-7.41 (q, 2H, Ar) 7.37-7.33 (m, 1H, Ar) 5.21 (s, 2H, CH₂) 4.32-4.27 (q, 2H, CH₂) 1.34-1.30 (t, 3H, CH₃); ¹³C NMR (400 MHz, CDCl₃, ppm): δ 166.2, 148.2, 130.3, 128.8, 128.3, 125.8, 120.8, 62.4, 50.9, 14.0; IR (ATR, cm⁻¹) 3134, 3064, 2966, 2874, 1752, 1462, 1440, 1347, 1216, 1182, 1075, 1014, 761, 693.

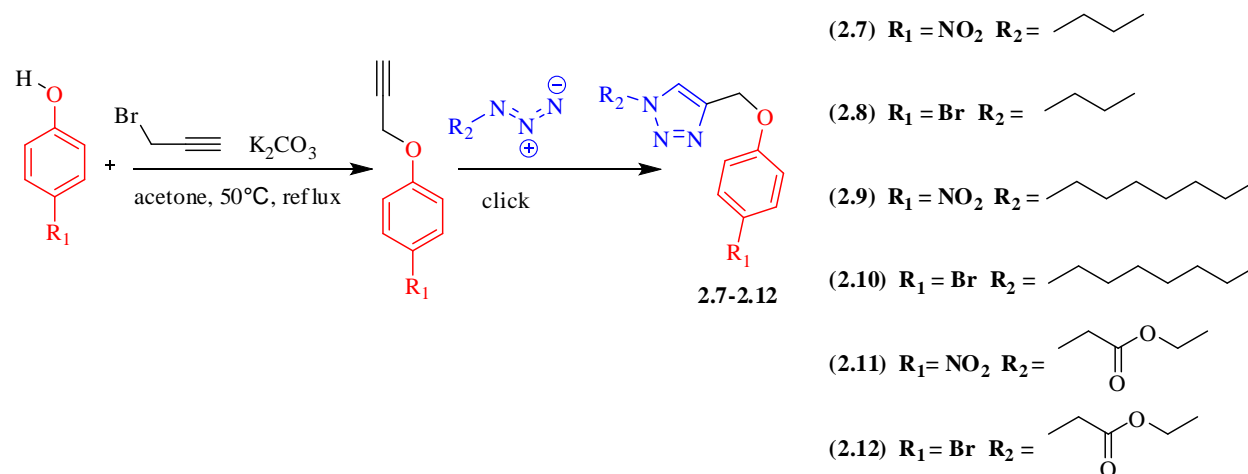
1-benzyl-4-phenyl-1H-1,2,3-triazole 2.6⁷

Starting materials were benzyl bromide (2.880 g, 16.8 mmol), NaN₃ (1.314 g, 20.2 mmol) and phenylacetylene (1.720 g, 16.8 mmol). White solid 3.33 g, 84% yield, mp 125 -126 °C. ¹H NMR (400 MHz, CDCl₃, ppm): δ 7.80-7.78 (d, 2H, Ar) 7.66 (s, 1H, triazole, C=CH) 7.41-7.26 (m, 8H,

Ar) 5.56 (s, 2H, CH₂); ¹³C NMR (400 MHz CDCl₃, ppm): δ 148.2, 134.6, 130.5, 129.1, 128.8, 128.7, 128.1, 128.0, 125.7, 119.5, 54.2; IR (ATR, cm⁻¹) 3143, 3083, 3029, 2977, 1694, 1606, 1469, 1450, 1362, 1223, 1046, 767, 728, 694.

2.2.2 General procedure for the synthesis of 1,4-disubstituted-1,2,3-triazoles 2.7-2.12

Into a 100 ml round bottomed flask was placed para nitro phenol 1.500 g, 10.8 mmol, propargyl bromide 1.28 g, 10.8 mmol, K₂CO₃ 2.99 g, 21.6 mmol and acetone 30 ml. The mixture was stirred under reflux for 18 hours. The reaction was then cooled and filtered over a pad of celite. The crude filtrate was concentrated using a vacuo and added to 1 equiv of *in situ* generated organic azide, 5% copper bromide, 10% sodium ascorbate and 5 ml of water were then added. The mixture was stirred for a further 18 hours at room temperature. The resulting suspension was partitioned between aqueous NH₄OH/EDTA (100 ml) and CH₂Cl₂ (100 ml) and the organic layer separated. The organic layer was washed with H₂O (100 ml) and dried over MgSO₄ and the solvent was removed under reduced pressure using rotary evaporation to give the triazole product.



Scheme 2.2: Synthesis of 1,4-disubstituted-1,2,3-triazoles 2.7-2.12.

1-butyl-4-((4-nitrophenoxy) methyl)-1H-1, 2, 3-triazole 2.7

Yellow crystals, 62.6% yield, mp 64-66 °C. ¹H NMR (400 MHz, CDCl₃, ppm): δ 8.22-8.20 (q, 2H, Ar) 7.63 (s, 1H, triazole, C=CH), 7.10-7.07 (m, 2H, Ar) 5.31 (s, 2H, CH₂), 4.40-4.36 (t, 2H, CH₂) 1.95-1.87 (q, 2H, CH₂) 1.42-1.32 (m, 2H, CH₂) 0.98-0.94 (t, 3H, CH₃) ¹³C NMR (400 MHz, CDCl₃, ppm): δ 163.1, 142.7, 141.9, 125.9, 122.7, 114.8, 62.5, 50.3, 32.2, 19.7, 13.4; IR (ATR, cm⁻¹): 3150, 3086, 2956, 2438, 2119, 1979, 1745, 1660, 1552, 1593, 1512, 1496, 1465; HRMS calcd for C₁₃H₁₆N₄NaO₃ 299.1120. Found 299.1114.

4-((4-bromophenoxy)methyl)-1-butyl-1H-1,2 3-triazole 2.8

White solid, 56% yield, mp 66-67 °C. ¹H NMR (400 MHz, CDCl₃, ppm): δ 7.57 (s, 1H, triazole, C=CH) 7.40-7.36 (m, 2H, Ar) 6.90-6.86 (m, 2H, Ar) 5.18 (s, 2H, CH₂) 4.38-4.34 (t, 2H, CH₂) 1.93-1.86 (m, 2H, CH₂) 1.41-1.32 (m, 2H, CH₂) 0.98-0.94 (t, 3H, CH₃) ¹³C NMR (400 MHz, CDCl₃, ppm): δ 157.3, 143.7, 132.3, 122.4, 116.6, 113.4, 62.3, 50.2, 32.2, 19.7, 13.4; IR (ATR, cm⁻¹): 3145, 3107, 3062, 2957, 2874, 2431, 1916, 1890, 1579, 1592, 1491, 1289, 1251. HRMS calcd for C₁₃H₁₆BrN₃NaO 333.0380. Found 332.0380.

4-((4-nitrophenoxy)methyl)-1-octyl-1H-1,2,3-triazole 2.9

Off white solid, 77% yield, mp 67-69 °C. ¹H NMR (400 MHz, CDCl₃, ppm): δ 8.83-8.20 (d, 2H, Ar) 7.62 (s, 1H, triazole, C=CH) 7.09-7.07 (d, 2H, Ar), 5.31 (s, 2H, Ar), 4.39-4.35 (t, 3H, CH₂), 1.94-1.90 (t, 2H, CH₂), 1.32-1.20 (m, 10H 5 x CH₂), 0.89-0.86 (t, 3H, CH₃) ¹³C NMR (400 MHz, CDCl₃, ppm): δ 163.1, 142.7, 141.9, 125.9, 122.7, 114.8, 62.5, 50.6, 31.6, 30.2, 29.0, 28.9, 26.4, 22.5, 14.0, IR (ATR, cm⁻¹): 3151, 3118, 2917, 2853, 2439, 1914, 1607, 1594, 1495, 1470, 1340; HRMS calcd for C₁₇H₂₄N₄NaO₃ 355.1746. Found 355.1739.

4-((4-bromophenoxy) methyl)-1-octyl-1H-1,2,3-triazole 2.10

Brown crystalline solid, 51.4% yield, mp 64-65 °C. ¹H NMR (400 MHz, CDCl₃, ppm): δ 7.58 (s, 1H, triazole, C=CH), 7.38-7.36 (d, 2H, Ar), 6.88-6.88 (d, 2H, Ar), 5.18 (s, 2H, CH₂), 4.36-4.33 (t, 2H, CH₂), 1.92-1.88 (t, 2H, CH₂), 1.31-1.25 (t, 10H 5 x CH₂), 0.89-0.87 (t, 3H, CH₃) ¹³C NMR (400 MHz, CDCl₃, ppm): δ 157.3, 143.7, 132.3, 122.5, 117.4, 116.1, 113.4, 62.2, 50.5, 31.6, 30.2,

28.9, 26.4, 22.5, 14.0, IR (ATR, cm^{-1}): 3135, 3101, 2923, 2853, 1871, 1644, 1592, 1578, 1489, 1469, 1283, 1236; HRMS calcd for $\text{C}_{17}\text{H}_{24}\text{BrN}_3\text{NaO}$ 388.1000. Found 388.1002.

2-(4-((4-nitrophenoxy)methyl)-1H-1,2,3-triazol-1-yl)acetate 2.11

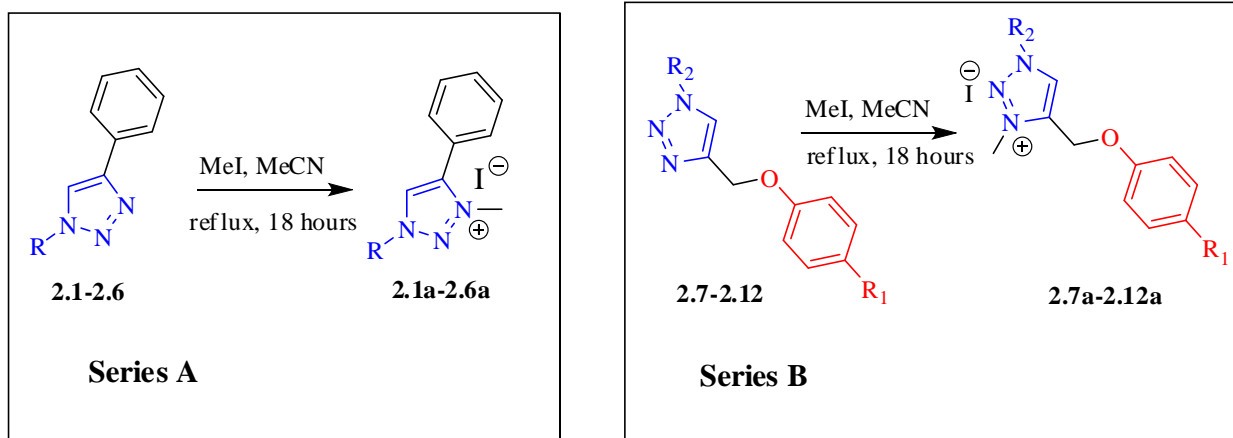
White crystalline solid, 47% yield, mp 110-112 °C. ^1H NMR (400 MHz, CDCl_3 , ppm): δ 8.22-8.20 (q, 2H, Ar) 7.81 (s, 1H, triazole, C=CH) 7.10-7.07 (q, 2H, Ar), 5.34 (s, 2H, CH_2), 5.19 (s, 2H, CH_2), 4.31-4.26 (q, 2H, CH_2), 1.33-1.29 (t, 3H, CH_3) ^{13}C NMR (400 MHz, CDCl_3 , ppm): δ 166.0, 163.0, 162.5, 143.2, 141.9, 125.8, 124.4, 115.0, 62.6, 50.9, 14.0, IR (ATR, cm^{-1}): 3462, 3263, 2996, 2907, 2451, 1935, 1738, 1607, 1592, 1521, 1343, 1243; HRMS calcd for $\text{C}_{13}\text{H}_{14}\text{N}_4\text{NaO}_5$ 329.0862. Found 329.0869.

ethyl 2-(4-((4-bromophenoxy)methyl)-1H-1,2,3-triazol-1-yl)acetate 2.12

White solid, 38% yield, mp 147-148 °C. ^1H NMR (400 MHz, CDCl_3 , ppm): δ 7.75 (s, 1H, triazole, C=CH), 7.36-7.36 (q, 2H, Ar) 6.90-6.87 (t, 2H, Ar), 5.21 (s, 2H, CH_2), 5.16 (s, 2H, CH_2), 4.30-4.25 (q, 2H, CH_2) 1.32-1.28 (t, 3H, CH_3) ^{13}C NMR (400 MHz, CDCl_3 , ppm): 166.1, 157.2, 144.3, 132.3, 124.1, 116.6, 113.5, 62.5, 62.1, 50.9, 14.0 IR (ATR, cm^{-1}): 3152, 3098, 2939, 2959, 1892, 1745, 1490, 1240; HRMS calcd for $\text{C}_{13}\text{H}_{14}\text{BrNaO}_3$ 362.0116. Found 362.0110.

2.2.3 N-alkylation of the 1,4-disubstituted-1,2,3-triazoles

N-alkylation of the 1,2,3-triazoles was achieved in a simple and straight forward protocol as depicted in Scheme 2.3. The reaction was afforded under mild conditions without the use of inert atmosphere. Alkylating reactions are usually done in polar aprotic solvents, therefore, acetonitrile was chosen as the operational solvent. In a typical procedure, 0.500 g of triazole **2.1-2.12** was added into a round bottomed flask, followed by 10 ml of acetonitrile and 1.2 equiv. of methyl iodide, the reaction was stirred under reflux at 80 °C for 18 hours. Excess methyl iodide and solvent were removed by vacuum distillation. The crude salt was then precipitated with dry ethyl acetate followed by filtration to afford triazolium salts **2.1a-2.12a** in moderate to high yields. Spectroscopic and analytical data are presented below.



Scheme 2.3: N-alkylation of triazolium salts.

3-methyl-4-phenyl-1-propyl-1H-1, 2, 3-triazol-3-ium iodide 2.1a

Pale yellow solid, 75% yield, mp 105-107 °C. ¹H NMR (400 MHz, CDCl₃, ppm): δ 9.52 (s, 1H, triazole, C=CH), 7.76-7.78 (t, 2H, Ar), 7.77-7.567 (m, 3H, Ar), 4.78-4.75 (t, 2H, CH₂) 4.34 (s, 3H NCH₃) 2.17-2.12 (q, 2H, CH₂), 1.07-1.03 (t, 3H, CH₃); ¹³C NMR (400 MHz, CDCl₃, ppm): δ 143.0, 131.9, 129.7, 129.9, 121.8, 55.9, 39.3, 23.0, 10.8; IR (ATR, cm⁻¹) 3056, 2953, 2873, 1754, 1609, 1583, 1489, 1468, 1429, 1223, 1157, 774.

1-butyl-3-methyl-4-phenyl-1H-1, 2, 3-triazol-3-ium iodide 2.2a

Pale yellow, 71% yield, mp 84-85 °C. ¹H NMR (400 MHz, CDCl₃, ppm): δ 9.52 (s, 1H, triazole, C=CH), 7.76-7.74 (t, 2H, Ar) 7.62-7.56, (m, 3H, Ar) 4.85-4.81 (t, 2H, CH₂) 4.312 (s, 3H, NCH₃) 2.13-2.06 (m, 2H, CH₂), 1.52-1.43 (m, 2H, CH₂), 1.01-0.98 (t, 3H, CH₃); ¹³C NMR (400 MHz, CDCl₃, ppm): δ 143.0, 132.0, 129.9, 129.8, 129.6, 121.7, 54.4, 39.0, 31.3 19.5, 14.2; IR (ATR, cm⁻¹) 3455, 3056, 2956, 2873, 13610, 1490, 1429, 1157, 774.

1-hexyl-3-methyl-4-phenyl-1H-1, 2, 3-triazol-3-ium iodide 2.3a

White solid, 88% yield, mp 96-98 °C. ¹H NMR (400 MHz, CDCl₃, ppm): δ 9.492 (s, 1H, triazole, C=CH), 7.788-7.758 (m, 2H, Ar) 7.626-7.546, (m, 3H, Ar) 4.82-4.78 (t, 2H, CH₂) 4.33 (s, 3H, NCH₃) 2.14-2.04 (m, 2H, CH₂), 1.45-1.40 (m, 2H, CH₂), 1.36-1.314(m, 4H, 2×CH₂), 0.91-0.87 (t,

3H, CH₃); ¹³C NMR (400 MHz, CDCl₃, ppm): δ 142.9, 132.0, 129.7, 129.7, 121.8, 54.6, 39.3, 31.0, 29.4, 25.8, 22.3, 13.9; IR (ATR, cm⁻¹) 3426, 3043, 2952, 2925, 2858, 1614, 1573, 1490, 1455, 1315, 1158, 1072, 762, 689.

3-methyl-1-octyl-4-phenyl-1H-1, 2, 3-triazol-3-ium iodide 2.4a

White solid, 87% yield, mp 98-99 °C. ¹H NMR (400 MHz, CDCl₃, ppm): δ 9.52 (s, 1H, triazole, C=CH), 7.77-7.76 (t, 2H, Ar) 7.61-7.55, (m, 3H, Ar) 4.82-4.78 (t, 2H, CH₂) 4.32 (s, 3H, NCH₃) 2.14-2.06 (m, 2H, CH₂), 1.44-1.27 (m, 10H, 5×CH₂), 0.90-0.86 (t, 3H, CH₃); ¹³C NMR (400 MHz, CDCl₃, ppm): δ 142.9, 132.0, 129.7, 121.8, 54.6, 39.2, 31.6, 29.4, 28.9, 28.8, 26.2, 22.5, 14.0; IR (ATR, cm⁻¹) 3092, 3022, 2922, 2853, 1581, 1490, 1452, 1240, 1233, 1159.

1-(2-ethoxy-2-oxoethyl)-3-methyl-4-phenyl-1H-1, 2, 3-triazol-3-ium iodide 2.5a

Pale yellow solid, 65%, yield, mp 96-98 °C. ¹H NMR (400 MHz, CDCl₃, ppm): δ 9.51 (s, 1H, triazole, C=CH), 7.72-7.70 (d, 2H, Ar) 7.63-7.57, (m, 3H, Ar) 5.94 (s, 2H, CH₂) 4.36 (s, 3H, NCH₃) 4.33-4.28 (t, 2H, CH₂), 1.38-1.35 (t, 3H, CH₃); ¹³C NMR (400 MHz, CDCl₃, ppm): δ 164.5, 142.9, 132.2, 131.4, 129.8, 129.6, 121.5, 63.5, 54.7, 39.2, 14.4; IR (ATR, cm⁻¹) 3134, 2969, 2950, 2875, 1752, 1462, 1441, 1214, 1197, 1015, 762, 693.

1-benzyl-3-methyl-4-phenyl-1H-1, 2, 3-triazol-3-ium iodide 2.6a

White solid, 96%, yield, mp 145-146 °C. ¹H NMR (400 MHz, CDCl₃, ppm): δ 9.42 (s, 1H, triazole, C=CH), 7.71-7.69 (d, 4H, Ar) 7.59-7.51, (m, 3H, Ar) 7.42-7.41, (t, 3H, Ar), 6.04 (s, 2H, CH₂), 4.316 (s, 3H, NCH₃); ¹³C NMR (400 MHz, CDCl₃, ppm): δ 143.0, 132.0, 131.2, 130.0, 129.7, 129.6, 129.4, 129.3, 128.0, 121.6, 57.5, 39.3; IR (ATR, cm⁻¹) 3459, 3098, 3064, 1747, 1614, 1583, 1310, 1153, 707, 693.

1-butyl-3-methyl-4-((4-nitrophenoxy) methyl)-1H-1, 2, 3-triazol-3-ium iodide 2.7a

Pale yellow solid, 86% yield, mp 129-130 °C. ¹H NMR (400 MHz, CDCl₃, ppm): δ 9.57 (s, 1H, triazole, C=CH), 8.18-8.16 (d, 2H, Ar) 7.27-7.24, (d, 2H, Ar) 5.87, (s, 2H, CH₂), 4.72-4.51 (t, 2H, CH₂), 4.51 (s, 3H, NCH₃), 2.10-2.02 (m, 2H, CH₂), 1.50-1.40 (m, 2H, CH₂) 1.00-0.97 (t, 3H, CH₃); ¹³C NMR (400 MHz, CDCl₃, ppm): δ 161.4, 142.6, 139.0, 131.4, 126.1, 115.4, 59.9, 54.4, 40.1,

31.2, 19.4, 13.3; IR (ATR, cm^{-1}) 3085, 2998, 2889, 1760, 1747, 1605, 1589, 1509, 1490, 1339, 1235, 1110, 1012, 997, 850; LRMS calcd for $[\text{C}_{14}\text{H}_{19}\text{N}_4\text{O}_3]^+$ 291.1457. Found 291.1405.

4-((4-bromophenoxy) methyl)-1-butyl-3-methyl-1H-1, 2, 3-triazol-3-ium iodide 2.8a

White solid, 96% yield, mp 179-181 °C. ^1H NMR (400 MHz, CDCl_3 , ppm): δ 9.54 (s, 1H, triazole, C=CH), 7.43-7.40 (d, 2H, Ar) 7.00-6.98, (d, 2H, Ar) 5.63, (s, 2H, CH_2), 4.69-4.65 (t, 2H, CH_2), 4.44 (s, 3H, NCH_3), 2.07-1.99 (m, 2H, CH_2), 1.46-1.38 (m, 2H, CH_2) 1.00-0.96 (t, 3H, CH_3); ^{13}C NMR (400 MHz, CDCl_3 , ppm): δ 155.8, 139.5, 132.8, 131.2, 116.8, 116.0, 59.4, 54.3, 39.8, 31.2, 19.4, 13.3; IR (ATR, cm^{-1}) 3084, 2987, 2889, 2185, 1759, 1582, 1487, 1367, 1231, 1158, 1021, 813; LRMS calcd for $[\text{C}_{14}\text{H}_{19}\text{BrN}_3\text{O}]^+$ 324.0711 Found 324.0726.

3-methyl-4-((4-nitrophenoxy) methyl)-1-octyl-1H-1, 2, 3-triazol-3-ium iodide 2.9a

White solid, 91% yield, mp 93-95 °C. ^1H NMR (400 MHz, CDCl_3 , ppm): δ 9.55 (s, 1H, triazole C=CH), 8.17-8.15 (d, 2H, Ar) 7.28-7.24, (d, 2H, Ar) 5.88, (s, 2H, CH_2), 4.71-4.669 (t, 2H, CH_2), 4.51 (s, 3H, NCH_3), 2.10-1.42 (m, 2H, CH_2), 1.41-1.21 (m, 10H, $2\times\text{CH}_2$) 0.89-0.85 (t, 3H, CH_3); ^{13}C NMR (400 MHz, CDCl_3 , ppm): δ 161.4, 142.6, 139.0, 131.3, 126.1, 115.4, 59.9, 54.7, 40.1, 31.6, 29.4, 28.9, 28.7, 26.1, 22.5, 14.0; (IR ATR, cm^{-1}) 3084, 3033, 2958, 2931, 2853, 1927, 1680, 1591, 1515, 1341, 1341, 1300, 1255, 855; LRMS calcd for $[\text{C}_{18}\text{H}_{27}\text{N}_4\text{O}_3]^+$ 347.2083 Found 347.2063.

4-((4-bromophenoxy) methyl)-3-methyl-1-octyl-1H-1, 2, 3-triazol-3-ium iodide 2.10a

White solid, 84% yield, mp 104-106 °C. ^1H NMR (400 MHz, CDCl_3 , ppm): δ 9.518 (s, 1H, triazole, C=CH), 7.43-7.41 (d, 2H, Ar) 7.00-6.98, (d, 2H, Ar) 5.63, (s, 2H, CH_2), 4.67-4.63 (t, 2H, CH_2), 4.44 (s, 3H, NCH_3), 2.08-2.00 (m, 2H, CH_2), 1.38-1.26 (m, 10H, $2\times\text{CH}_2$) 0.89-0.86 (t, 3H, CH_3); ^{13}C NMR (400 MHz, CDCl_3 , ppm): δ 155.7, 139.5, 132.8, 131.2, 116.8, 115.1, 59.4, 54.5, 39.8, 31.6, 29.4, 28.9, 28.7, 26.1, 22.5, 14.0; IR (ATR, cm^{-1}) 3092, 2962, 2926, 2853, 1581, 1490, 1465, 1435, 1239, 1048, 828; LRMS calcd for $[\text{C}_{18}\text{H}_{27}\text{BrN}_3\text{O}]^+$ 382.1317 Found 382.1284.

**1-(3-ethoxy-2-oxopropyl)-3-methyl-4-((4-nitrophenoxy)methyl)-1H-1,2,3-triazol-3-ium
iodide 2.11a**

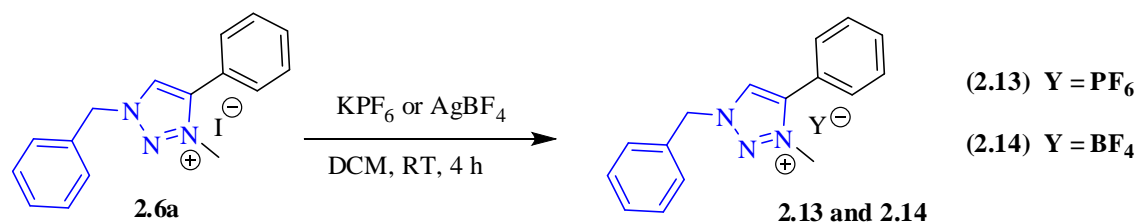
Pale yellow solid, 53% yield, mp 127-128 °C. ¹H NMR (400 MHz, CDCl₃, ppm): δ 9.58 (s, 1H, triazole C=CH), 8.24-8.22 (d, 2H, Ar) 7.22-7.20 (d, 2H, Ar) 5.80 (s, 2H, CH₂), 5.763 (s, 2H, CH₂) 4.50 (s, 3H, NCH₃), 4.35-4.29 (q, 2H, CH₂), 1.36-1.33 (t, 3H, CH₃); ¹³C NMR (400 MHz, CDCl₃, ppm): δ 164.2, 161.3, 142.8, 138.8, 133.0, 126.2, 115.2, 63.7, 59.7, 54.5, 40.1, 14.0; IR (ATR, cm⁻¹) 3453, 3041, 2975, 1919, 1749, 1911, 1590, 1511, 1339, 1224, 1109, 1011, 850; LRMS calcd for [C₁₄H₁₇N₄O₅]⁺ 321.1199 Found 321.1208.

**4-((4-bromophenoxy)methyl)-1-(2-ethoxy-2-oxoethyl)-3-methyl-1H-1,2,3-triazol-3-ium
iodide 2.12a**

White solid, 51% yield, mp 124-126 °C. ¹H NMR (400 MHz, CDCl₃, ppm): δ 9.55 (s, 1H, triazole C=CH), 7.44-7.42 (d, 2H, Ar) 6.96-6.94 (d, 2H, Ar) 5.77 (s, 2H, CH₂), 5.57 (s, 2H, CH₂) 4.45 (s, 3H, NCH₃), 4.34-4.28 (q, 2H, CH₂), 1.36-1.32 (t, 3H, CH₃); ¹³C NMR (400 MHz, CDCl₃, ppm): δ 164.2, 155.8, 139.3, 132.8, 132.7, 116.7, 63.6, 59.3, 54.5, 40.0, 14.0; IR (ATR, cm⁻¹) 3443, 3100, 2985, 2914, 2869, 1881, 1757, 1581, 1489, 1230, 1157, 1006, 815; LRMS calcd for [C₁₄H₁₇BrN₃O₃]⁺ 354.0453 Found 354.0399.

2.2.4 Typical procedure for salt metathesis of triazolium salts

Salt metathesis of **2.6a** was conducted with KPF₆ and AgBF₄ in dichloromethane at room temperature to afford **2.13** and **2.14** respectively (Scheme 2.4). In a typical procedure, 0.450 g of **2.6a** was charged into a Schleck tube followed by 2 mole equiv. of the respective source of counter anion (KPF₆ or AgBF₄) and 15 ml of dichloromethane. The mixture was stirred for four hours at room temperature to yield a brown suspension which was filtered over celite. The filtrate was concentrated in vacuo to give a solid product in high yield.



Scheme 2.4: salt metathesis of **2.6a**.

1-benzyl-3-methyl-4-phenyl-1H-1,2,3-triazol-3-ium hexafluorophosphate **2.13**

White solid, 75% yield, mp 117-119 °C. ^1H NMR (400 MHz, CDCl_3 , ppm): δ 9.22 (s, 1H, triazole) 7.69-7.65 (m, 3H, Ar), 7.58-7.53 (m, 3H, Ar), 7.44-7.42 (m, 3H, Ar), 5.987 (s, 2H, CH_2), 4.28 (s, 3H, NCH_3); ^{13}C NMR (400 MHz, CDCl_3 , ppm): 143.2, 132.0, 131.1, 130.0, 129.9, 129.7, 129.5, 129.5, 129.1, 121.7, 57.7; ^{31}P NMR (400 MHz, CDCl_3) ; δ -153.4 (m, PF_6^-); IR (ATR, cm^{-1}); 3453, 3037, 1612, 1580, 1491, 1454, 1156, 832.

1-benzyl-3-methyl-4-phenyl-1H-1,2,3-triazol-3-ium tetrafluoroborate **2.14**

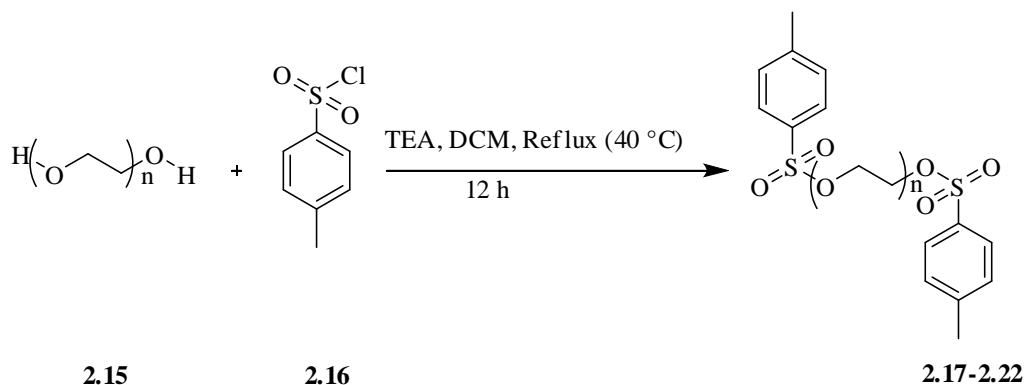
Yellow solid, 100% yield, mp 139-141 °C ^1H NMR (400 MHz, CDCl_3 , ppm): δ 9.38 (s, 1H, triazoles $\text{C}=\text{CH}$), 7.70-7.69 (m, 4H, Ar) 7.57-7.523 (m, 3H, Ar) 7.43-7.41 (m, 3H, Ar), 6.03 (s, 2H, CH_2), 4.29 (s, 3H, NCH_3); ^{13}C NMR (400 MHz, CDCl_3 , ppm): δ 143.1, 132.0, 131.2, 130.0, 129.9, 129.7, 129.6, 129.4, 129.3, 121.7, 57.6, 39.2; IR (ATR cm^{-1}) 3393, 3037, 2926, 2962, 2418, 1612, 1490, 1453, 1154, 739, 707.

2.5 Attempted immobilization of triazoles on silanes

In our initial stride towards the development of immobilized triazolium organocatalysts, click chemistry was applied to build the triazole heterocyclic ring onto 3-chloropropyltriethoxysilane. The objective was to quaternize the triazole via *N*-alkylation and later immobilize it on silica. We were successful in constructing the triazole heterocyclic ring, however our attempt to *N*-alkylate it was futile. We only generated polymeric adducts which were unreactive towards silica. We therefore shifted our focus towards the use of polymers.

2.6 General procedure for synthesis of PEG ditosylates

To a stirred mixture of polyethylene glycol PEG Mn₃₀₀, (3.000 g, 10 mmol) and p-toluenesulfonyl chloride **3.2** (3.813 g, 20 mmol) in 20 ml dichloromethane at 0°C was added triethylamine 2, 2 equiv. dropwise for 10 minutes. The reaction mixture was stirred under reflux for 12 hours, followed by cooling to ambient temperature. The reaction mixture was poured into 100 ml of water in a separation funnel. Extraction was done three times using 40 ml dichloromethane; the combined organic layers were washed with 100 ml of brine and dried over anhydrous MgSO₄. Evaporation of dichloromethane produced the PEG ditosylate as a colourless oil in high yield. The method is generic for all PEG ditosylates.



Scheme 2.5: Synthesis of PEG ditosylate.

PEG Mn₃₀₀ ditosylate 2.17

The starting materials used: p-toluenesulphonyl chloride (2.542 g, 13.3 mmol), triethylamine (1.348 g, 13.3 mmol) and polyethylene glycol Mn 300 (3.000 g, 0.01 mol). Colourless oil, 2.731g 88% yield. ¹H NMR (400 MHz, CDCl₃, ppm): δ 7.81-7.77 (q, 4H, Ar), 7.45-7.43 (d, 4H, Ar), 3.67-3.55 (m, 33H, (OCH₂CH₂)_n), 2.45 (s, 6H, 2×CH₃); ¹³C NMR (400 MHz, CDCl₃, ppm): δ 146.5, 134.4, 133.6, 131.2, 129.1, 55.1, 49.8, 49.6, 49.4, 49.2, 49.0, 48.8, 48.6, 21.8 IR; (ATR cm⁻¹): 3412, 2873, 2113, 1650, 1598, 1452, 1350, 1293, 1245.

PEG Mn₆₀₀ ditosylate 2.18

The starting materials used: p-toluenesulphonyl chloride (1.907 g, 0.01 mol), triethylamine (1.012 g, 0.01 moles) and PEG Mn₆₀₀ (3.000 g, 5 mmol). Colourless oil 4.096 g, 90% yield. ¹H NMR (400 MHz, CDCl₃, ppm): δ 7.93-7.91 (d, 1H, Ar), 7.80-7.78 (d, 3H, Ar), 7.43-7.41 (1H, d, Ar) 7.36-7.32

(3H, t, Ar) 3.72-3.58 (m, 58H, (OCH₂CH₂)_n), 2.45 (s, 6H, 2×CH₃); ¹³C NMR, (400 MHz, CDCl₃, ppm): δ 146.8, 144.7, 141.6, 132.9, 130.2, 129.8, 129.5, 127.0, 72.5, 71.3, 70.6, 70.5, 70.4, 70.2, 69.2, 68.6, 21.7, 21.6; IR (ATR cm⁻¹) 3469, 2870, 1797, 1452, 1352, 1293, 1174, 1095.

PEG Mn₁₀₀₀ ditosylate 2.19

The starting materials used: p-toluenesulphonyl chloride (1.907 g , 10.0 mmol) and triethylamine (1.012 g , 10.0 mmol) and polyethylene glycol Mn₁₀₀₀ (5.000 g, 5 mmol). Colourless oil 5.568 g, 85% yield. ¹H NMR (400 MHz, CDCl₃, ppm): δ 7.93-7.91 (d, 2H, Ar), 7.93-7.91 (d, 2H, Ar), 7.43-7.41b(2H, d, Ar) 7.36-7.33 (2H, t, Ar) 3.73-3.58 (m, 110H, (OCH₂CH₂)_n), 2.50 (s, 3H, CH₃) 2.45 (s, 3H CH₃); ¹³C NMR, (400 MHz, CDCl₃, ppm): δ 146.8, 144.7, 141.6, 132.9, 130.2, 129.7, 127.9, 126.9, 72.5, 70.6, 70.5, 70.2, 69.2, 68.6, 61.6, 53.5, 52.1, 21.7, 21.5; IR (ATR, cm⁻¹) 3392, 2928, 1615, 1498, 1451, 1301, 1151, 1041, 729, 505.

PEG Mn₂₀₀₀ ditosylate 2.20

The starting materials used: p-toluenesulphonyl chloride (0.953 g , 5 mmol), PEG Mn₂₀₀₀ (5.000 g, 2.5 mmol) triethylamine (0.506 g, 5 mmol). White solid, 5.313 g, 92% yield. ¹H NMR (400 MHz, CDCl₃, ppm): δ 7.94-7.92 (d, 2H, Ar), 7.81-7.79 (d, 2H, Ar), 7.43-7.40 (2H, d, Ar) 7.36-7.33 (2H, d, Ar) 4.17-3.58 (m, 130H, (OCH₂CH₂)_n), 2.49 (s, 3H, CH₃) 2.45 (s, 3H, CH₃); ¹³C NMR (400 MHz, CDCl₃, ppm): δ 146.8, 144.7, 141.7, 133.0, 130.2, 129.8, 127.0, 71.3, 70.7, 70.5, 69.2, 68.6, 21.8, 21.6; IR (ATR, cm⁻¹) 3700, 3085, 2965, 2876, 2364, 1954, 1621, 1239, 1161, 1155, 1004, 679.

PEG Mn₄₀₀₀ ditosylate 2.21

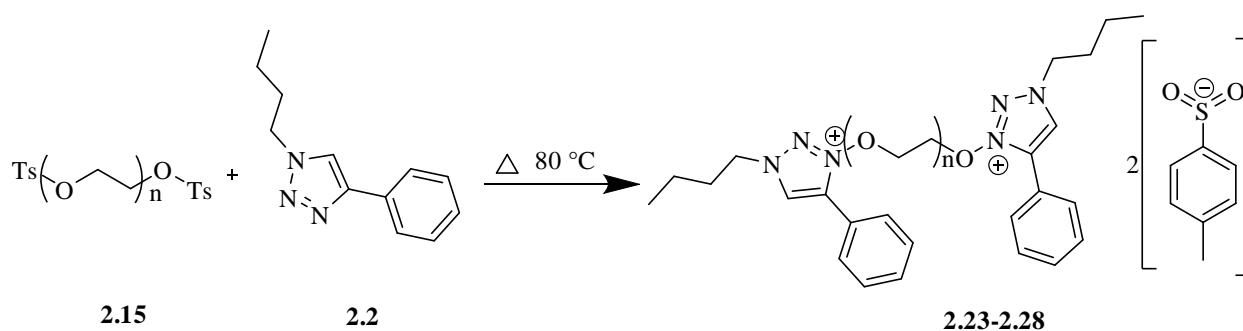
The starting materials used: p-toluenesulphonyl chloride (0.456 g , 2 mmol), PEG Mn₄₀₀₀ (4.000 g, 1 mmole) triethylamine (0.243 g , 2 mmol). White solid, 3.405 g, 79% yield. ¹H NMR (400 MHz, CDCl₃, ppm): δ 7.93-7.91 (d, 4H, Ar), 7.43-7.41 (d, 4H, Ar), (m, 78H, (OCH₂CH₂)_n), 2.49 (s, 6H, CH₃); ¹³C NMR, (400 MHz, CDCl₃, ppm): δ 146.8, 144.7, 141.6, 132.9, 130.2, 129.8, 128.6, 127.9, 127.0, 126.1, 71.3, 70.7, 70.5, 69.2, 68.6, 21.8, 21.6; IR (ATR, cm⁻¹) 3060, 3085, 2965, 2876, 2364, 1954, 1621, 1594, 1493, 1239, 1155, 679, 562.

PEG Mn₈₀₀₀ ditosylate 2.22

The starting materials used: p-toluenesulphonyl chloride (0.191 g, 1 mmol), PEG Mn₈₀₀₀ (4.000 g, 0.5 mmole) triethylamine (0.101 g, 0.5 mmol). White solid, 3.698 g, 89% yield. ¹H NMR (400 MHz, CDCl₃, ppm): δ 7.93-7.91 (d, 3H, Ar), 7.80-7.78 (d, 1H, Ar), 7.42-7.40 (3H, d, Ar) 7.35-7.33 (1H, d, Ar) 4.17-3.58 (m, 163H, (OCH₂CH₂)_n), 2.49 (s, 3H, CH₃) 2.45 (s, 3H CH₃); ¹³C NMR, (400 MHz, CDCl₃, ppm): δ 146.7, 144.7, 141.6, 133.0, 130.2, 129.8, 127.9, 70.7, 70.5, 69.2, 68.6, 21.8, 21.6; IR (ATR, cm⁻¹) 3434, 2882, 2740, 2226, 1958, 1650, 1466, 1454, 1413, 1359, 1341, 1279, 1146, 1060, 946, 841.

2.7 General procedure for the immobilization of 1-butyl-4-phenyl-1H-1,2,3-triazole onto PEGs

Our immobilization protocol involves the tosylation of PEG diols (Scheme 2.5) followed by a neat reaction between the synthesized tosylate and the triazole at moderate temperature. It is a high yielding reaction with simple work up. Illustrated in (Scheme 2.6) is the immobilization protocol. A mixture of PEG Mn₃₀₀ ditosylate 2.500 g, 4.10 mmol and 1-butyl-4-phenyl-1H-1,2,3-triazole 1.650 g, 8.20 mmole were ground using a pestle and mortar, the resulting paste was heated at 80 °C for 6 hours. The reaction mixture was cooled to ambient temperature and washed several times with ether to afford a brown oil 3.11 g, 75% yield.



2.23 = Mn 300; 2.24 = Mn 600; 2.25 = Mn 1000; 2.26 = Mn 2000; 2.27 = Mn 4000; 2.28 = Mn 8000

Scheme 2.6: Covalent immobilization of 1-butyl-4-phenyl-1H-1,2,3-triazole onto PEG.

2.23

A mixture of PEG Mn₃₀₀ ditosylate 2.500 g, 4.10 mmol and 1-butyl-4-phenyl-1H-1,2,3-triazole 1.650 g, 8.20 mmole were ground using a pestle and mortar, the resulting paste was heated at 80 °C for 6 hours. The reaction mixture was cooled to ambient temperature and washed several times with ether to afford a brown oil 3.11 g, 75% yield. ¹H NMR (400 MHz, CDCl₃, ppm): δ 8.74 (s, 1H, triazole) 7.865—7.861 (d, 2H, Ar), 7.85-7.85 (t, 2H, Ar), 7.36-7.33 (m, 3H, Ar) 7.15-7.13 (d, 2H, Ar) 4.499-4.462 (t, 2H, CH₂) 3.766-3.573(m, 16H, (OCH₂CH₂)_n), 2.33 (s, 3H, CH₃) 1.93-1.86 (m, 2H, CH₂) 1.33-1.26 (d, 2H, CH₂) 0.92-0.88 (t, 3H, CH₃); ¹³C NMR (400 MHz, CDCl₃, ppm): δ 145.0, 144.5, 142.0, 140.6, 133.1, 130.0, 129.5, 128.1, 126.9, 125.0, 124.0, 71.5, 70.9, 70.8, 70.7, 69.5 68.8, 52.7, 42.9, 31.8, 21.8, 19.6, 13.5. IR (ATR, cm⁻¹) 3702, 3085, 2966, 2876, 2399, 1953, 1621, 1594, 1493, 1371, 1239, 678, 562; HRMS: calcd for [C₁₂H₁₅N₃ + H]⁺ 202.1344 found 202.1347, 303.1945 (M⁺, n = 7), 347.2204 (M⁺, n = 8), 396.2043 (M⁺, n = 9), 440.2310 (M⁺, n = 10), 484.2572 (M⁺, n = 11), 528.2837 (M⁺, n = 12), 572.3102 (M⁺, n = 13), 620.3002 (M⁺, n = 14), 664.3262 (M⁺, n = 15), 708.3514 (M⁺, n = 16), 752.3781 (M⁺, n = 17).

2.24

A mixture of PEG Mn 600 ditosylate 3.620 g, 3.977 mmole and 1-butyl-4-phenyl-1H-1,2,3-triazole 1.601 g, 7.95 mmole were ground using pestle and mortar to form a paste. The resulting paste was heated at 80 °C for 6 hours. The reaction mixture was cooled to ambient temperature and washed several times with diethyl ether to afford a brown oil, 4.177 g, 80% yield. ¹H NMR (400 MHz, CDCl₃, ppm): δ 8.53 (s, 1H, triazole), 7.87-7.84 (q, 2H, Ar), 7.81-7.78 (q, 3H, Ar), 7.38-7.30 (m, 4H, Ar), 7.15-7.13 (d, 2H, Ar), 4.48-4.45 (t, 3H, Ar), 3.66-3.57 (m, 39H (OCH₂CH₂)_n), 1.94-1.87 (m, 2H, CH₂), 1.37-1.28 (m, 2H, CH₂), 0.937-0.90 (t, 3H, CH₃); ¹³C NMR (400 MHz, CDCl₃, ppm): 145.0, 144.8, 142.1, 140.1, 132.9, 131.6, 129.8, 128.7, 126.4, 122.7, 122.1, 72.5, 71.3, 70.6, 70.5, 70.2, 69.2, 68.6, 51.8, 42.7, 31.7, 21.6, 19.4, 13.3; IR (ATR, cm⁻¹) 3442, 2875, 1639, 1594, 1465, 1349, 1299, 1225, 1175, 1095, 768, 680.

2.25

A mixture of PEG Mn₁₀₀₀ ditosylate 3.889 g, 2.97 mmole and 1-butyl-4-phenyl-1H-1,2,3-triazole 1.195 g, 5.94 mmole were ground using a pestle and mortar to form a paste. The resulting paste was heated at 80 °C for 6 hours. The reaction mixture was cooled to ambient temperature and washed

several times with diethyl ether to afford a brown oil 4.626 g, 91% yield. ^1H NMR (400 MHz, CDCl_3 , ppm): δ 8.27 (s, 1H, triazole) 7.85-7.83 (d, 2H, Ar) 7.80-7.78 (d, 2H, Ar) 7.41-7.33 (m, 3H, Ar), 7.17-7.15 (d, 1H, Ar), 4.46-4.43 (t, 2H, CH_2), 3.66449-3.61 (m, 55H, $(\text{OCH}_2\text{CH}_2)_n$), 2.35 (s, 3H, CH_3), 1.96-1.88 (m, 2H, CH_2), 1.40-1.31 (m, 2H CH_2), 0.96-0.92 (t, 3H, CH_3); ^{13}C NMR (400 MHz, CDCl_3 , ppm): 145.0, 144.8, 144.0, 132.9, 131.6, 129.9, 129.8, 129.7, 129.6, 129.4, 129.1, 128.7, 127.9, 126.4, 126.4, 122.7, 122.1, 71.1, 70.6, 70.5, 70.2, 69.2, 68.6, 51.8, 42.7, 31.7, 21.6, 21.2, 19.4, 13.3; IR (ATR, cm^{-1}) 3080, 2876, 2421, 1955, 1621, 1594, 1466, 1239, 1008, 953, 680; HRMS: calcd for $[\text{C}_{12}\text{H}_{15}\text{N}_3 + \text{H}]^+$ 202.1344 found 202.1352, 807.4143 (M^+ , $n = 18$), 851.4143 (M^+ , $n = 19$), 895.4647 (M^+ , $n = 20$), 939.4922 (M^+ , $n = 21$), 983.5173 (M^+ , $n = 22$), 1027.454 (M^+ , $n = 23$), 1071.5713 (M^+ , $n = 24$), 1115.5974 (M^+ , $n = 25$), 1159.6223 (M^+ , $n = 26$), 1203.6493 (M^+ , $n = 2$), 1247.6821 (M^+ , $n = 28$), 1291.7068 (M^+ , $n = 29$), 1335.7328 (M^+ , $n = 30$).

2.26

A mixture of PEG Mn₂₀₀₀ ditosylate 3.623 g, 1.57 mmole and 1-butyl-4-phenyl-1H-1,2,3-triazole 0.631 g, 3.14 mmole were ground using a pestle and mortar, the resulting paste was heated at 80 °C for 6 hours. The reaction mixture was cooled to ambient temperature and washed several times with diethyl ether to afford a brown oil 3.489 g, 82% yield. ^1H NMR (400 MHz, CDCl_3 , ppm): 8.56 (s, 1H, triazole) 7.87-7.85 (m, 2H, Ar) 7.81-7.79 (d, 2H, Ar) 4.48-4.45 (t, 2H, CH_2) 3.75-3.58 (m, 83H, $(\text{OCH}_2\text{CH}_2)_n$) 2.35 (s, 1H, CH_3) 1.95-1.87 (m, 2H, CH_2) 1.36-1.30 (q, 2H, CH_2) 0.94-0.91 (t, 3H, CH_3) ^{13}C NMR (400 MHz, CDCl_3 , ppm): 144.2, 141.0, 140.7, 130.4, 130.0, 129.8, 129.6, 129.5, 129.3, 127.9, 126.7, 126.1, 124.7, 123.3, 71.3, 70.6, 70.4, 69.2, 68.6, 54.1, 52.5, 42.7, 31.5, 21.6, 21.3, 19.4, 13.3; IR (ATR, cm^{-1}) 3816, 2884, 2739, 1956, 1466, 1340, 1239, 1107, 1060, 680; HRMS calcd for $[\text{C}_{12}\text{H}_{15}\text{N}_3 + \text{H}]^+$ 202.1344 found 202.1348, 998, 5419 (M^+ , $n = 22$), 1042.5641 (M^+ , $n = 23$), 1086.5907 (M^+ , $n = 24$), 1130.6154 (M^+ , $n = 25$), 1175.6438 (M^+ , $n = 26$), 1263.7159 (M^+ , $n = 27$), 1308.7385 (M^+ , $n = 28$), 1352.7708 (M^+ , $n = 30$).

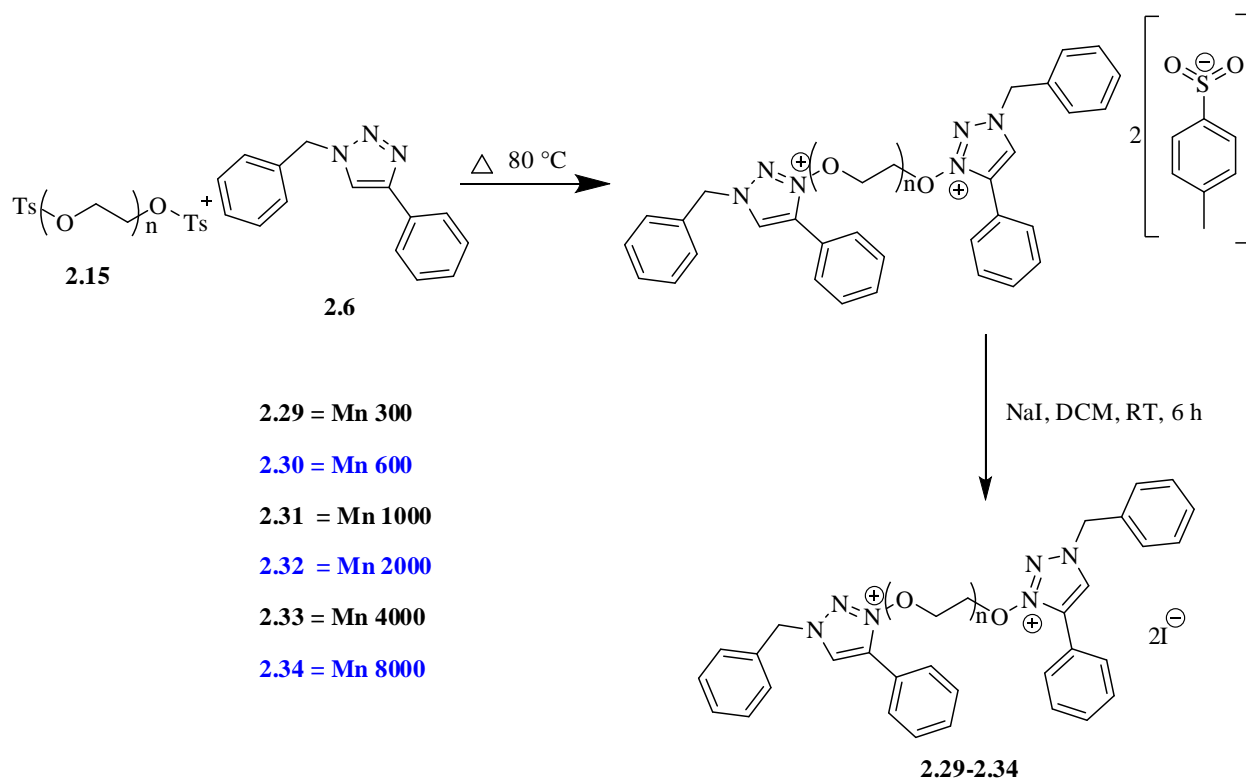
2.27

A mixture of PEG Mn₄₀₀₀ ditosylate 4.543 g, 1.05 mmole and 1-butyl-4-phenyl-1H-1,2,3-triazole 1.208g, 2.10 mmole were ground using a pestle and mortar, the resulting paste was heated at 80 °C for 6 hours. The reaction mixture was cooled to ambient temperature and washed several times with ether to afford a brown oil 4.172 g, 86% yield. ^1H NMR (400 MHz, CDCl_3 , ppm): 8.807 (s, 1H,

triazole) 7.87-7.82 (d, 2H, Ar) 7.84-7.80 (t, 2H, Ar) 7.79-7.33 (m, 4H, Ar) 7.19-7.17 (d, 2H, Ar) 4.46-4.42 (t, 2H, CH₂) 3.77-3.58 (m, 142H, (OCH₂CH₂)_n) 2.36 (s, 3H, CH₃) 1.96-1.90 (q, 2H, CH₂) 1.41-1.35 (q, 2H, CH₂) 0.98-0.95 (t, 3H, CH₃) ¹³C NMR 400 MHz, CDCl₃, ppm): 141.3, 140.5, 130.2, 129.8, 129.1, 129.0, 128.8, 127.9, 127.0, 126.1, 121.1, 71.3, 70.7, 70.6, 70.5, 69.2, 68.6, 51.2, 42.7, 31.9, 21.6, 21.3, 13.3; IR (ATR, cm⁻¹) 2882, 2740, 1962, 1466, 1340, 1107, 1060, 956; HRMS calcd for [C₁₂H₁₅N₃ + H]⁺ 202.1344 found; 202.1349, 776.4134 (M⁺, n = 17), 818.4507 (M⁺, n = 18), 864.4628 (M⁺, n = 19), 952.5233 (M⁺, n = 20), 996.5433 (M⁺, n = 21), 1040.5581 (M⁺, n = 22), 1084.5581 (M⁺, n = 23), 1128.6208 (M⁺, n = 24), 1172.6208 (M⁺, n = 25), 1216.6810 (M⁺, n = 26), 1303.7344 (M⁺, n = 28), 1348.7446 (M⁺, n = 29), 1392.7759 (M⁺, n = 30), 1437.8013 (M⁺, n = 31), 1480.8148 (M⁺, n = 32), 1524.8528 (M⁺, n = 33).

2.28

A mixture of PEG Mn₈₀₀₀ ditosylate 4.827g, 0.581 mmole and 1-butyl-4-phenyl-1H-1,2,3-triazole 0.233 g, 1.16 mmole were ground using a pestle and mortar, the resulting paste was heated at 80 °C for 6 hours. The reaction mixture was cooled to ambient temperature and washed several times with ether to afford a brown oil 4.454 g, 88% yield ¹H NMR (400 MHz, CDCl₃, ppm): 8.14 (s, 1H, triazole) 7.87-7.85 (d, 2H, Ar) 7.80-7.78 (d, 2H, Ar) 7.43-7.40 (q, 3H, Ar) 7.20-7.18 (d, 2H, Ar) 4.47-4.43 (t, 2H, CH₂) 3.77-3.58 (m, 249H, (OCH₂CH₂)_n) 2.37 (s, 1H, triazole) 1.98-1.91 (q, 2H, CH₂) 1.41-1.34 (m, 2H, CH₂) 0.99-0.95 (t, 3H, CH₃); ¹³C NMR (400 MHz, CDCl₃, ppm): 140.8, 130.2, 129.8, 129.6, 129.2, 128.8, 127.9, 127.0, 126.3, 126.2, 71.3, 70.5, 51.6, 31.8, 21.3, 19.5, 13.3; IR (ATR, cm⁻¹) 3092, 2881, 2740, 1967, 1622, 1594, 1456, 1341, 1240, 1100, 841, 682; HRMS calcd for [C₁₂H₁₅N₃ + H]⁺ 202.1344 found 202.1439, 440.2298 (M⁺, n = 10), 488.2890 (M⁺, n = 11), 529.3179 (M⁺, n = 12), 573.3418 (M⁺, n = 13), 616.3418 (M⁺, n = 14), 660.3553 (M⁺, n = 15), 748.4348 (M⁺, n = 17), 792.4382 (M⁺, n = 18), 836.4804 (M⁺, n = 19), 967.5497 (M⁺, n = 22), 1056.6064 (M⁺, n = 24), 1277.7453 (M⁺, n = 29), 1628.9402 (M⁺, n = 37).



Scheme 2.7: Covalent Immobilization of 1-benzyl-4-phenyl-1H-1,2,3-triazole onto PEG.

2.8 Typical Procedure for covalent immobilization of 1-benzyl-4-phenyl-1H-1,2,3-triazole onto PEG.

A 100 ml round bottomed flask was charged with PEG Mn₃₀₀ ditosylate (**2.15**) 2.000 g, 3.3 mmol, and 1-benzyl-4-phenyl-1H-1,2,3-triazole (**2.6**) 0.769 g, 6.6 mmol. The mixture was stirred at 80 °C for 9 hours to yield 84% of a brown oil 2.117 g. The resulting brown oil was dissolved in DCM (30 ml) followed by addition of NaI (2.5 equiv.) and stirred for 6 hours at room temperature. The reaction mixture was then filtered over a pad of celite, the filtrate was concentrated in vacuo to yield a brick red ionic liquid (**2.29**).

2.29

1-benzyl-4-phenyl-1H-1,2,3-triazole, 0.825 g, 3.51 mmol was charged into a round bottomed flask followed PEG Mn₃₀₀ ditosylate 1.074 g, 1.75 mmol. The mixture was heated for 8 hours and cooled to ambient temperature followed by the addition of dichloromethane 20 ml and sodium iodide 1.052 g, 7.02 mmol. The reaction was then stirred at room temperature for four hours followed by filtering over a pad of celite. Excess solvent was removed using a vacuo to afford a brick red ionic liquid

1.581 g, 88% yield. ^1H NMR (400 MHz, CDCl_3 , ppm): δ 8.89 (s, 1H, triazole) 7.96-7.95 (d, 2H, Ar), 7.79-7.36 (m, 6H, Ar), 5.82 (s, 2H, CH_2) 3.77-3.49 (m, 25H, $(\text{OCH}_2\text{CH}_2)_n$); ^{13}C NMR (400 MHz, CDCl_3 , ppm): 146.5, 135.9, 131.4, 130.5, 129.2, 129.1, 190.0, 128.8, 127.8, 125.1, 69.7; (ATR, cm^{-1}) 2869, 1918, 1597, 1495, 1351, 1291, 1246, 1174, 1095, 916; HRMS calcd for $[\text{C}_{15}\text{H}_{13}\text{N}_3 + \text{H}]^+$ 236.2838 found 236.1192, 331.1229 (M^+ , $n = 7$), 385.1170 (M^+ , $n = 8$), 430.1877 (M^+ , $n = 9$), 474.2156 (M^+ , $n = 10$), 518.2422 (M^+ , $n = 11$), 566.2264 (M^+ , $n = 12$), 610.2563 (M^+ , $n = 13$), 654.2843 (M^+ , $n = 14$), 698.311 (M^+ , $n = 15$), 742.3390 (M^+ , $n = 16$), 786.3654 (M^+ , $n = 17$), 870.3342 (M^+ , $n = 19$), 914.3605 (M^+ , $n = 20$).

2.30

The ionic liquid was synthesized following the general procedure with the following masses being used, 1-benzyl-4-phenyl-1H-1,2,3-triazole 0.789, 3.36 mmol, PEG Mn_{600} ditosylate 1.530 g, 1.68 mmol to yield a brick red ionic liquid 1.977 g, 89% yield. ^1H NMR (400 MHz, CDCl_3 , ppm): δ 8.42 (s, 1H, triazole) 7.88-7.88 (d, 2H, Ar), 7.88-7.31 (m, 8H, Ar), 5.70 (s, 2H, CH_2) 3.68-3.63 (m, 83H, $(\text{OCH}_2\text{CH}_2)_n$); ^{13}C NMR (400 MHz, CDCl_3 , ppm): 147.6, 137.4, 134.5, 131.8, 130.1, 130.1, 130.0, 129.9, 129.7, 129.6, 129.6, 129.4, 129.0, 128.8, 128.5, 128.3, 128.1, 125.8, 121.8, 120.3, 71.8, 71.6, 71.1, 70.369.0, 54.3; (ATR, cm^{-1}) 3439, 3015, 2871, 2503, 1902, 1615, 1349, 1209, 1094, 946, 768, 717; HRMS calcd for $[\text{C}_{15}\text{H}_{13}\text{N}_3\text{Na}]^+$ 258.1007 found 258.1059, 745.1083 (M^+ , $n = 17$), 789.1354 (M^+ , $n = 18$), 833.1626 (M^+ , $n = 19$), 1053.3004 (M^+ , $n = 24$).

2.31

Starting materials used were 1-benzyl-4-phenyl-1H-1,2,3-triazole (0.652 g, 2.77 mmol), PEG Mn_{1000} ditosylate (1.817 g, 1.30 mmol). Brick red viscous liquid, 1.864 g, 78% yield. ^1H NMR (400 MHz, $(\text{CD}_3)_2\text{SO}$, ppm): δ 8.64 (s, 1H, triazole) 7.85-7.85 (d, 2H Ar), 7.85-7.84 (d, 2H, Ar) 7.83-7.74 (m, 4H, Ar) 7.48-7.32 (m, 3H, Ar), 5.64 (s, 2H, CH_2) 3.53-3.43 (m, 51H, $(\text{OCH}_2\text{CH}_2)_n$); ^{13}C NMR (400 MHz, $(\text{CD}_3)_2\text{SO}$, ppm): 130.6, 129.7, 129.0, 128.8, 128.7, 128.1, 127.8, 125.1, 121.5, 69.7; (IR, ATR, cm^{-1}) 3469, 3061, 2868, 1963, 1635, 1456, 1348, 1297, 1249, 1091, 946, 697; HRMS calcd for $[\text{C}_{15}\text{H}_{13}\text{N}_3\text{Na}]^+$ 258.1007 found 258.1215, 557.3431 (M^+ , $n = 12$), 623.3912 (M^+ , $n = 14$), 711.6539 (M^+ , $n = 16$), 799.5116 (M^+ , $n = 18$).

2.32

Starting materials used were 1-benzyl-4-phenyl-1H-1,2,3-triazole (0.782 g, 3.33 mmol), PEG Mn₂₀₀₀ (3.84 g, 1.66 mmol). Brick red viscous liquid, 3.262 g, 72% yield. ¹H NMR (400 MHz, (CD₃)₂SO, ppm): δ 8.65 (s, 1H, triazole) 7.87-7.85 (d, 2H, Ar), 7.83-7.32 (m, 8H, Ar), 5.764 (s, 2H, CH₂) 3.56-3.46(m, 71H, (OCH₂CH₂)_n); ¹³C NMR (400 MHz, CDCl₃, ppm): 140.8, 133.0, 129.9, 129.3, 128.9, 128.7, 126.2, 126.1, 70.5; (IR, KBr, cm⁻¹) 3462, 3142, 2977, 1966, 1469, 1449, 1361, 1223, 1075, 1046, 728, 767, 694; HRMS calcd for [C₁₅H₁₃N₃Na]⁺ 258.1007 found 258.1104, 748.0179 (M⁺, n = 17).

2.33

Starting materials used were 1-benzyl-4-phenyl-1H-1,2,3-triazole (0.498 g, 2.12 mmol), PEG Mn₄₀₀₀ (2.449 g, 1.05 mmol). Brick red viscous liquid, 4.102 g, 82% yield. ¹H NMR (400 MHz, CDCl₃, ppm): δ 8.03 (s, 1H, triazole) 7.93-7.91 (m, 2H, Ar), 7.84-7.78 (m, 6H, Ar), 5.61 (s, 2H, CH₂) 3.69-3.58 (m, 161H, (OCH₂CH₂)_n); ¹³C NMR (400 MHz, CDCl₃, ppm): 130.2, 129.8, 129.2, 129.0, 128.8, 128.3, 127.9, 127.0, 126.2, 126.1, 70.5; (IR, KBr, cm⁻¹) 3440, 3143, 2977, 2872, 1607, 1469, 1450, 1362, 1224, 1076, 747, 728, 694; HRMS calcd for [C₁₅H₁₃N₃Na]⁺ 258.1007 found 258.1366, 459.1501 (M⁺, n = 10), 679.3110 (M⁺, n = 15).

2.34

Starting materials used were 1-benzyl-4-phenyl-1H-1,2,3-triazole (0.461 g, 1.96 mmol), PEG Mn₈₀₀₀ (8.149 g, 0.98 mmol). Brick red viscous liquid, 7.270 g, 85% yield. ¹H NMR (400 MHz, CDCl₃, ppm): δ 8.79 (s, 1H, triazole) 7.83-7.77 (q, 4H, Ar), 7.42-7.28 (t, 4H, Ar), 7.20-7.18 (d, 2H, Ar) 5.62 (s, 2H, CH₂), 3.77-3.58 (m, 290H, (OCH₂CH₂)_n); ¹³C NMR (400 MHz, CDCl₃, ppm): 140.8, 129.2, 129.0, 128.9, 128.3, 126.2, 126.0, 71.3, 70.5, 54.9; (IR, KBr, cm⁻¹) 3439, 3142, 3029, 2977, 1986, 1966, 1607, 1582, 1469, 1450, 1362, 1223, 1046, 767; HRMS calcd for [C₁₅H₁₃N₃Na]⁺ 258.1007 found 258.1389, 679.3200 (M⁺, n = 15).

2.9 Results and discussion

2.9.1 NMR

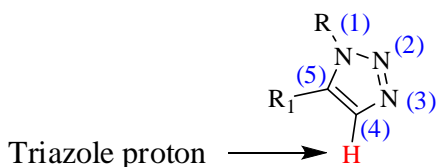


Figure 2.1: Typical triazole numbering.

The triazole numbering as described in this discussion is depicted in Figure 2.1. Well resolved ^1H NMR and ^{13}C NMR spectra were obtained for the triazoles and their corresponding salts. For instance the ^1H NMR for compound **2.1** showed strong evidence of successful triazoles synthesis where the typical triazole fingerprint proton appeared at 7.63 ppm (Figure 2.2). While its ^{13}C NMR spectrum showed a triazole C(5) resonance signal at 122.7 ppm (Figure 2.3). This is consistent with related triazoles reported in literature.⁹

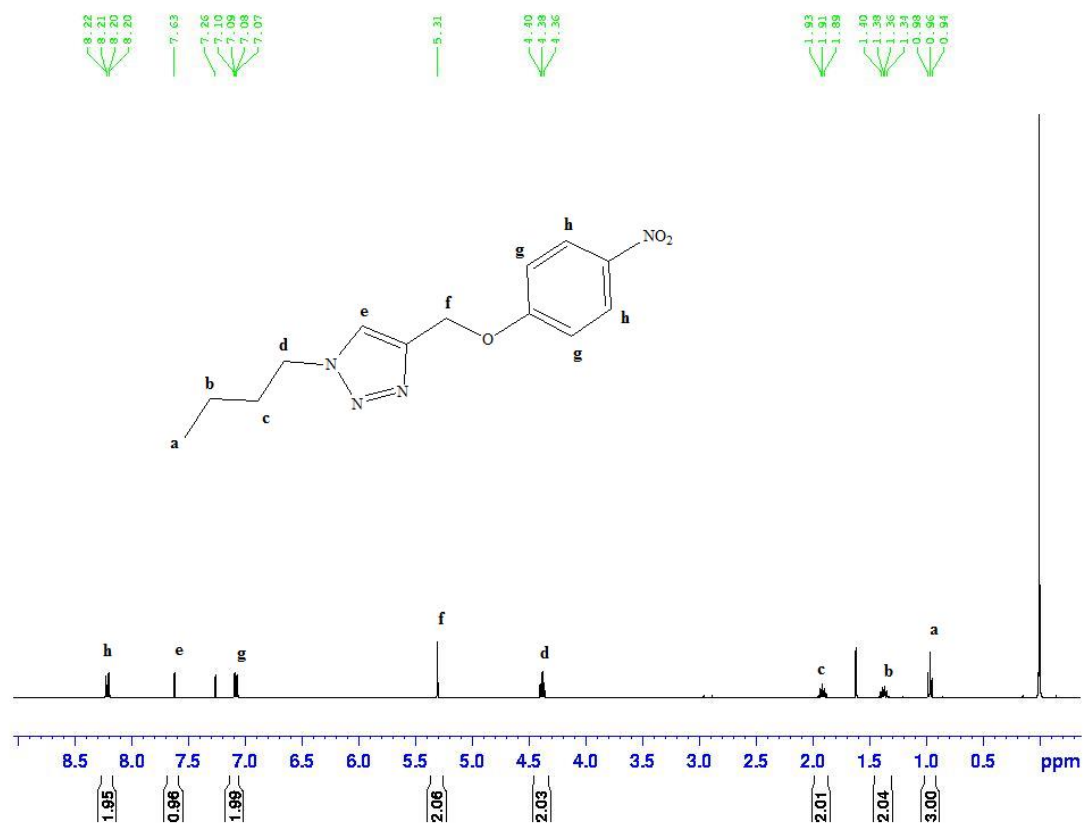


Figure 2.2: ¹H NMR spectrum of **2.7**.

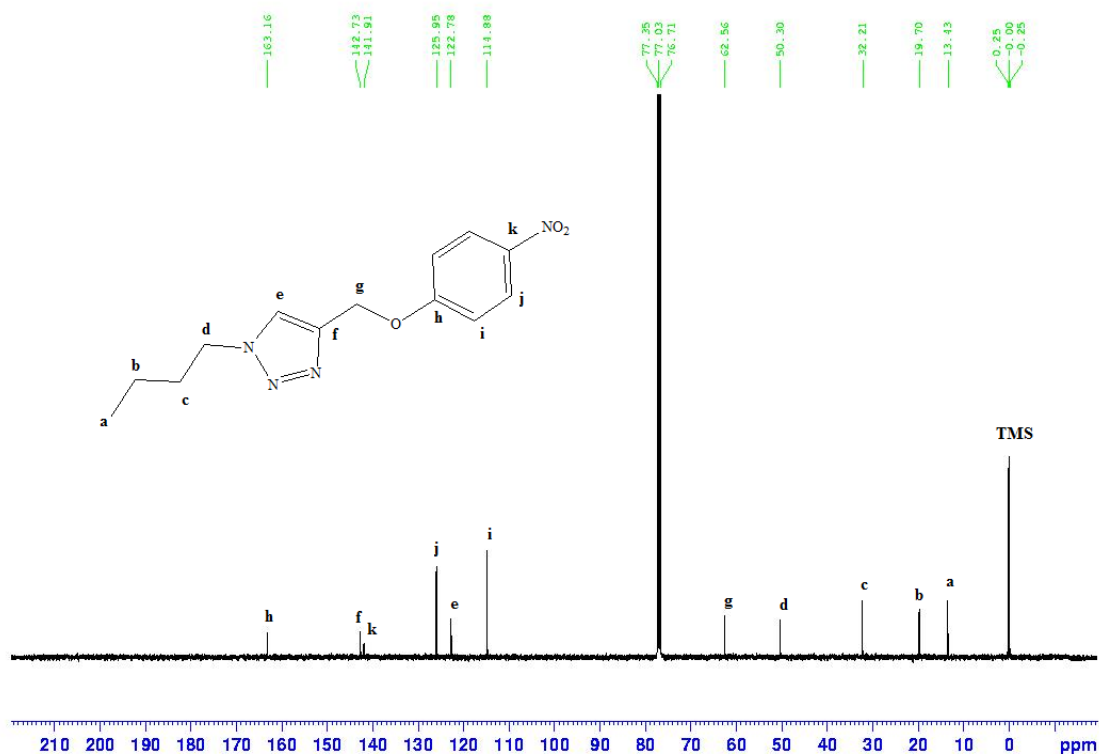


Figure 2.3: ^{13}C NMR spectrum of **2.7**.

Upon conversion of the triazole to the triazolium salt, complete methyl alkylation was evidenced by the appearance of a singlet signal at 4.51 ppm (Figure 2.4) which integrated to 3 protons of the methyl group. The downfield shift of the triazole proton to 9.57 ppm also confirmed successful *N*-alkylation. This downfield shift is attributed to the introduction of a positive charge to the heterocyclic ring upon N(3) alkylation thereby reducing the overall electron density of the ring thus effectively deshielding all the hydrogen environments.¹⁰

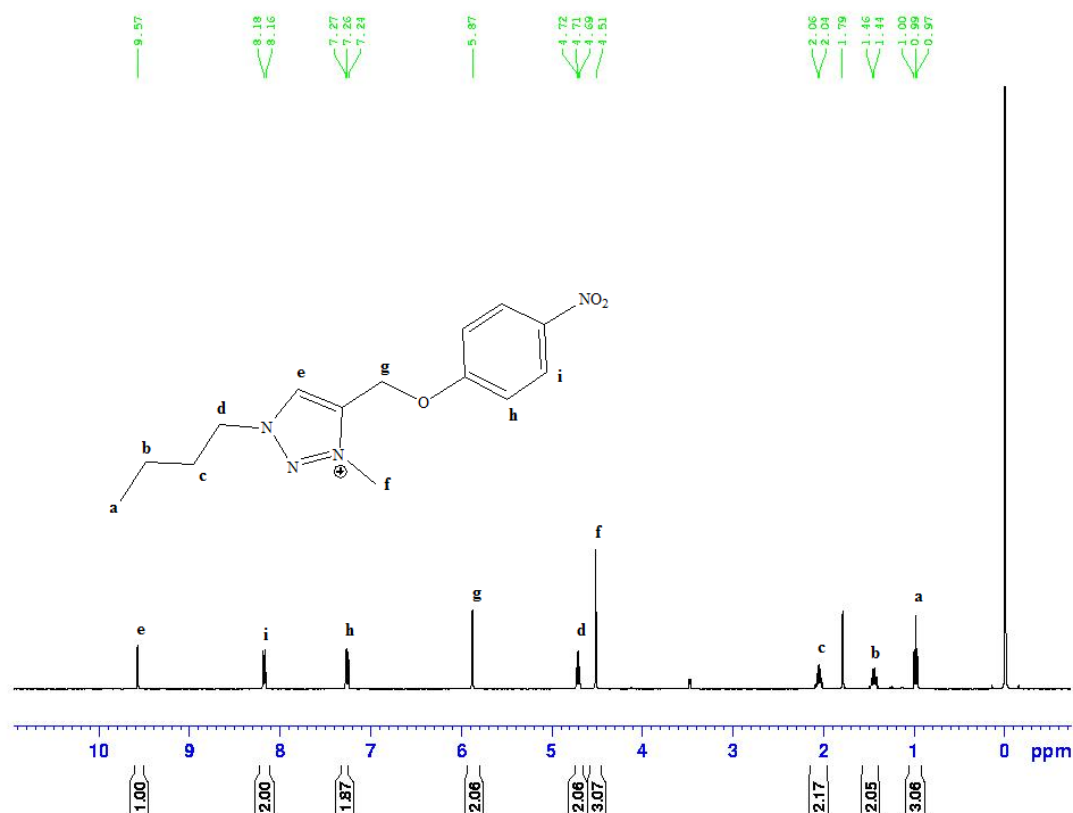


Figure 2.4: ¹H NMR spectrum of **2.7a**.

This phenomenon was also observed in the ¹³C NMR spectra of the triazolium salts. When compared to neutral triazoles, triazolium salts showed a slight downfield shift of the C₅ heterocyclic ring carbon (figure 2.5) with an average shift of 5 ppm.

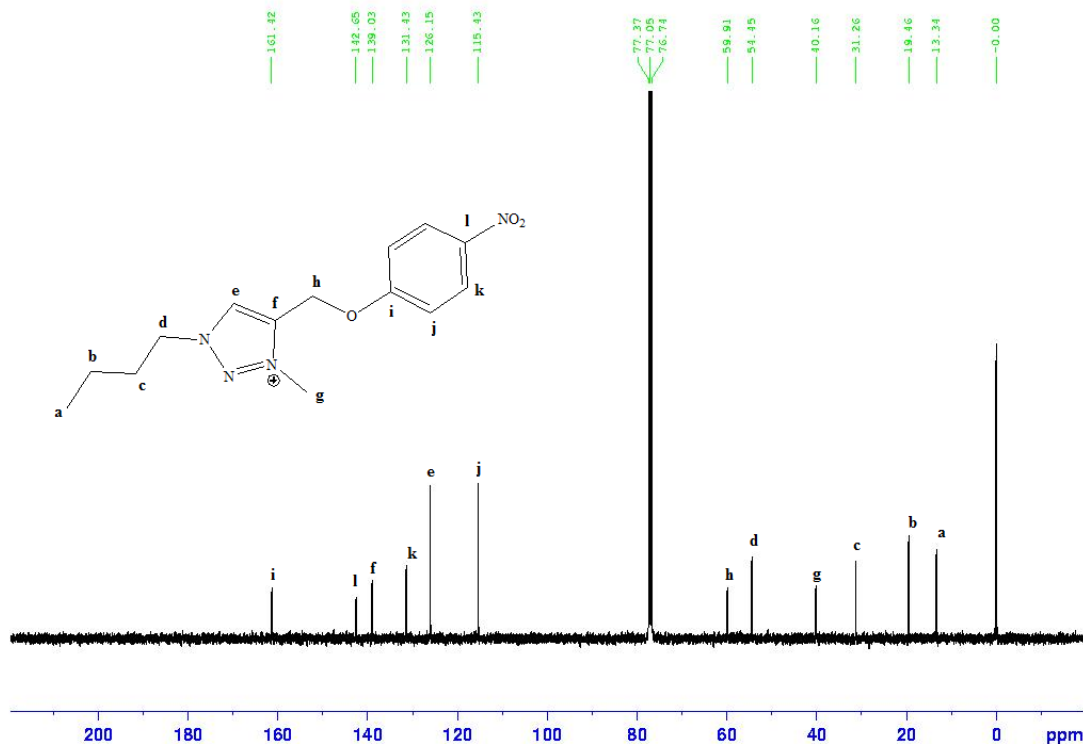


Figure 2.5: ^{13}C NMR spectrum of **2.7a**.

This is caused by the formation of cationic species bearing a formal (+) charge and has been reported before in other triazole system of related compounds.¹¹ The formation of only N(3) substituted regioisomer was confirmed by 2D ^1H - ^1H NOESY NMR analysis (Figure 2.6). Generally, NOE cross peaks are caused by cross relaxation between adjacent protons that are spatially in close proximity (approximately less than 5\AA apart)¹². The NOESY spectrum of **2.8a**, **2.10a** and **2.11a** showed NOE correlation between the methyl protons attached to N(3) and methylene protons attached to the phenoxy ring suggesting that they are in close proximity. A result that is in harmony with findings of similar compounds reported in the literature.^{10a} N(3) was alkylated in preference to N(2) because the central nitrogen atom N(2) of the 1,2,3-triazole bears less electron density than the C-bond N(3), in essence N(3) is more nucleophilic than N(2).¹³ Hence triazoles with electron withdrawing substituents gave relatively lower yields of N(3) methyl alkylated products when compared to their electron donating counter parts. This can be attributed to a decreased electron density of the

heterocyclic ring which subsequently decreases its basicity and hence the availability of a lone pair of electrons at N(3).

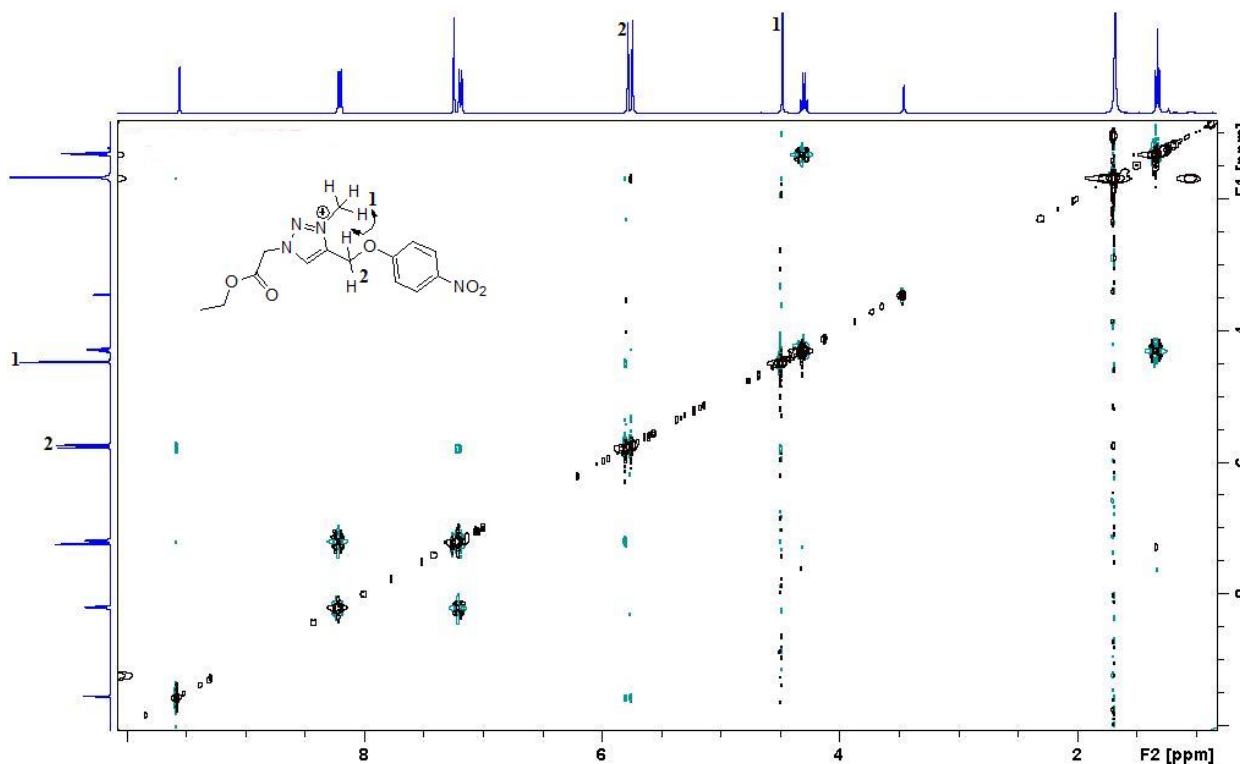


Figure 2.6: NOESY NMR spectrum of **2.11a**.

2.9.2 Tosylation of PEG diols

Traditionally, tosylated alcohol derivatives were prepared by a procedure involving the use of pyridine as both the base and solvent and the method requires over 10 equiv. of the pyridine base to prevent the formation of undesired intermediates.¹⁴ Tanabe¹⁴ *et al.*, developed a pyridine free amine catalyzed tosylation of alcohols in water, however the method suffered from hydrolysis of sulfonyl chlorides by water and requires pH adjustments. Herein a facile method for the tosylation of alcohols in refluxing dichloromethane¹⁵ was adopted. Well resolved ¹H NMR and ¹³C NMR spectra were obtained for all the synthesized tosylates. Figure 2.7 shows the ¹H NMR spectrum of PEG₃₀₀ ditosylate **2.17**. The appearance of a singlet signal at 2.45 ppm which integrated to six protons confirms the presence of two methyl groups attached to the benzene ring as constituted. The presence of the polymer backbone was confirmed by the appearance of a multiplet between 3.68-3.51 ppm.

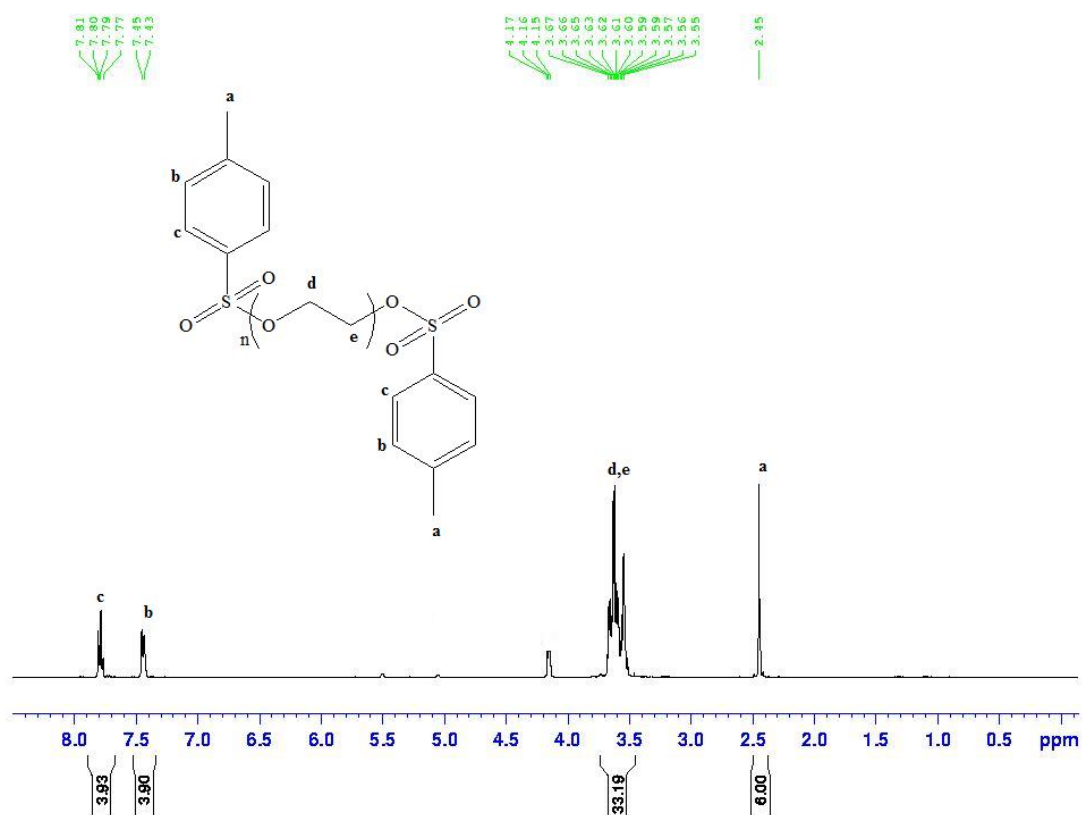


Figure 2.7: ^1H NMR spectrum of PEG₃₀₀ ditosylate **2.17**.

2.9.3 Covalent immobilization of triazoles onto PEGs

The use of PEGs as thermo-regulated organocatalyst supports was first reported by Luo⁸ using imidazole to yield ionic liquids which exhibited remarkable temperature-dependent phase behavior in toluene. In light of the advantages and disadvantages of both homogeneous and heterogeneous catalyzed reactions, we were inspired to develop a new methodology to immobilize triazolium salts on PEGs. We envisaged the possibility of combining the advantages offered by homogeneous and heterogeneous catalysis while eliminating the disadvantages of both catalytic systems. Our

protocol involves the tosylation of PEG diols followed by a neat reaction between the synthesized tosylate and the triazole at moderate temperature. It is a high yielding reaction with simple work up. The ^1H NMR analysis confirmed successful triazole immobilization onto PEGs. For example the ^1H NMR spectrum of **2.29** shows the appearance of protons from the 1,2,3-triazolium moiety as constituted. The downfield shift of the typical triazole fingerprint proton (Figure 2.8) to 8.74 ppm suggested that a formal positive charge was formed on the triazolium heterocyclic ring upon PEG immobilization.

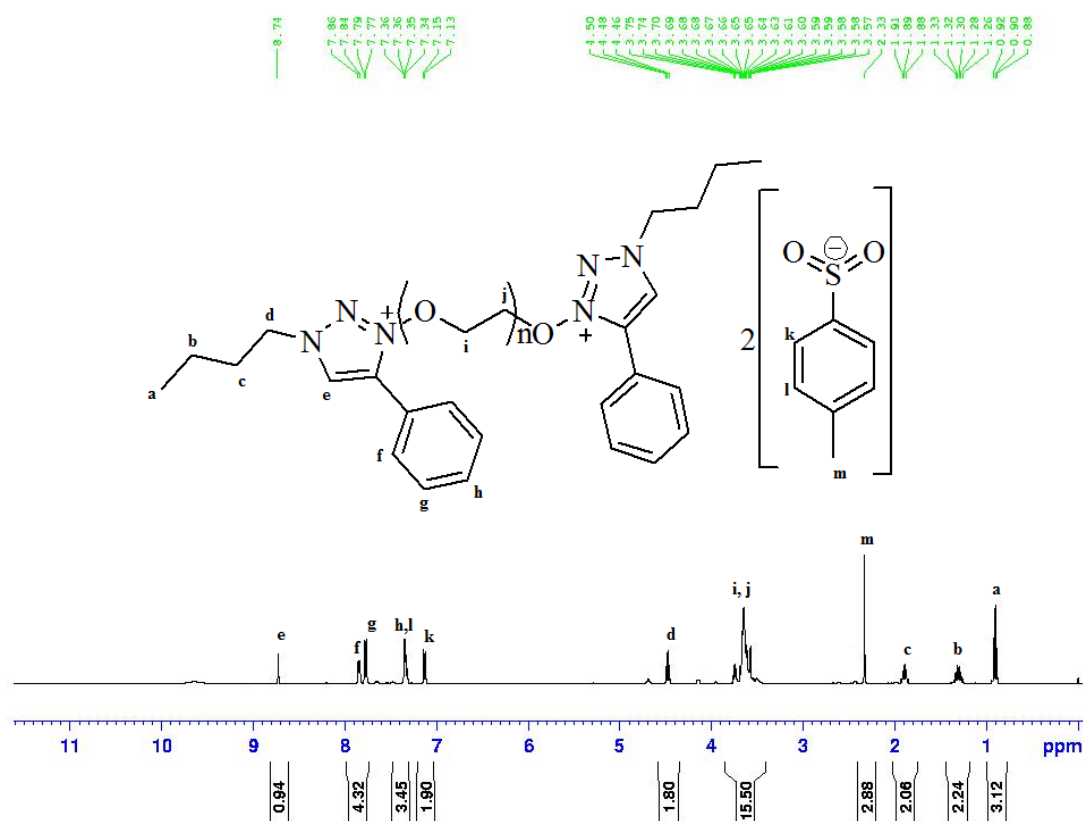


Figure 2.8: ^1H NMR spectrum of PEG₃₀₀ ditriazole **3a**.

2.10 Melting point

The melting point and range of a substance give a rough indication of the purity of that substance. The presence of impurities usually lowers the melting point and increases the melting range. The

melting point of 1,2,3-triazoles and their corresponding salts were measured. The triazolium salts retained the thermal stability of the 1,2,3-triazole derivatives.¹⁶ Unlike neutral triazoles, triazolium salts melt at higher temperatures because of the presence of oppositely charged ions (a large organic cation and a smaller inorganic anion) hence the bonding is dominantly ionic. On the other hand, simple 1,2,3-triazoles are covalently bonded thus they melt at lower temperatures. Evidence of the existence of ionic bonding in triazolium salts was shown by the melting points of salts **2.1a** and **2.4a**, one would expect the melting point of **2.4a** to be higher than that of **2.1a** because of its bigger size. Both compounds consist of the phenyl group at C(1) and an iodide counter ion. The only difference is at N(1), **2.1a** has a propyl group while **2.4a** has an octyl group, **2.1a** melts at 106 °C while **2.4a** has a melting point of 98 °C. The apparent melting point difference might be due to the influence of the electron donating octyl group which reduces the availability of the positive charge on the triazolium heterocyclic ring. This subsequently weakens the strength of the ionic bonding hence **2.4a** has a lower melting point than **2.1a** as observed. This apparent melting point difference can also be attributed to a disruption in the crystal packing of the triazolium salts as the molecular size of the alkyl chain increases.¹⁷ The observed melting points of compounds **2.6a**, **2.13**, and **2.14** is very interesting. The three compounds consist of a similar positive triazolium heterocyclic ring. The only difference is the counter ion, **2.6a** has an iodide, while **2.13** and **2.14** contain PF_6^- and BF_4^- respectively. The melting points decreased as the size of the counter ion increased (Table 2.1). This is caused by an increasing tendency at the disruption in the ability of the counter-ions to neatly pack in the lattice as the size and binding abilities of the various counter-ions vary.¹⁷

Table 2.1: Variations in mp and the triazole chemical shift of the compounds.

Compound	Mp °C	Counter ion X ⁻	¹ H NMR (ppm)
2.1	42	-	7.75
2.2	46	-	7.74
2.3	64	-	7.74
2.4	75	-	7.75
2.5	90	-	7.91
2.6	125	-	7.66

2.7	64	-	7.63
2.8	66	-	7.57
2.9	64	-	7.62
2.10	68	-	7.58
2.11	110	-	7.81
2.12	147	-	7.75
2.13	117	PF ₆	9.22
2.14	139	BF ₄	9.38
2.1a	106	I	9.52
2.2a	84	I	9.52
2.3a	96	I	9.49
2.4a	89	I	9.52
2.5a	96	I	9.51
2.6a	145	I	9.42
2.7a	129	I	9.57
2.8a	180	I	9.53
2.9a	94	I	9.55
2.10a	105	I	9.52
2.11a	127	I	9.58
2.12a	125	I	9.55

2.11 IR spectra

IR spectroscopy is one of the fastest analytical instruments available for modern scientists and virtually any sample in any state can be analyzed in a few minutes. Important IR bands observed for the triazoles corresponded to C-H stretch (3000-2850 cm⁻¹), =C-H stretch (3100-3000 cm⁻¹), C=C

stretch ($1680\text{--}1640\text{ cm}^{-1}$) and C=O stretch ($1750\text{--}1735\text{ cm}^{-1}$). Absorption band at $1254\text{--}1131\text{ cm}^{-1}$ were assigned to N=N of the 1,2,3-triazoles.¹⁸ Figure 2.7 is an illustration of the IR spectrum of **2.7**.

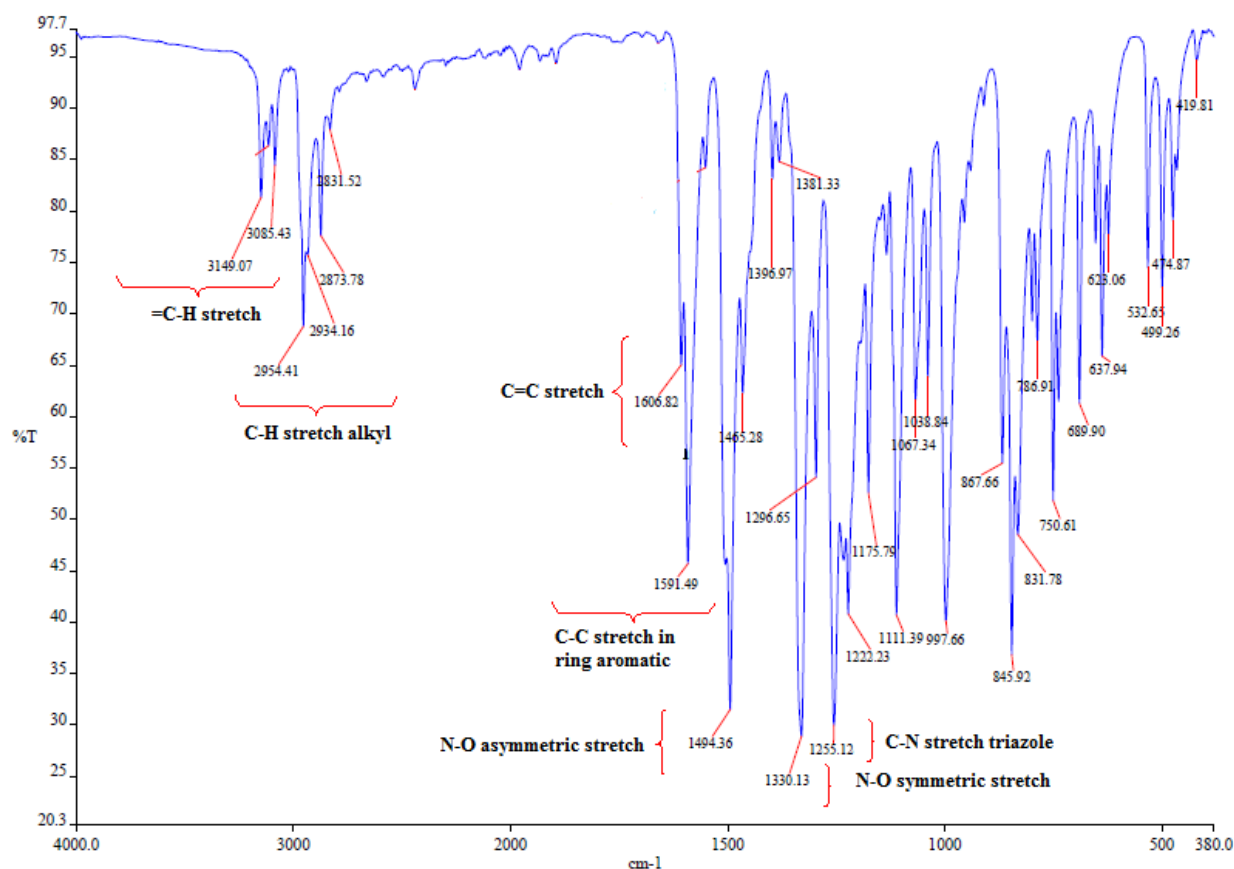


Figure 2.9: IR spectrum of **2.7**.

2.12 Mass spectrometry

The MS results further confirmed successful synthesis of the triazolium compounds, the observed molecular ion peaks were comparable to the calculated molecular formulae. Tables 2.2 and 2.3 show sets of the MS results obtained for the triazoles and the corresponding triazolium salts.

Table 2.2: Values of m/z ratios obtained for the triazoles.

Compound	$[M + Na]^+$ Found	Calculated
2.7	299.1114	299.1120
2.8	332.0380	332.0374

2.9	355.1739	355.1746
2.10	388.1000	388.1002
2.11	329.0869	329.0862
2.12	362.0110	362.0116

Table 2.3: Values of m/z ratios obtained for the triazolium salts.

Compound	[M - I] ⁺ Found	Calculated
2.7a	291.1405	291.1457
2.8a	324.0726	324.0727
2.9a	347.2063	347.2083
2.10a	382.1284	382.1317
2.11a	321.1208	321.1199
2.12a	354.0399	354.0453

The calculated m/z values correlated well with the observed m/z values for all the compounds. The fragmentation patterns showed peaks at [M]⁺ (100% abundance) and [M+1]⁺ (1.1% abundance) which is attributed to ¹²C and ¹³C isotopes respectively. As constituted, the MS of triazoles **2.8**, **2.10** and **2.12** and their corresponding triazolium salts **2.8a**, **2.10a** and **2.12a** showed the presence of the bromide substituent. Bromine has two isotopes, ⁷⁹Br and ⁸¹Br in approximately 1:1 abundance ratio, compounds containing one bromine atom will show two peaks in the molecular ion region, depending on which bromine isotope the molecular ion contains.¹⁹ The ⁷⁹Br isotope shows a base peak at [M]⁺ (Figure 2.8) whereas that of ⁸¹Br appears at [M + 2]⁺ as observed in figure 2.8.

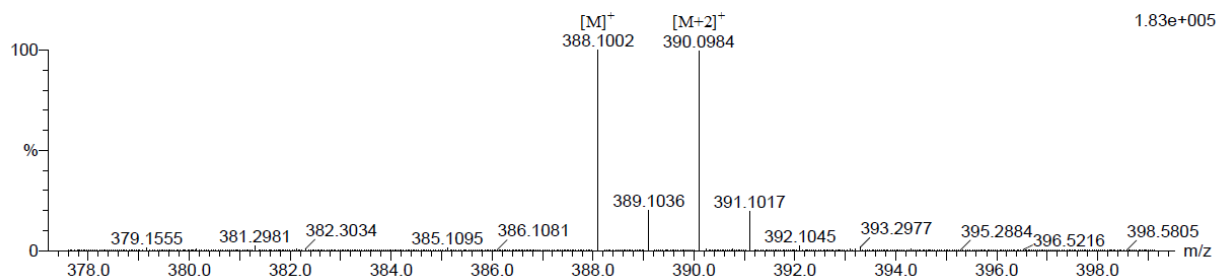


Figure 2.10: Mass spectrum of 2.10.

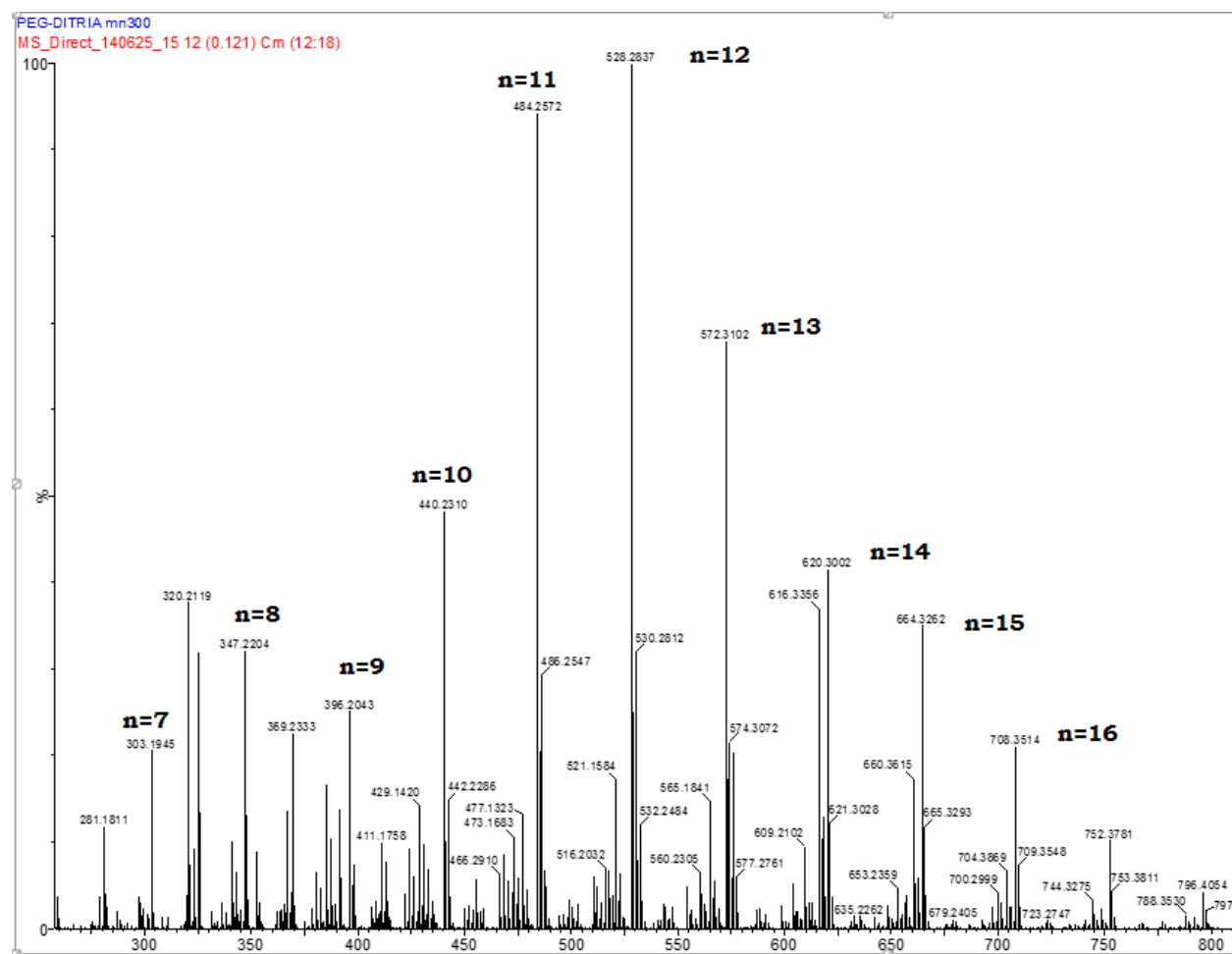


Figure 2.11: Mass spectrum of 2.29

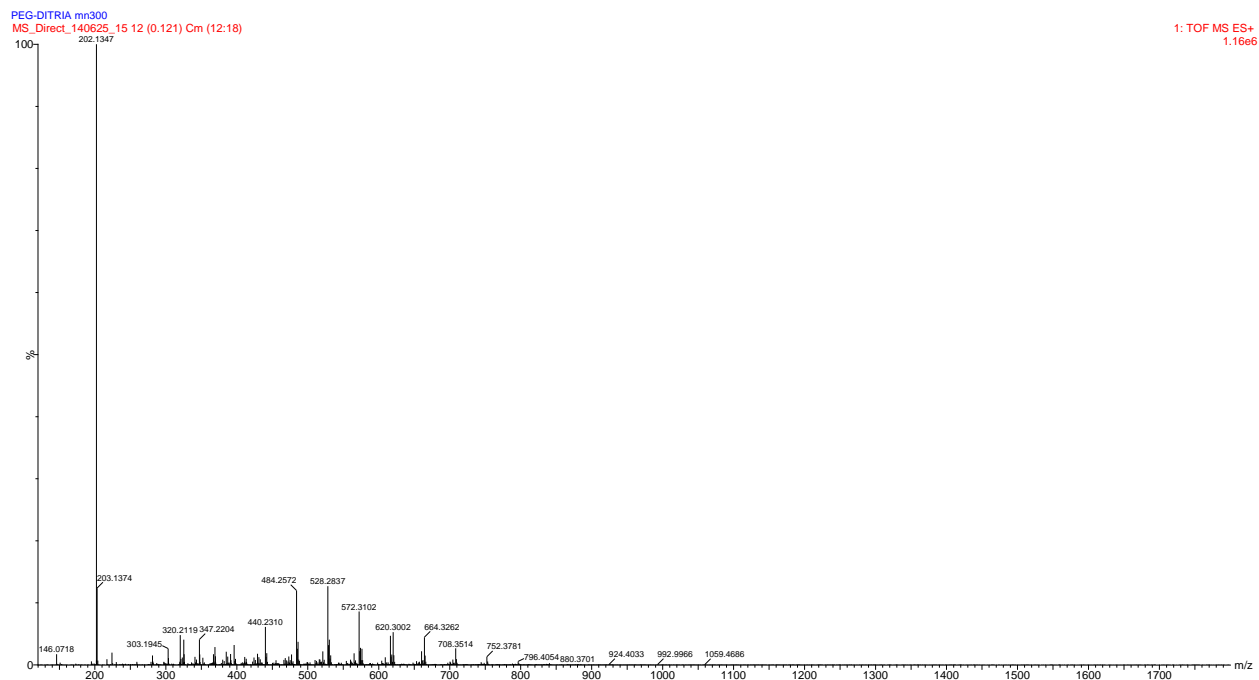


Figure 2.12: Mass spectrum of **2.29**

The Mass spectrum of **2.29** (Figures 2.11 and 2.12) additionally confirmed the successful triazole immobilization onto PEG. The fragmentation pattern shows the molecular weight of the triazolium moiety (202.1347, MH^+) and the PEG backbone. The fragmentation pattern of the PEG backbone shows molecular weights of different oligomeric units separated by the mass of the repeating unit as identified in Figure 2.11.

2.13 Elemental analysis (EA)

Elemental analysis (EA) on carbon, hydrogen and nitrogen CHN is a powerful technique used to determine the bulk purity of a compound. The obtained micro analysis results of the triazoles and their corresponding salts correlated well with theoretical values (Table 2.3) which further reaffirmed the successful synthesis of the compounds.

Table 2.4: CHN elemental analyses results for the triazoles and triazolium salts.

Compound	Mass fraction C%	Mass fraction N%	Mass fraction H%
	Found (Calculated)	Found (Calculated)	Found (Calculated)
2.7	56.80 (56.51)	21.51 (20.28)	5.04 (5.84)
2.8	50.47 (50.34)	14.23 (13.55)	4.80 (5.20)
2.9	60.93 (61.43)	18.16 (16.86)	6.38 (7.28)
2.10	56.00 (55.74)	11.48 (11.47)	6.13 (6.60)
2.11	50.98 (52.58)	18.34 (18.29)	4.61 (4.28)
2.12	47.20 (45.90)	12.96 (12.35)	3.99 (4.15)
2.7a	39.91 (40.21)	13.22 (13.40)	4.53 (4.8)
2.8a	36.72 (37.19)	9.17 (9.29)	4.18 (4.24)
2.9a	44.98 (45.58)	11.69 (11.81)	5.66 (5.74)
2.10a	42.43 (42.54)	8.26 (8.27)	5.40 (5.35)
2.11a	34.930 (37.56)	11.82 (12.50)	3.53 (3.82)
2.12a	34.34 (34.88)	8.59 (8.72)	3.44 (3.55)

2.14 Single crystal X-ray diffraction studies

To unambiguously elucidate the atom connectivity in selected triazoles and their corresponding salts, single crystal X-ray data of **2.7**, **2.11**, **2.8a**, and **2.12a** were collected and analyzed. The single crystals were grown by slow diffusion of hexane into a concentrated solution of the respective compound in CH₂Cl₂. The solid state structure of compounds **2.7** and **2.11** shows the presence of two molecules in the asymmetric unit cell (Figures 2.9 and 2.11). Compounds **2.7** and **2.11** crystalizes in the triclinic crystal system with P-1 space group. The crystal structures are consistent with other experimental data obtained. Selected bond lengths and angles are listed in Table 2.6. The atom numbering is depicted in Figures 2.5-2.8 respectively. The crystal packing consist of periodically alternating triazole layers aligned parallel to each other. The formation of 3-methyl-1,2,3-triazolium cation by

N-alkylation of the N(3) atom resulted in minimal changes in the triazole ring geometry. The cationic rings are mutually oriented parallel to each other. When compared to neutral triazoles, triazolium salts showed only slight shortening of the N(3)-N(2), N(2)-N(1), N(3)-C(6), N(1)-C(5), bond distances (Table 2.6). This is caused by the delocalization of the positive charge in the triazolium heterocyclic ring. A result that is in agreement to related heterocyclic ring systems reported in literature.²⁰ The triazolium salts **2.8a** and **2.12a** belong to the monoclinic crystal system, space group C2/c and triclinic crystal system, space group P-1 respectively. In **2.8a** there are two molecules in the asymmetric unit cell (Figure 2.14) aligned parallel to each other while **2.12a** has eight molecules in its asymmetric unit cell (Figure 2.16). Interestingly, the solid state structures of **2.8a** and **2.12a** shows the presence of halogen bond contacts (Figure 2.17) with bond angles of 180° and bond length of 3.735Å and 3.692Å respectively. Halogen bonding is a non-covalent interaction that occurs when there is net attractive forces between a positively polarized halogen atom, frequently bromine or iodine, with a Lewis base.²¹

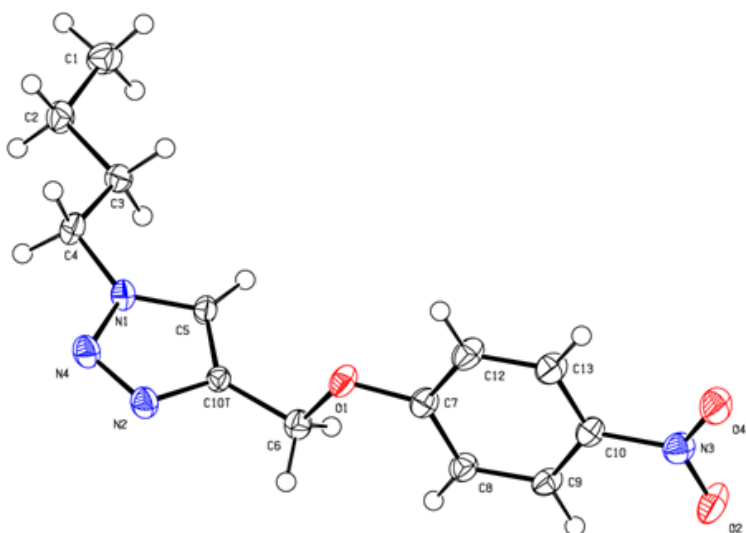


Figure 2.13: ORTEP representation of the structure of **2.7** with the displacement ellipsoids drawn at the 50% probability level.

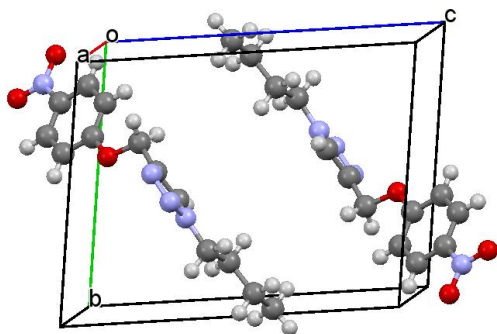


Figure 2.14: Crystal packing of **2.7**.

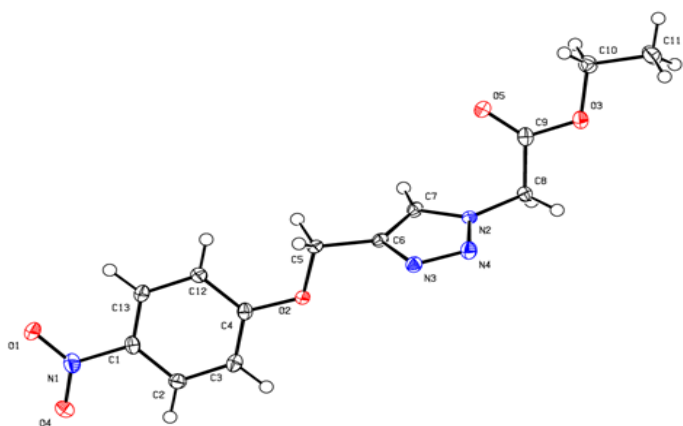


Figure 2.15: ORTEP representation of the structure of **2.11** with the displacement ellipsoids drawn at the 50% probability level.

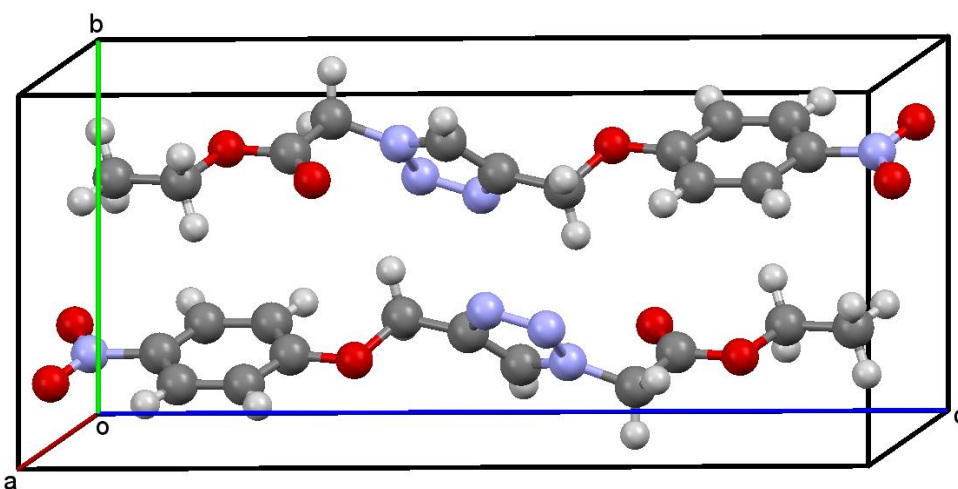


Figure 2.16: Crystal Packing of **2.11**.

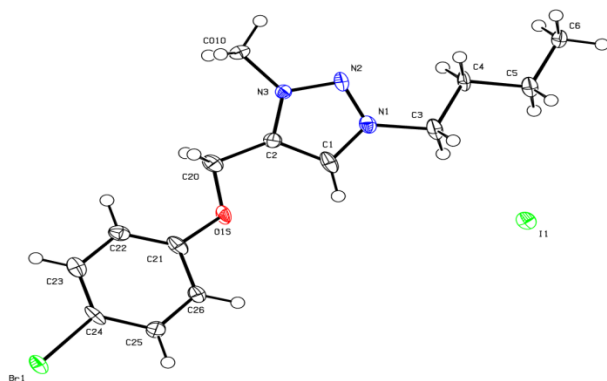


Figure 2.17: ORTEP representations of the structure of **2.8a** with the displacement ellipsoids drawn at the 50% probability level.

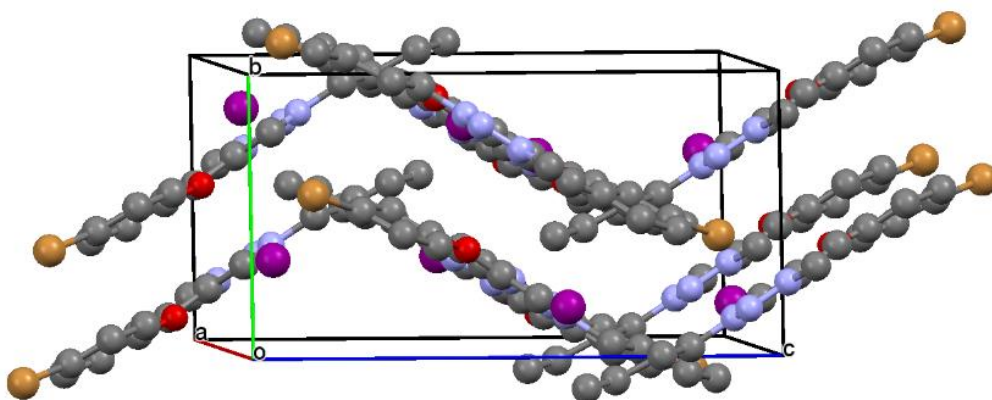


Figure 2.18: Crystal packing of **2.8a**.

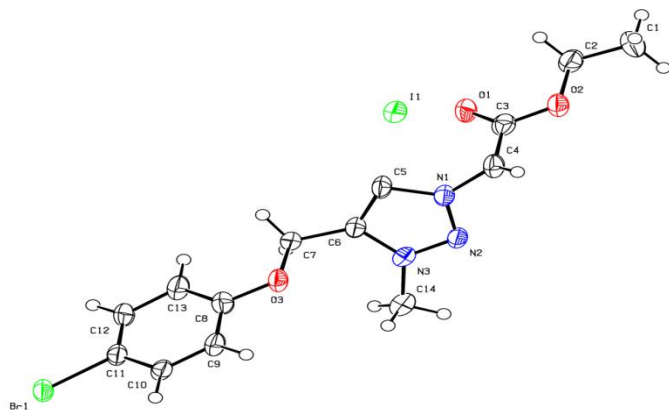


Figure 2.19: ORTEP representations of the structure of **2.12a** with the displacement ellipsoids drawn at the 50% probability level.

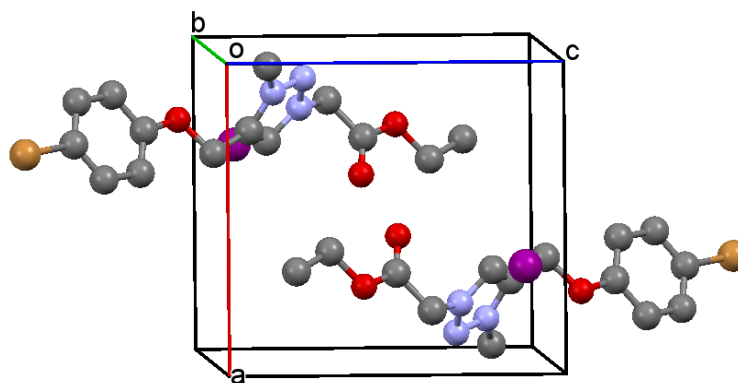


Figure 2.20: Crystal packing of **2.12a**.

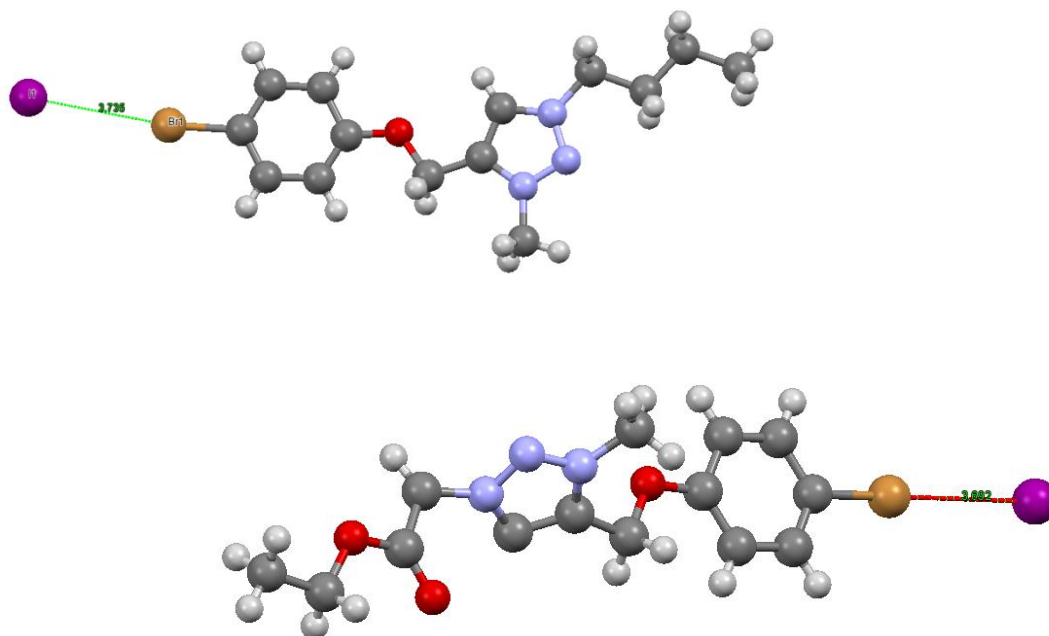


Figure 2. 21: Solid state structure of **2.8a** (top) and **2.12a** (bottom) showing halogen bonding; (brown = bromide purple = iodide).

Table 2.5: Summary of crystallographic data for **2.7**, **2.11**, **2.8a** and **2.12a**.

Compound	2.7	2.11	2.8a	2.12a
Empirical formula	C ₁₂ H ₁₆ N ₄ O ₃	C ₁₃ H ₁₄ N ₄ O ₅	C ₁₄ H ₁₉ BrIN ₃ O ₅	C ₁₄ H ₁₅ BrIN ₃ O ₃
Formula weight	276.30	306.28	452.13	480.10
Temperature (K)	173 (2)	173(2)	173(2)	173(2)
Wavelength (Å)	0.71073	0.71073	0.71073	0.71073
Crystal system	Triclinic	Triclinic	Monoclinic	Triclinic
Space group	P-1	P-1	C2/c	P-1
a (Å)	5.3477(5)	5.51900(10)	29.303(4)	9.5083(17)
b (Å)	10.3514(9)	7.6183(2)	7.9988(11)	9.6199(18)
c (Å)	12.5584(11)	17.4487(4)	17.099(3)	10.2075(19)
α (°)	97.797(4)	90.9480(10)	90	79.654(8)
β (°)	98.530(4)	98.0430(10)	122.900(11)	84.984(8)
γ (°)	99.752(4)	108.7400(10)	90	76.935(7)
Volume (Å ³)	668.28(10)	686.43(3)	3365.1(9)	893.6(3)
Z	2	2	8	2
Absorption coefficient mm ⁻¹	0.100	0.116	4.278	4.041
F(000)	292	320	1760	464
Crystal size mm ³	0.47 x 0.30 x 0.16	0.44 x 0.26 x 0.12	0.20 x 0.19 x 0.19	0.30 x 0.28 x 0.21
Density (Mg/m ³)	1.373	1.482	1.785	1.784
Theta range (°)	1.66 to 28.50	2.83 to 28.49	2.38 to 28.71	2.03 to 28.82°.
Index range	6<=h<=7, 13<=k<=12, 16<=l<=14	-5<=h<=6, 10<=k<=10, 22<=l<=12	-39<=h<=37, 10<=k<=10, 22<=l<=22	-12<=h<=12, 12<=k<=12, 13<=l<=13
Reflection collected	14085	1947	17310	14721
Completeness to theta	97.1% (28.50°)	47.5% (28.47°)	80.1% (28.71°)	85.0% (28.82°)
Max. and min. transmission	0.9841 and 0.9543	0.9862 and 0.9506	0.4970 and 0.4816	0.4841 and 0.3769
Refinement method	Full-matrix least-squares on F ²	Full-matrix least-squares on F ²	Full-matrix least-squares on F ²	Full-matrix least-squares on F ²
Data / restraints / parameters	3294 / 0 / 183	1660 / 0 / 200	3500 / 0 / 182	3969 / 0 / 202
Goodness-of-fit on F ²	1.096	1.059	1.681	1.234
Final R indices [I>2sigma(I)]	R1 = 0.1207, wR2 = 0.3976	R1 = 0.0350, wR2 = 0.0971	R1 = 0.1055, wR2 = 0.3333	R1 = 0.0896, wR2 = 0.2674
R indices (all data)	R1 = 0.1234, wR2 = 0.3989	R1 = 0.0380, wR2 = 0.1017	R1 = 0.1093, wR2 = 0.3440	R1 = 0.0981, wR2 = 0.2841
Largest diff peak and hole e.Å ⁻³	0.756 and -0.551	0.187 and -0.229	10.282 and -4.751	2.603 and -4.854

Table 2.6: Selected bond lengths (Å) and angles (°) for **2.7**, **2.11**, **2.8a** and **2.12a**.

2.7	2.11	2.8a	2.12a
Bond lengths	Bond lengths	Bond lengths	Bond lengths
N1-N4 1.338(6)	N2-N4 1.342(3)	N1-N2 1.312 (13)	N1-N2 1.326 (11)
N1-C4 1.475(7)	N2-C7 1.3556(19)	N2-N3 1.323 (10)	N2-N3 1.314 (11)
N1-C5 1.342(6)	N2-C8 1.458(2)	N3-C2 1.354 (11)	N3-C6 1.370 (11)
N4-N2 1.312(7)	N4-N3 1.316(16)	C2-C1 1.396 (13)	C6-C7 1.490 (12)
N2-C10T 1.352(7)	N3-C6 1.365(3)	C1-N1 1.353 (11)	C6-C 1.376 (14)
C10T-C6 1.492(7)	C6-C5 1.4931(16)	N1-C3 1.498 (11)	C5-N1 1.382 (11)
C10T-C5 1.384(7)	C6-C7 1.368(3)		
Bond angles	Bond angles	Bond angles	Bond angles
N4-N1-C5 110.7(4)	N4-N2-C7 111.38(15)	N1-N2-N3 104.4 (8)	N1-N2-N3 105.1 (7)
N2-N4-N1 107.9(4)	N3-N4-N2 107.32	N2-N3-C2 112.7 (8)	N2-N3-C2 113.2 (8)
N2-C10T-C5 108.2(4)	N2-C7-C6 103.9(2)	C1-N1-N2 113.6 (8)	C1-N1-N2 111.4 (8)

2.15 References

- (1) Crowley, J. D.; Bandeen, P. H.; Hanton, L. R. *Acta Crystallogr. Sect. E: Struct. Rep. Online* **2009**, 65, o999.
- (2) Uppal, B. S.; Booth, R. K.; Ali, N.; Lockwood, C.; Rice, C. R.; Elliott, P. I. P. *Dalton Trans.* **2011**, 40, 7610.
- (3) González, J.; Pérez, V. M.; Jiménez, D. O.; Lopez-Valdez, G.; Corona, D.; Cuevas-Yañez, E. *Tetrahedron Lett.* **2011**, 52, 3514.
- (4) Veerakumar, P.; Velayudham, M.; Lu, K.-L.; Rajagopal, S. *ChemInform* **2012**, 43, no.
- (5) Wang, D.; Li, N.; Zhao, M.; Shi, W.; Ma, C.; Chen, B. *Green Chem.* **2010**, 12, 2120.
- (6) Albadi, J.; Keshavarz, M.; Shirini, F.; Vafaie-nezhad, M. *Catal. Commun.* **2012**, 27, 17.
- (7) Mukherjee, N.; Ahammed, S.; Bhadra, S.; Ranu, B. C. *Green. Chem.* **2013**, 15, 389.
- (8) Zhi, H.; Lü, C.; Zhang, Q.; Luo, J. *Chem. Commun.* **2009**, 2878.
- (9) (a) Creary, X.; Anderson, A.; Brophy, C.; Crowell, F.; Funk, Z. *J. Org. Chem.* **2012**, 77, 8756
- (10) (a) Drake, G.; Kaplan, G.; Hall, L.; Hawkins, T.; Larue, J. *J. Chem. Crystallogr.* **2007**, 37, 15(b) Mudraboyina, B. P.; Obadia, M. M.; Abdelhedi-Miladi, I.; Allaoua, I.; Drockenmuller, E. *Eur. Polym. J.* **2015**, 62, 331.
- (11) Drake, G.; Hawkins, T.; Brand, A.; Hall, L.; McKay, M.; Vij, A.; Ismail, I. *Propellants, Explosives, Pyrotechnics* **2003**, 28, 174.
- (12) Zhang, J.; Higashi, K.; Ueda, K.; Kadota, K.; Tozuka, Y.; Limwikrant, W.; Yamamoto, K.; Moribe, K. *Int. J. Pharm.* **2014**, 465, 255.
- (13) (a) Schweinfurth, D.; Strobel, S.; Sarkar, B. *Inorg. Chim. Acta* **2011**, 374, 253(b) Urankar, D.; Pinter, B.; Pevec, A.; De Proft, F.; Turel, I.; Košmrlj, J. *Inorg. Chem.* **2010**, 49, 4820.
- (14) Morita, J.-i.; Nakatsuji, H.; Misaki, T.; Tanabe, Y. *Green. Chem.* **2005**, 7, 711.
- (15) Huang, Y.; Gard, G. L.; Shreeve, J. n. M. *Tetrahedron Lett.* **2010**, 51, 6951.
- (16) Ivashkevich, O.; Matulis, V. E.; Lyakhov, A.; Grigorieva, I.; Gaponik, P.; Sukhanov, G.; Filippova, Y. V.; Sukhanova, A. *Chem. Heterocycl. Comp.* **2009**, 45, 1218.
- (17) Ikhile, M. I.; Bala, M. D.; Nyamori, V. O.; Ngila, J. C. *Appl. Organomet. Chem.* **2013**, 27, 98.

- (18) Garudachari, B.; Isloor, A. M.; Satyanarayana, M. N.; Fun, H.-K.; Hegde, G. *Eur. J. Med. Chem.* **2014**, 74, 324.
- (19) Holdsworth, D. K. *J. Chem. Educ.* **1982**, 59, 780.
- (20) Matulková, I.; Němec, I.; Teubner, K.; Němec, P.; Mička, Z. *J. Mol. Struct.* **2008**, 873, 46.
- (21) (a) *The Oxford handbook of comparative evolutionary psychology*; Vonk, J.; Shackelford, T. K., Eds.; Oxford University Press: New York, 2012(b) Mercurio, J. M.; Knighton, R. C.; Cookson, J.; Beer, P. D. *Eur. J. Chem.* **2014**, 20, 11740(c) Vick, S. J.; Bovet, D.; Anderson, J. R. *Animal Cognition* **2010**, 13, 351.

Chapter three

Covalent immobilization of triazoles onto PEGs and their application as catalysts for the transfer hydrogenation of ketones

3.1 Introduction

This chapter describes the application of triazolium compounds as organocatalysts for the transfer hydrogenation of ketones. Triazolium salts with different electronic and steric contributions were screened by testing their catalytic activity for the transfer hydrogenation of acetophenone. This was followed by testing selected immobilized triazolium ionic liquids for the transfer hydrogenation of acetophenone. The major objective was to develop heterogenized homogeneous systems to achieve ease of separation and recycling which are benefits of heterogeneous catalysis.

3.2 Organocatalytic transfer hydrogenation of ketones

The hydrogenation of double bonds is important for living organisms as well as in industry for the manufacture of chemicals.¹ The direct reduction of ketones to secondary alcohols in principle requires either a combination of the use of molecular hydrogen and a transition metal catalyst or stoichiometric amounts of a hydride donor.² In this section transfer hydrogenation of ketones in isopropanol and triazolium organocatalysts is presented.

3.3 Experimental

All reactions were conducted in air. Isopropanol was distilled prior to use. The ketones were purchased from Aldrich and used without further purification. All other starting materials were commercially available and used as received. The reactions were monitored by GC analysis with an Agilent capillary gas chromatograph model 6820 fitted with a DB wax polyethylene column (0.25 mm in diameter, 30 m in length), and a flame ionization detector. Nitrogen gas was used as carrier gas at a flow rate of 2 ml/min. The oven temperature for the aromatic and the cyclic ketones was 70 °C, while for the remaining ketones the oven temperature was 50 °C. Samples (0.5 µl) were injected at 180 °C front inlet temperature.

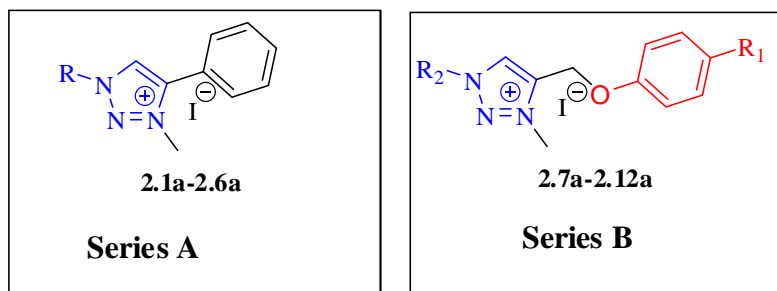


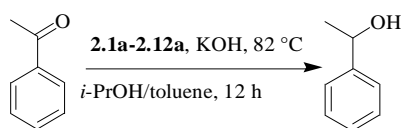
Figure 3.1: Triazolium salts **2.1a-2.12a**.

3.4 Typical protocol for transfer hydrogenation of ketones

Catalytic amount of triazolium salts **2.1a-2.12a** (2.5 mol%) and KOH (0.112 g, 0.2 M) in isopropanol (10 ml) as solvent and hydrogen donor were placed in a Schlenk tube followed by the addition of the respective ketones (2.2 mmol). The mixture was refluxed at 82 °C for 12 hours. The reaction progress was monitored by taking aliquots at time intervals, passed through a pad of silica and injected into a GC. The identities of the products were assessed by comparison of their retention time with commercially available (Aldrich Chemical Co.) samples. The percentage conversions were obtained from integration values of the GC peaks which were related to residual unreacted ketones.

3.5 Transfer hydrogenation of acetophenone by triazolium ionic salts

In view of the growing concern for sustainable processes, we envisioned a recyclable immobilized triazolium organocatalyst that exhibits thermoregulated phase separated behavior in isopropanol. As a prelude of the study, towards the development of the immobilized triazolium organocatalyst, acetophenone was chosen as a model substrate. An initial screening of conditions was conducted, which included reaction temperature, the role of KOH promoter and the triazolium salts, the results are summarized in Table 3.1.

Table 3.1: Transfer hydrogenation of acetophenone catalyzed by triazolium salts **2.1a-2.12a**.

Entry	Organocatalyst	(Conversion %) ^a	TON
1 ^b	2.5a	0	
2 ^c	-	42	
3 ^d	2.5a	0	
4 ^e	2.5a	0	
5 ^f	2.5a	38	25
6 ^g	2.5a	56	37
7	2.5a	93	62
8	2.1a	91	61
9	2.2a	85	57
10	2.3a	52	35
11	2.4a	56	37
12	2.6a	87	58
13	2.13	53	35
14	2.14	65	43
16	2.7a	56	37
17	2.8a	41	27
18	2.9a	62	41
19	2.10a	57	38
20	2.11a	65	43
21	2.12a	58	39

Except for conditions a-g; reactions were conducted in air at 82 °C using acetophenone 2.2 mmole, KOH 0.112g and isopropanol 10 ml. ^aConversion was determined by GC analysis after 12 h. ^bNo base used. ^cNo catalyst used. ^dReaction done at 24 °C. ^eReaction done at 50 °C. ^fReaction done at 60 °C. ^gReaction done at 70 °C.

Conducting a blank run (without catalyst and base) yielded no reduction product, but when KOH (2M) was added a 42% conversion of acetophenone to 1-phenylethanol was observed after 12 hours. This correlates well with similar reactions conducted to establish the role of basic media in promoting transfer hydrogenation reactions.³ Inspired by this initial progress, an investigation of the influence of reaction temperature on this transfer hydrogenation of ketones was conducted. The reaction was conducted at room temperature with catalyst **2.5a** and no reaction was observed. There was also no observable reaction upon increasing the reaction temperature to 50 °C. Generally, low temperature gave poor conversion with the highest conversion observed only after refluxing at 82 °C (the boiling point of isopropanol). Numerous explanations either exclusively or in combination can be presented for this observation: i) increasing the reaction temperature up to reflux increased the rate of reaction according to the Arrhenius equation and ii) increasing the reaction temperature increased the solubility of the triazolium catalyst in isopropanol and iii) the viscosity of triazolium ionic salt catalyst was significantly decreased with increasing reaction temperature, thereby resulting in increased mass and heat transfer. The influence of reaction time was then investigated using cyclohexanone as the substrate. Aliquots were taken from the reaction media at 1h intervals and filtered through a pad of silica followed by GC injections. The results obtained are illustrated in Figure 3.5, where it is observed that after one hour there was no detectable cyclohexanol formed. However, after two hours cyclohexanol started forming and increased gradually with time up to 8 hours, thereafter the graph leveled off.

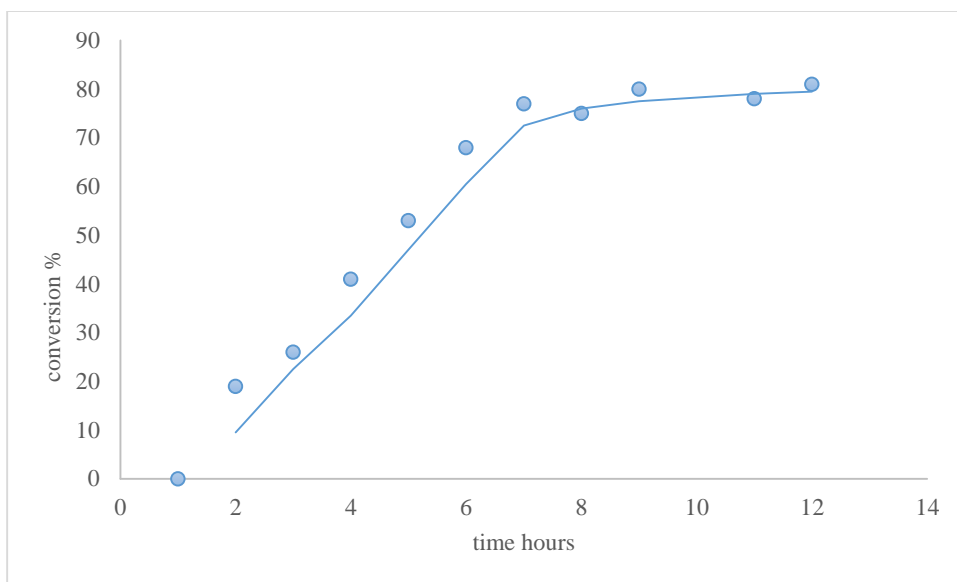
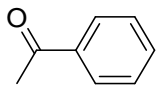
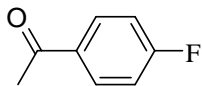
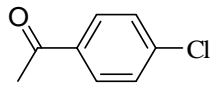
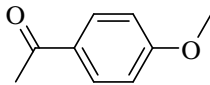
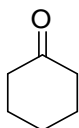
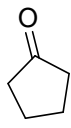
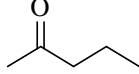
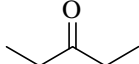


Figure 3.2: Time dependance of the transfer hydrogenation of cyclohexanone catalysed by **2.5a**.

Triazolium salts **2.1a-2.12a** were tested for activity in the reduction of acetophenone and it was found that salts **2.1a-2.12a** were active in this transfer hydrogenation protocol resulting in moderate to high conversions of acetophenone to phenylethanol. Triazolium organocatalyst **2.5a** showed the highest activity with a conversion of 93% after 9h. Generally, triazolium salts with electron withdrawing substituents produced higher conversion of acetophenone into 1-phenylethanol compared to their electron donating substituents functionalized equivalents. This can be attributed to the effects of the withdrawing groups which render the triazolium C(5) position more susceptible to nucleophilic attack by nucleophiles such as the ketonic C=O bond. This observation was consistent with findings of related studies reported in the literature.³ Hence triazolium salt **2.5a** bearing the acetate and phenyl substituents showed the highest conversion. To establish the scope, limitations and functional group tolerance of this transfer hydrogenation protocol, a variety of ketones were investigated. The results obtained are presented in Table 3.2.

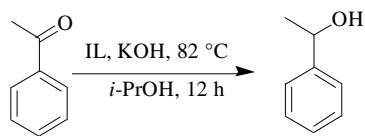
Table 3.2: Transfer hydrogenation of a variety of ketones.

<div><div><div><div>$\text{R}-\overset{\text{O}}{\parallel}{\text{C}}-\text{R}$</div><div>entry 1-8</div></div><div>$\xrightarrow[\textit{i}\text{-PrOH, 12 h}]{\text{2.5a, KOH, 82 }^\circ\text{C}}$</div><div><div>$\text{R}-\text{CH}(\text{OH})-\text{R}$</div></div></div></div>			
Entry	Substrate	Conversion (%)	TON
1		93	62
2 ^a		18	12
3 ^b		93	62
4 ^c		12	8
5		81	54
6 ^d		3	2
7		58	39
8		8	5

^aconversion determined after 24h. ^bconversion after 6h. ^cconversion after 24h. ^dconversion after 24h.

Generally, the reductions proceeded smoothly for both aromatic and aliphatic ketones. The presence of electron withdrawing groups which increase the electrophilicity of the ketone double bond (entry 3) shortens the reaction time. However replacing the chloride with a fluoride (entry 2) resulted in a reduced % conversion to the product due to the positive inductive effect of the small fluoride group para to the ketonic double bond.⁴ The substrates with an electron donating methoxy group (entry 4) also gave lower yields even after 24 hours. This is because electron donating groups reduces the electrophilicity of the carbon atom in the C=O bond. This is consistent to findings of similar studies reported in the literature in which ketones with electron donating substituents reacted less readily and required more residence time.^{2,5} 2-ketones entry 7 reacted with ease when compared to 3-ketones entry 8 this might be attributed to restricted access of the ketonic double bond due to steric hinderance.⁶

In order to achieve the overall aim of developing a recyclable homogeneous catalyst, the immobilization of triazole **2.5a** was conducted since it was the most active. However this immobilization, which makes use of mild alkylating agent (tosylate) was futile. This is a result of the electron withdrawing groups flanked at positions N(1) and C(4) of the triazolium heterocyclic ring. These groups considerably reduce the basicity of the ring both in solution and gas phase, which complicated the process of *N*-alkylation.⁷ This phenomenon was also observed while alkylating **2.5** with methyl iodide in which relatively low yields were obtained. Hence, triazoles **2.2** and **2.6** were immobilized onto PEGs of various chain length to yield ionic liquid catalysts. All the immobilized ionic liquid catalysts were successfully tested for activity in the transfer hydrogenation reaction and the results are presented in Table 3.3.

Table 3.3: Effect of polymer chain length on catalysis.

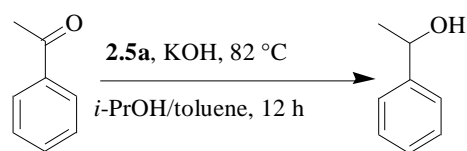
Entry	Ionic liquid Catalyst	(Conversion %)
1	3.10	0
2	3.11	0
3	3.12	0
4	3.13	0
5	3.14	0
6	3.15	0
7	3.18	73
8	3.19	87
9	3.20	66
10	3.21	51
11	3.22	49
12	3.23	44

Conversion was determined by GC analysis after 12 h.

Unexpectedly, with the tosylate counter ion, no conversion was obtained. This might probably be a result of the tosyl group being preferentially reduced to hydrosulfonylbenzene in competition to the ketonic double bond. However, replacing the tosylate with iodide ion via salt metathesis yielded interesting results. The catalytic activity decreased with an increase in polymer molecular weight, presumably due to poor substrate-catalyst transfer caused by the high viscosity of higher molecular weight polymers. It may also be attributed to a decrease in catalytic loading associated with high molecular weights since the triazolium organocatalysts are flanked at either ends of a straight chain polymer. These findings are in harmony with catalytic systems involving PEGs reported in literature.⁸ As a result, PEG₆₀₀ was found to be the ideal polymer chain for this catalytic systems. Wang *et al.*, found PEG₁₀₀₀ to be the optimum polymer chain length for both the esterification and acetalization of aromatic acids and aldehydes.⁸

In an effort to develop a PEG anchored organocatalyst that exhibits thermoregulated phase separated behavior with isopropanol it was observed that the optimum catalyst PEG₆₀₀ ditriazole is sparingly soluble in isopropanol and also prone to leaching in it. Therefore, the blending of isopropanol with a less polar solvent was done in order to improve its association with the catalyst. Da Rosa *et al.*, utilized a two organic liquid biphasic system consisting of poly(ethylene glycol), heptane and either CH₂Cl₂ or methanol in the catalytic hydrogenation of hex-1-ene using Wilkinson's catalyst or a cationic rhodium complex respectively.⁹ Hence, toluene was chosen for the current system and different ratios of isopropanol/toluene were tested as solvents and hydrogen sources for the transfer hydrogenation of acetophenone. The results obtained is presented in Table 3.4.

Table 3.4: Effect of toluene blending on catalysis



Isopropanol :Toluene	(Conversion %)
1:1	70
3:1	81
1:3	61
1:4	37

Conversion was determined by GC analysis after 12 h.

An isopropanol/toluene ratio of 3:1 was found to be the optimum ratio. The results indicates that the introduction of toluene reduced the concentration of isopropanol available for the reduction of acetophenone hence conversion decreased with an increase in isopropanol to toluene ratio. The blending of isopropanol with toluene was very crucial in reducing the polarity of the former and improving potential catalyst recovery. Our next focus was centered on conducting recycling studies using the PEG₆₀₀ ditriazole (**2.19**) toluene/isopropanol system at the optimum 3:1 ratio. However , it

was observed that the toluene/isopropanol system was still very polar and resulted in appreciable leaching of the ionic liquid catalyst into the solution that prevented any possibility of thermoregulated phase separated behavior. An alternative method for catalyst recovery was therefore envisaged, which involved solvents that are totally immiscible with ionic liquid catalysts. Generally, ionic liquid catalysts are immiscible with non polar solvents like dialkyl ethers and saturated hydrocarbon solvents.¹⁰ The addition of diethyl ether to the current system enabled distinct separation between the PEG bound ionic liquid catalysts and isopropanol. Hence the catalyst system was easily recycled by the decantation of the supernatant layer (Figure 3.6).

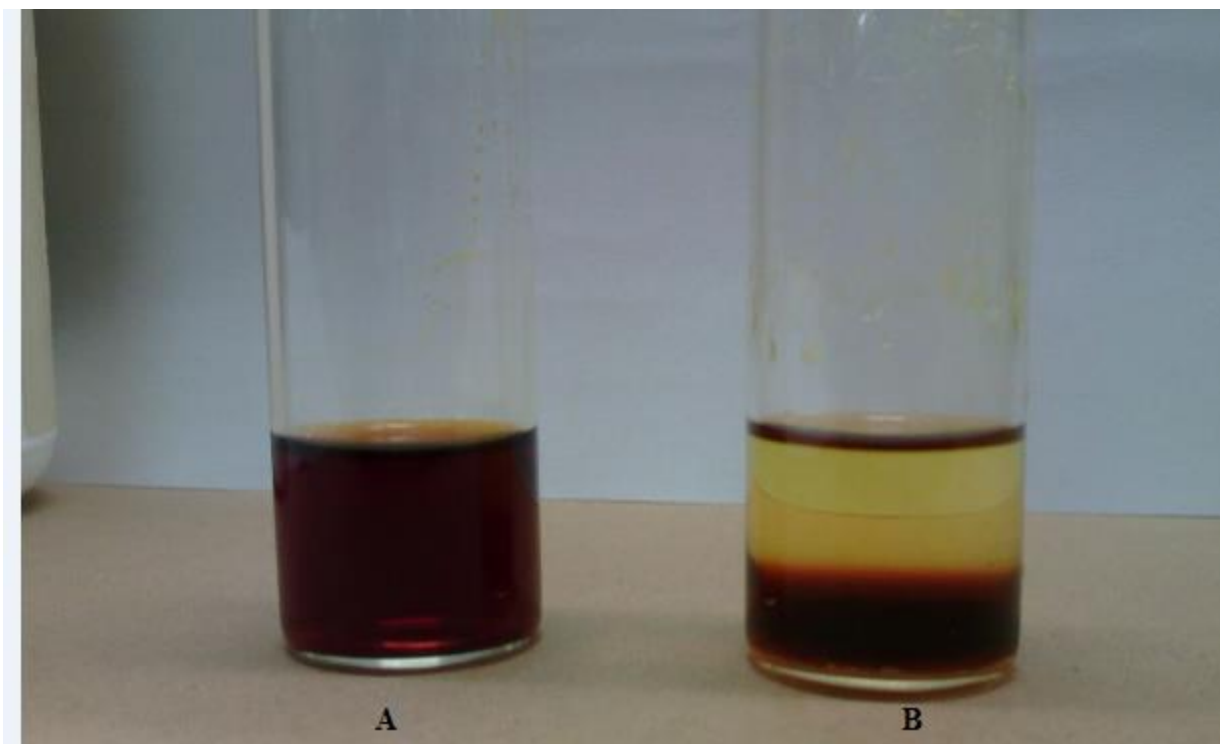


Figure 3.3: Behaviour of PEG₆₀₀ IL in ether.

- (A) Homogeneous layer after the completion of reaction (B) complete phase separation after the addition of ether.

3.6 Catalyst recycle

To investigate the recyclability of the ionic liquid catalyst, the reduction of acetophenone was investigated. The PEG immobilized ionic liquid organocatalyst combined the advantages of single phase homogeneous catalysis with the ease of catalyst separation of heterogeneous catalysis. Hence

after the completion of the first reaction cycle, diethyl ether was added, the catalyst separated and settled at the base of the reaction vessel as illustrated in Figure 3.6. The supernatant consisting of the organic product and solvent was then decanted while the lower ionic liquid layer was extracted with dichloromethane to remove KOH base. Analysis of the extract liquor showed no transfer hydrogenation product implying that the products remained in the supernatant layer. Then the ionic liquid layer was then recycled by the addition of fresh solvent, substrates and KOH base. Figure 3.7 is an illustration of the the recycling studies of PEG₆₀₀ (**2.19**).

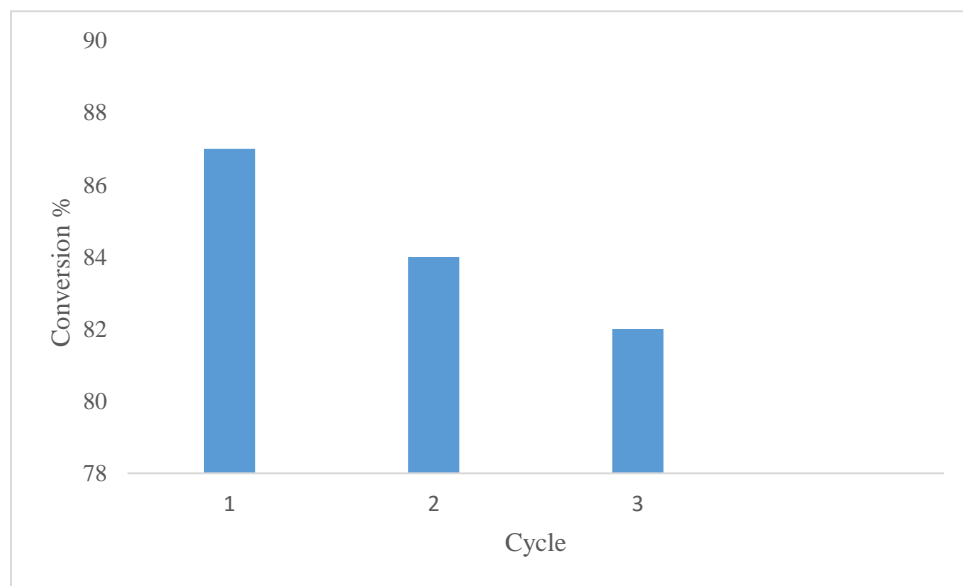


Figure 3.4: Recycling studies for the PEG immobilized catalyst **3.19**.

The catalyst system was recycled 3 times without any significant loss of activity, however after the third cycle white sediments settled at the base of the reaction upon the addition of diethyether. This was a result of the triazolium organocatalyst becoming detached from the polymer support. The inclusion of basic KOH in this catalytic system had a major detrimental effect on the recyclability of the ionic liquid system. It resulted in the cleavage of the N-O bond between the polymer backbone and the organocatalyst. In addition, the presence of a strong base like KOH will deprotonate the triazolium C(5)proton thereby generating highly reactive free cabenes that complicate the process of recycling.

3.7 References

- (1) Yang, J. W.; Hechavarria Fonseca, M. T.; List, B. *Angew. Chem. Int. Ed* **2004**, *43*, 6660.
- (2) Sedelmeier, J.; Ley, S. V.; Baxendale, I. R. *Green Chem.* **2009**, *11*, 683.
- (3) Ikhile, M. I.; Nyamori, V. O.; Bala, M. D. *Tetrahedron Lett.* **2012**, *53*, 4925.
- (4) Ikhile, M. I.; Bala, M. D.; Nyamori, V. O.; Ngila, J. C. *Appl. Organomet. Chem.* **2013**, *27*, 98.
- (5) Polshettiwar, V.; Varma, R. S. *Green Chem.* **2009**, *11*, 1313.
- (6) Bala, M. D.; Ikhile, M. I. *J. Mol. Catal. A: Chem.* **2014**, 385, 98.
- (7) Ivashkevich, O.; Matulis, V. E.; Lyakhov, A.; Grigorieva, I.; Gaponik, P.; Sukhanov, G.; Filippova, Y. V.; Sukhanova, A. *Chem. Heterocycl. Comp.* **2009**, *45*, 1218.
- (8) Wang, Y.; Zhi, H.; Luo, J. *J. Mol. Catal. A: Chem.* **2013**, *379*, 46.
- (9) da Rosa, R. G.; Martinelli, L.; da Silva, L. H.; Loh, W. *Chem. Commun.* **2000**, 33.
- (10) Song, C. E.; Roh, E. J. *Chem. Commun.* **2000**, 837.

Chapter four

Conclusion and recommendations

4.1 Synthesis and N-alkylation of triazoles

In this research 1,4-disubstituted-1,2,3-triazoles (Figure 4.1) and their corresponding 1,3,4-trisubstituted salts (Figure 4.2) were successfully synthesized and characterized. Among the synthesized triazoles six were known and available in the literature while the other six compounds were reported for the first time. The 1,4-disubstituted-1,2,3-triazoles were synthesized by adopting the versatile, green and regioselective Cu (I) catalyzed cycloaddition reaction of organic azides and terminal alkynes. The unreported compounds were synthesized in a two-step reaction process. First the reaction between propargyl bromide and the respective para substituted phenols was conducted to generate terminal alkynes. The second step was a click reaction between the alkynes and *in situ* generated organic azides. Due to safety concerns, the isolation of organic azides was avoided because while bearing short carbon chains they are highly energetic and potentially explosive, hence they were used *in situ*. Generally, moderate to high yields were obtained for most of the compounds. Presented in Figure 4.1 is a summary of the synthesized triazoles. Successful synthesis of the triazoles was confirmed by NMR, in which the typical triazole fingerprint proton appeared at around 7.77 ppm while the corresponding triazoles C(5) signal appeared at around 120 ppm. These findings were consistent to those reported in the literature. The triazolium salts were synthesized by *N*-alkylation of the 1,2,3-triazoles. *N*-alkylation was done using the mild alkylating methyl iodide in acetonitrile. This produced only N(3) substituted 1,3,4-trisubstituted-1,2,3-triazoles, hence both the synthesis and the *N*-alkylation was done in a highly regioselective protocol. The formation of only N(3) substituted *N*-alkylated triazolium salts was confirmed by NOESY NMR and single crystal X-ray crystallography data of selected triazolium salts. Generally, both N(2) and N(3) substituted products are usually formed when strong alkylating reaction conditions are used, which present problems of regioselectivity. Figure 4.2 is an illustration of the synthesized triazolium salts. The formation of the triazolium salts resulted in a significant down field shift of the triazolium fingerprint proton to values around 9.50 ppm. This is caused by the formation of a cationic specie bearing a formal positive charge which decreases the overall electron density of the triazolium heterocyclic ring.

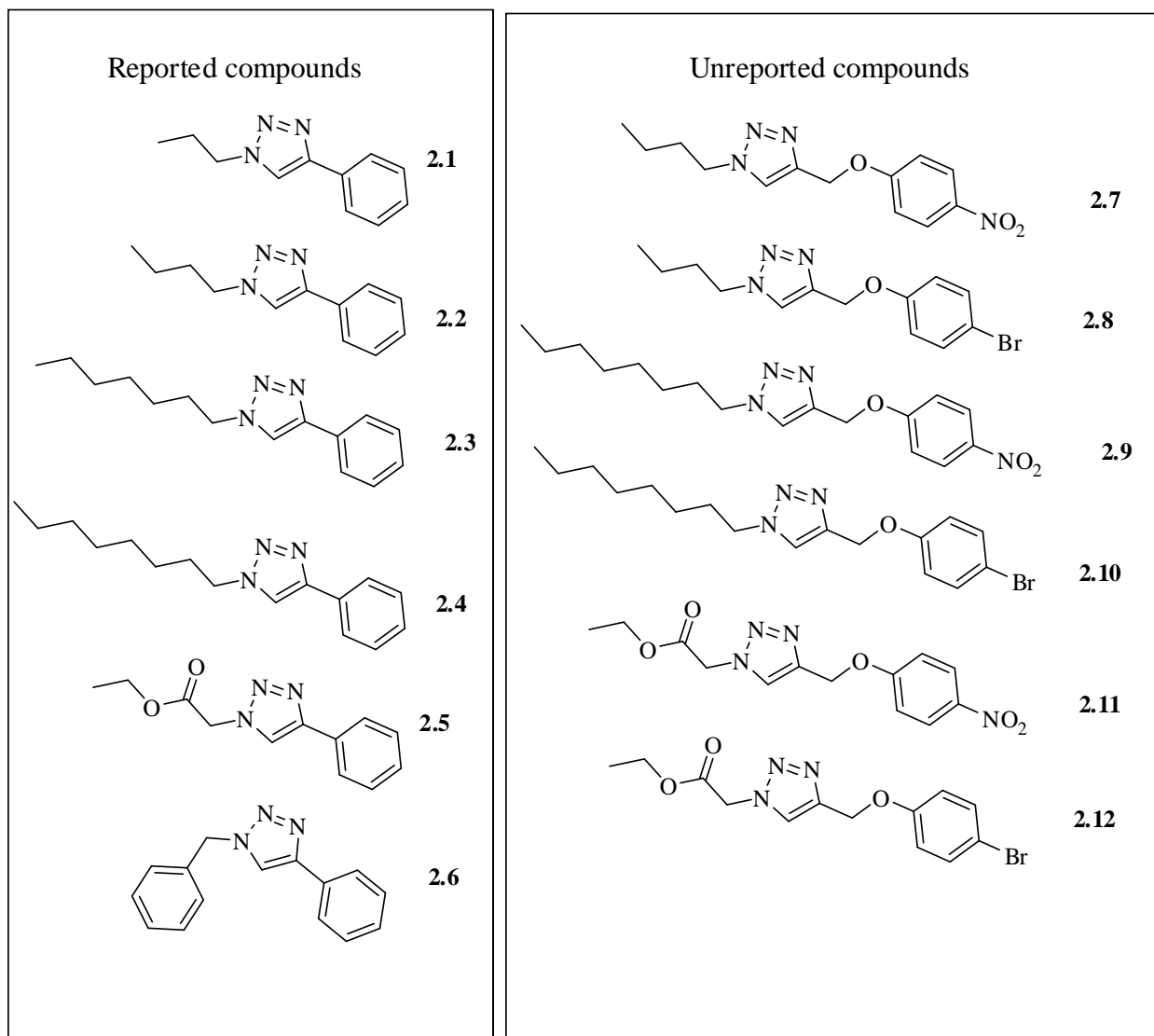


Figure 4.1: Summary of the synthesized triazoles.

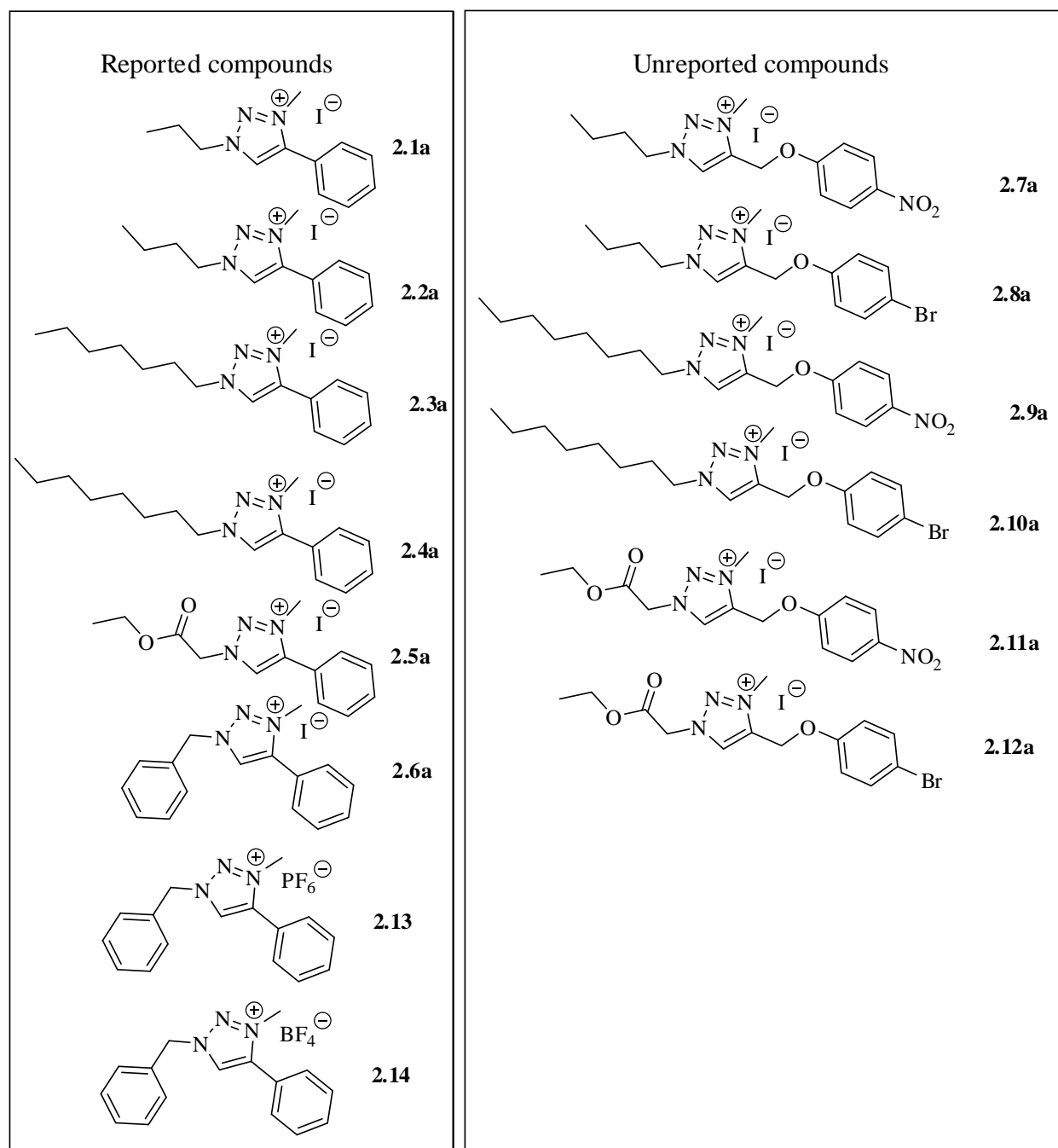


Figure 4.2: Summary of the synthesized triazolium salts.

4.2 Immobilization and catalysis

The triazole immobilization onto PEGs was achieved by tosylation of the PEGs followed by *N*-alkylation reaction between the triazoles and the PEG ditosylates. Salt metathesis was done to replace the tosyl group with an iodide ion. Successful salt metathesis was evidenced by the disappearance of proton and carbon signals of the tosyl group from the ^1H and ^{13}C NMR respectively. All the synthesized triazolium salts were successfully tested for catalytic activity in transfer hydrogenation of ketones. Among the triazolium salts, those with electron withdrawing groups showed the highest activity in the transfer hydrogenation reaction. However, an attempt to immobilize the most active triazolium catalyst **2.5a** onto PEG was unsuccessful. This was attributed to the electron withdrawing groups flanked at positions N(1) and C(4) which reduced the basicity of N(3). As a result **2.2** and **2.6** were immobilized on PEGs of various chain lengths forming immobilized ionic liquid catalysts. The catalysts were active up to three cycles before the onset of degradation and total loss of activity due to the basic conditions of the reaction set up.

4.3 Future outlook

Mechanistic study of the transfer hydrogenation protocol will be investigated. Apart from being a support, the influence of the polymer backbone on the catalysis need to be investigated. It is important to note that although the ionic liquid catalysts are generally insoluble in isopropanol at lower temperatures, the lower molecular weight ones are generally soluble. Lower molecular weight immobilized triazolium ionic liquids were also the most active due to their high catalytic loading and lower viscosity. Conversely, triazolium ionic liquid catalysts immobilized on high molecular weight PEGs were insoluble in isopropanol and exhibited remarkable temperature dependent phase separated behavior. However, their main drawback is the poor catalytic activity which is attributed to high viscosity and low catalytic loading. In addition, the inevitable inclusion of basic KOH during transfer hydrogenation made potential catalyst recovery unrealistic and impractical. It was perceived that the base resulted in the hydrolysis of the N-O bond thereby causing catalyst leaching. In order to make full use of PEG immobilized triazolium catalysts, their application in reactions that do not require the use of strong bases is recommended. Oxidation and condensation reactions are good examples. These reactions can easily be carried out in non-polar solvents, thereby automatically eliminating any

possibility of catalyst leaching. Although transfer hydrogenation of ketones with triazolium organocatalysts gave moderate to high conversions the system cannot really replace the existing transition metal catalysts due to long reaction times (8-12 h) required. More research need to be carried out in this realm of catalysis if high turnover numbers comparable to transition metals are to be achieved.